Thin film microextraction

by

Zhipei Qin

A thesis

presented to the University of Waterloo

in fulfillment of the

thesis requirement for the degree of

Doctor of Philosophy

in

Chemistry

Waterloo, Ontario, Canada, 2010

AUTHOR'S DECLARATION

I hereby declare that I am the sole author of this thesis. This is a true copy of the thesis, including any required final revisions, as accepted by my examiners.

I understand that my thesis may be made electronically available to the public.

Abstract

This thesis developed thin film extraction technique, which is a solid phase microextraction (SPME) technique with enhanced sensitivity, without sacrificing analysis time due to the large surface area-to-volume ratio of thin film. Thin film extraction was applied for both spot sampling and time weighted average (TWA) sampling in laboratory and on site.

First, an electric drill coupled with a SPME polydimethylsiloxane (PDMS) fiber or a PDMS thin film was used for active spot sampling of polycyclic aromatic hydrocarbons (PAHs) in aqueous samples. Laboratory experiments demonstrated that the sampling rates of fiber and thin film can be predicted theoretically. The performance of a PDMS-coated stir bar at a constant stirring speed was also investigated. Compared with the fiber or the stir bar, the thin film sampler exhibited a higher sampling rate and much better sensitivity due to its higher surface-to-volume ratio and its larger extraction-phase volume. A new thin film active sampler was developed; field tests illustrated that it was excellent for rapid on-site water sampling due to its short sampling period, high sampling efficiency and durability.

Second, modeling was applied to study the kinetics of fiber SPME and thin film extraction by COMSOL Multiphysics. The symmetry of absorption of analyte onto the fiber (or thin film) and desorption of calibrant from the fiber in static aqueous solution and a flow through system, was demonstrated by modeling. Furthermore, kinetic calibration method was illustrated to be feasible for fiber SPME in complex aqueous matrix and then

was used to calculate the total concentration of analyte in the system.

Third, thin film extraction was used in on-site sampling in Hamilton Harbour and for the determination of TWA concentrations of PAHs based on the kinetic calibration. When the thin film sampler, a fiber-retracted SPME field water sampler, and a SPME rod were used simultaneously, the thin film sampler exhibited the highest sampling rate compared to the other water samplers, due to its large surface-to-volume ratio.

Fourth, partition equilibriums and extraction rates of PAHs were examined for live biomonitoring with black worms and for the PDMS thin-film in passive sampling mode. In the initial extraction stage, the extracted amounts per surface area by two samplers were similar indicating that thin-film samplers could mimic the behavior of black worms for passive monitoring. A good linear relationship between bioconcentration factors and film-water partition coefficients of PAHs demonstrated the feasibility of thin-film sampler for determining the bioavailability of PAHs in water.

Finally, thin film extraction was used for the analysis of human skin and breath under different experimental conditions. Thin film technique could study several skin areas of one person, characterize the skins of different persons, and measure volatile fractions of cosmetic products that were released from the skin. The sampling time in the breath analysis could be further reduced to only 20 seconds when the thin film was rotated with a portable drill.

Acknowledgements

I would like to thank my supervisor, Dr. Janusz Pawliszyn, for providing me the opportunity to work on this interesting and challenging project and for guiding me in this work.

I thank the members of my committee, Dr. George Dixon, Dr. Dan Thomas and Dr. Morris Tchir for their advice and efforts during the years of graduate research. I also thank my external examiner Dr. Abdul Malik for his advice on the thesis.

I would like to thank Dr. Mehran Alaee from Environment Canada for his collaboration work in field sampling in Hamilton Harbour. I appreciate the help from Technical Operations Services Research Support Branch at Environment Canada.

I would also like to express my thanks to all the group members for their help and friendship, especially Dr. Wennan (Joy) Zhao, Leslie Bragg, Dr. Gangfeng Ouyang, Dr. Heather Lord, Sanja Risticevic, Ying Gong, Jie (Jet) Wu, Yanwei (Wendy) Zhan, Dr. Xu (Shine) Zhang, Melissa Morley, Francois Breton, Dr. Shokouh Hosseinzadeh, Dr. Lucie Setkova and Dr. Vadoud Niri.

I would like to thank my parents for their love, support and encouragement.

Dedication

I dedicate this thesis to my parents for their love, encouragement and understanding.

Table of Contents

List of Figures

List of Tables

List of Abbreviations

Ace	Acenaphthene
Anth	Anthracene
ATAS	A total analytical system
BCF	Bioconcentration factor
BTEX	Benzene, toluene, ethylbenzene, and xylene
CAD	Computer-aided design
CIS	Cooled injection system
DTD	Direct thermal desorption
EI	Electron ionization
Fl	Fluorene
Fla	Fluoranthene
GC	Gas chromatography
HOM	Humic organic matter
HPLC	High performance liquid chromatography
HSA	High surface area
Log K_{ow}	Log octanol/ water partition coefficient
Log K_{tfw}	Log thin film/ water partition coefficient
LPME	Liquid-phase microextraction
LTPRI	Linear temperature programmed retention index
LVI	Large volume injection
MPS	Multipurpose sampler

MS	Mass spectrometer
NIST	National institute of standards and technologies
PAHs	Polycyclic aromatic hydrocarbons
PDE	Partial differential equation
PDMS	Poly(dimethylsiloxane)
PFE	Pressurized fluid extraction
PFTBA	Perfluorotributylamine
ppb	Parts per billion
ppm	Parts per million
Pyr	Pyrene
RI	Retention index
RSD	Relative standard deviation
SBSE	Stir bar sorptive extraction
SLH	Septum-less head
SPE	Solid phase extraction
SPMD	Semipermeable membrane device
SPME	Solid-phase microextraction
TDS	Thermal desorption system
TDU	Thermal desorption unit
TWA	Time weighted average
U. S. EPA	United States Environmental Protection Agency

Chapter 1

Introduction

1.1 Sample Preparation

The sample preparation step of an analytical process consists of an extraction procedure that isolates and enriches the components of interest from a sample matrix. Traditional extraction techniques (such as liquid-liquid extraction and Soxhlet extraction), consume large amounts of solvents, thus creating environmental hazards, which increases the risk of cancer and contributes to the depletion of the ozone layer. Some less-solvent-consuming procedures, such as: solid phase extraction (SPE); new pressurized fluid extraction (PFE); hot-water extraction; microwave-assisted extraction and solid phase microextation (SPME) are alternative methods.[1]

Figure 1-1 illustrates a classification of extraction techniques based on their fundamental processes.[2] Exhaustive extraction approaches do not require calibration, because most analytes are transferred to the sampler by employing overwhelming volumes of the extraction phase. To reduce the use of a solvent and the time required to accomplish exhaustive removal, batch equilibrium techniques are frequently replaced by flow-through techniques.[2] Large volumes of sample can be passed through a small cartridge, and the flow through the sorbent bed facilitates efficient mass transfer. The desorption of analytes into a small volume of solvent would then follow; this strategy is used in sorbent trap and SPE.[3-4] However, the sorbent in SPE suffers from overloading or high carryover and batch-to-batch variation of the sorbents, which results in poor reproducibility.
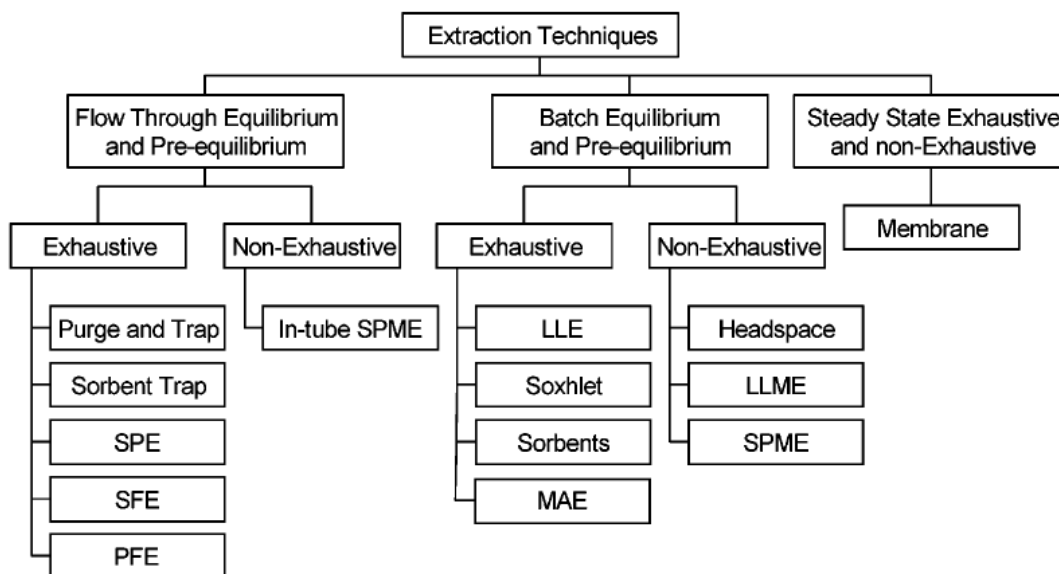
Figure 1-1 Classification of extraction techniques.

In non-exhaustive techniques, the capacity of the extraction phase is small and is therefore insufficient to remove most of the analytes from the sample matrix. The non-exhaustive approaches can be classified based on equilibrium, pre-equilibrium and permeation.[5] Equilibrium techniques involve employing a small volume of the extraction phase relative to the large sample volume, or a low partition coefficient between the extraction phase and sample matrix. Pre-equilibrium methods are performed when the extraction is terminated before equilibrium between two phases has been reached. The process happening at the extraction phase/sample matrix interface, determines the kinetics of the overall extraction procedure. Membrane extraction is a typical permeation technique, in which sorption into and desorption out of the extraction phase occur simultaneously during the continuous transport of analytes through the membrane.[6] The semi-permeable membrane device (SPMD) is also based on permeation through a non-porous membrane, but its disadvantage is the complex and time-consuming procedure

required to recover the analytes from the trioleine collecting medium.[7]

Despite substantial efforts made towards highly selective separation and sensitive instrumentation, there is an increasing demand for new, solvent-free extraction methods with speed, sensitivity, convenience and automation.

1.2 Solid Phase Microextraction (SPME)

Analytical microextraction is non-exhaustive sample preparation with a very small volume of solid or semi-solid polymeric material, which addresses the issues of miniaturization, automation, on-site analysis, and time efficiency.[8-9] Solid phase microextraction (SPME) was invented in 1990 and later became commercially available.[10-11] It requires no solvent or complicated apparatus and provides linear results over a wide range of analyte concentrations. It is also fast, sensitive, inexpensive and efficient, and combines sampling, isolation, concentration, and sample introduction into one step.[12-13]

1.2.1 Introduction to SPME

In the commercial version of SPME, a small diameter fused-silica fiber, coated with a small volume of stationary phase is contained in a specially designed syringe whose needle protects the fiber when septa are pierced (Figure 1-2). The fiber is exposed to a liquid or a gaseous sample to extract, and the analytes partition between the sample and extracting phase. After a well-defined period of time, the fiber is withdrawn into the needle and introduced into an injector of a gas chromatography (GC). The analytes are

subsequently thermally desorbed and analyzed, thus minimizing the loss of analyte due to multi-step processes. SPME can be performed manually or by an autosampler. Other advantages of this method are that it has a low cost and it is reusable. It is easily cleaned by desorbing any contaminants in a hot condition station with helium gas flow and can be immediately available for a subsequent sampling session. SPME is also readily amenable to field portability. Over the past decade, the SPME related methods (direct or headspace) have been applied for the trace determination of various organic compounds in the environmental and biological fields.[14-17]
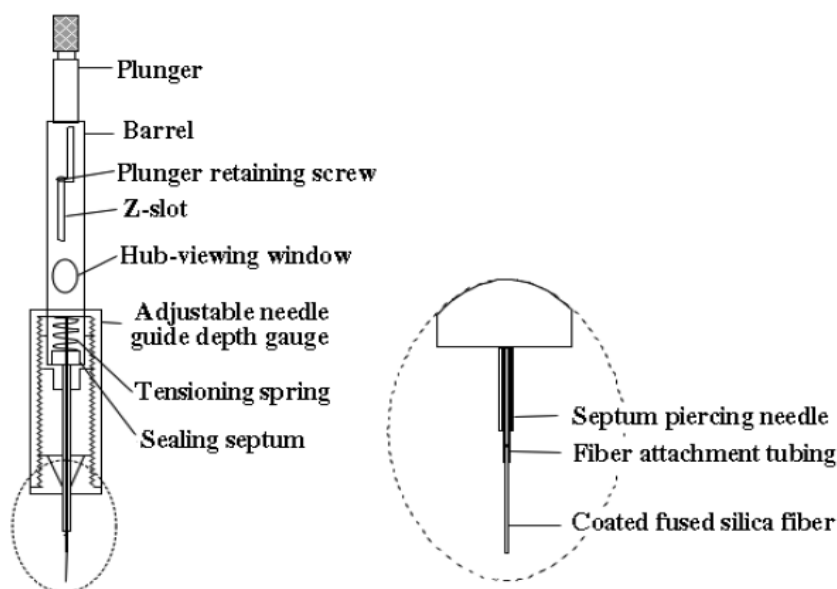
Figure 1-2 SPME device.

The geometry of the SPME system is optimized to facilitate speed, convenience of use, and sensitivity. Figure 1-3 provides a list of several implementations of SPME that have been considered to date.[18] These include mainly open-bed extraction concepts; such as coated fiber, vessels, suspended particles, agitation mechanism, and disks/membrane. Some of the implementations are better suited to address the issues associated with

agitation and ease of performing sample introduction to the analytical instrument. For example, stir bar sorptive extraction (SBSE) consists of a magnetic rod incorporated into a glass jacket coated with a layer of stationary phase; the stir bar is placed in the sample, where it performs extraction during stirring, followed by thermal desorption.[19] An in-tube approach is also considered, which is based on a piece of internally coated tubing. This tubing can consist of the needle of a syringe itself or it can be mounted in a needle.[20] Aside from the configurations in Figure 1-3, another simple construction − a rod − was developed based on the SPME technique.[21] The rod contains a much larger volume of stationary phase than the volume of the fiber coating. By shaking the sample solution containing the rod, the analytes are enriched in the extraction phase.
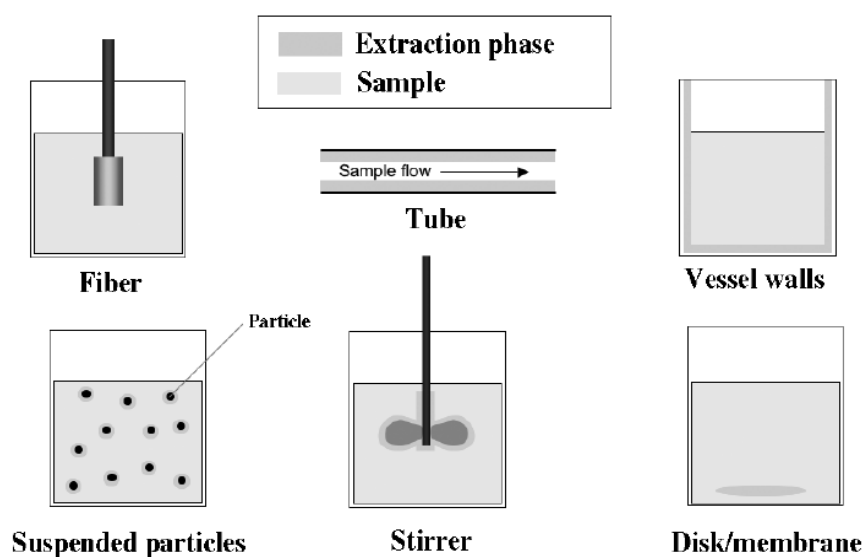
Figure 1-3 Configurations of SPME.

Based on thermodynamics and kinetics, there are two important reasons for developing these alternative approaches. The first reason is to enhance sensitivity by using a large volume of the extracting phase. The second one is to improve the mass transfer at

the interface of the sample and coating, by increasing the surface to volume ratio of the extraction phase.

Recently, introducing newly designed configurations of the SPME technique has generated increased interest in high sensitivity, improved kinetics and ease of implementation.

1.2.2 SPME with High Surface Area

In the SPME process, the movement of analytes follows a concentration gradient according to Fick's first law of diffusion; the fluid in contact with the extraction phase's surface is always stationary. To model mass transport, the gradation in fluid motion and convection of molecules in the space surrounding the extraction phase can be simplified using a Prandtl boundary layer, as seen in Figure 1-4. [11]
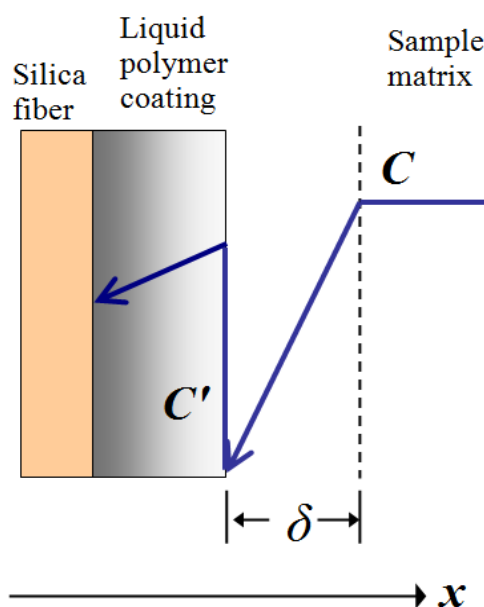
Figure 1-4 Boundary layer model in SPME process.

The thickness of the boundary layer determines the equilibration time and extraction rate, as extraction rate is controlled by diffusion from the sample matrix through the boundary layer to the extraction phase.[11] The boundary layer thickness can be calculated for given convection conditions by using principles of engineering.

Koziel *et al.* found that the initial extraction rate of SPME process was proportional to the surface area of the extraction phase.[22]

$$\mathrm{d}n/\mathrm{d}t = \left(D_s A / \delta\right) C_s \qquad \text{Equation 1.1}$$

where n is the mass of analyte extracted over the sampling time (t) and A is the surface area of the extraction phase. D_s is the analyte's diffusion coefficient in the sample fluid; δ is the effective thickness of a boundary layer; and C_s is the initial concentration of analytes in the sample matrix. Therefore, the increased surface area of the extraction phase should lead to an increase in the uptake rate of analyte and a lower detection limit.

1.2.2.1 Thin Film Extraction

In direct SPME extraction for a large sample volume, the amount of analyte in equilibrium condition, n, is expressed by equation 1.2:[11]

$$n_e = K_{es} V_e C_s \qquad \text{Equation 1.2}$$

where K_{es} is the analyte's partition coefficient between the extraction phase and sample matrix and V_e is the volume of extraction phase. Because the amount of analyte is proportional to the volume of extraction phase, the sensitivity in SPME can be improved by increasing the extraction phase volume. However, much longer equilibration time (t_e) is required if a thick extraction phase is employed; if the equilibrium time is assumed to be

achieved when 95% of the equilibrium amount of analyte is extracted from the sample, the

time required to reach equilibrium can be estimated by the following equation:[11]

$$t_e = t_{95\%} = B \frac{\delta K_{es}(b-a)}{D_s} \qquad \text{Equation 1.3}$$

where (b-a) is the thickness of extraction phase, and B is a geometric factor referring to the

geometry of the supporting material on which the extracting phase is dispersed − this

value is 3 for cylinder geometry.

The optimal way to increase the volume of the extraction phase and thus the

sensitivity of the method, is to use a thin extraction phase with a large surface area. In

other words, the extraction phase should have a large surface area-to-volume ratio. This

results in enhanced sensitivity without sacrificing analysis time.

Bruheim *et al.* examined a thin sheet of poly(dimethylsiloxane) (PDMS) membrane as

an extraction phase and compared it to SPME PDMS-coated fiber for application to

semivolatile analytes in direct and headspace modes.[23] As shown in Figure 1-5, the

membrane was attached to a deactivated stainless steel rod and positioned inside the

sample container. In both direct and headspace extraction, care was taken to ensure that

the membrane was shaped like a flag. After the extraction, the membrane was rolled

around the rod and finally placed in the GC injector (positioned in the center of the liner)

for immediate thermal desorption. The samples were stirred at either 1250

revolutions/minute (rpm) or at 600 rpm.[23]
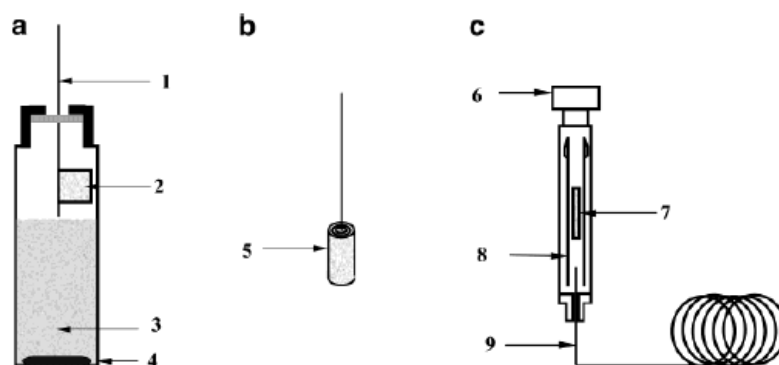
Figure 1-5 Headspace membrane SPME system. 1. Deactivated stainless steel rod. 2. Flat sheet membrane. 3. Sample solution. 4. Teflon-coated stirring bar. 5. Rolled membrane. 6. Injector nut. 7. Rolled membrane. 8. Glass liner. 9. Capillary column.

The surface area of a 1 cm x 1 cm membrane sheet is 200 mm^2, which is about 20 times that of a 100 μm PDMS fiber (A = 10 mm^2). Direct extraction of seven polycyclic aromatic hydrocarbons (PAHs) from a 1 L sample solution (at a concentration of 4 ng/mL), stirred at 600 rpm was performed by both fiber SPME and membrane extraction. Table 1-1 provides the extracted amount ratio by the direct membrane extraction and direct fiber extraction when extraction times were 1 minute, 3 minutes and 45 minutes. After 3 minutes, the amounts extracted by the membrane were 18 and 20 times higher (fluoranthene and pyrene, respectively) than the 100 μm fiber. By reducing the extraction time to only 1 minute, the ratios increased to 8, 14, 16, and 19 for naphthalene, acenaphthene (ACE), acenaphthylene (ACEY), and fluorene, respectively. These results clearly illustrate that at the initial stages of extraction, the extraction rate is proportional to the surface area as predicted by equation 1.1.

Table 1-1 Amount extracted by direct membrane (1 cm x 1cm) SPME relative to direct fiber (100 μm) SPME.

	Amount ratio						
Time (min)	Naphthalene	ACEY	ACE	Fluorene	Anthracene	Fluoranthene	Pyrene
1	8	14	16	19	ND	ND	ND
3	7	10	11	11	16	18	20
45	5	6	6	5	8	8	8

ND, not detected

In Figure 1-6 A, the extraction time profile for naphthalene and ACEY by membrane extraction shows that the compounds are at (or close to) equilibrium after 10 minutes. Equation 1.2 shows that the amount extracted at equilibrium is proportional to the extraction-phase volume. The extraction phase volume of a membrane sheet ($V_e = 2.55$ mm^3) is about 4.2 times larger than that of a 100 μm PDMS fiber ($V_e = 0.61$ mm^3). Table 1-1 and Figure 1-6 show that after 45 minutes of extraction, the ratio of the amount extracted by the membrane compared to the fiber was 5-6 for all the compounds that had reached equilibrium (naphthalene, ACE, ACEY, fluorene), and 8 for the compounds not at equilibrium (anthracene, fluoranthene, pyrene). The results demonstrate that the benefit of direct membrane SPME is not only in the enhancement of the surface area, but also in the extraction-phase volume. When these two advantages are combined, they lead to enhanced sensitivity without sacrificing analysis time.[23]
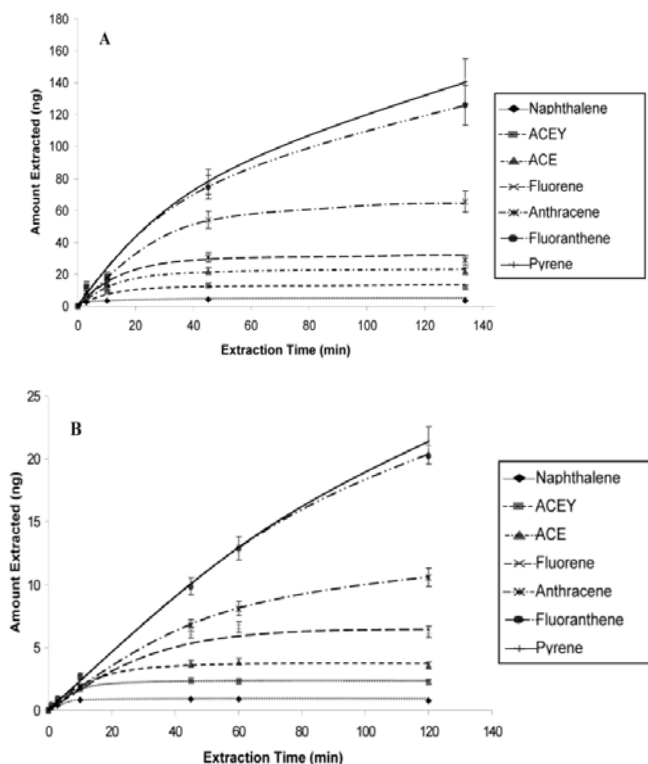
Figure 1-6 Extraction time profiles for seven PAHs. (A) Direct membrane extraction (B) Direct fiber extraction.

The extraction efficiency in headspace was compared between a 100 μm PDMS fiber and two pieces of PDMS membranes of different sizes (1 cm x 1 cm; and 1 cm x 2 cm). As expected, the amount of analytes extracted by membrane SPME was much higher than the amount obtained by fiber, due to a larger extraction-phase volume (V_e). The volume of a 1 cm x 2 cm membrane sheet ($V_e = 5.1$ mm^3) is more than 8 times larger than that of a 100 μm PDMS fiber ($V_e = 0.61$ mm^3). However, the amount of analytes extracted by the 1 cm x 2 cm membrane was only 5-7 times larger than that obtained by the 100 μm fiber and did not double the amount obtained by the 1 cm x 1 cm membrane. This difference can be easily understood when the small sample volume and relatively large membrane volume used for extraction are considered.[23]

1.2.2.2 High Surface Area SPME Phase between Two Glass Tubes

A sampler based on high-surface area solid phase microextraction (HSA-SPME) was employed for dynamic sampling at high air velocities of up to several hundred centimeters per second. The sampling device consisted of a thin wire coated with helical carboxen/ polydimethylsiloxane (carboxen/PDMS) material wound in the annular space between two concentric glass tubes, providing a large trapping surface (Figure 1-7). The sensitivity of the approach for the benzene, toluene, ethylbenzene and xylene (BTEX) compounds exceeded that of traditionally used SPME approaches, with a minimal extraction time of less than 1 minute.[24]
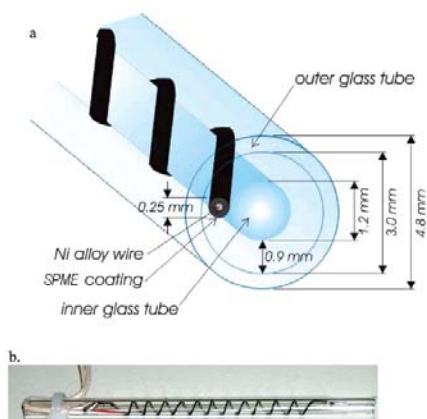
Figure 1-7 (a) Cross section of the HSA-SPME sampler design. (b) A picture of the HSA-SPME device (78.5 mm in length).

By coating the stationary phase on a 100 mm length of nickel alloy wire to a thickness of 65 μm, the polymeric surface area in direct contact with sample air flow was 10 times greater than that of the widely used conventional straight SPME fibers (81 mm^2 vs. 8.1 mm^2). As discussed in equation 1.1, the *A* term defining the surface area of the fiber in

contact with air flow compared to that of a fiber, is clearly higher by an order of magnitude. An increase in the uptake rate of the analyte should be observed. Calibration curves were obtained based on the benzene extracted from a 1 ppm gas mixture via the HSA-SPME device, and by dynamic and static headspace SPME. The HSA-SPME sampler response curve was approximately 1 order of magnitude higher than both conventional SPME methods over the concentration range studied. The steep linear response from HSA-SPME translates to an increased sensitivity relative to both dynamic and static sampling using conventional SPME fibers.[24]

Extraction time using HSA-SPME was also significantly decreased, as observed in the time-based sampling results by comparing HSA-SPME and conventional headspace SPME of a 40 ppb benzene and toluene gas mixture. The improved performance of the HSA-SPME sampler could be contributed to the 10-fold increase of the surface area in contact with the air flow, and perhaps subtle geometry factors as well. The HSA-SPME method provides increased analyte sorption per unit time.[24]

The detection limits of the HSA-SPME method were 1 to 2 orders of magnitude lower than the dynamic SPME method under similar extraction parameters, and 1 to 2 orders of magnitude lower than static headspace SPME that required up to 4 minutes for extraction.[24]

Field application results indicate that the HSA-SPME sampler provided similar quantification of the BTEX compounds as the conventional dynamic flow fiber SPME method under identical sampling conditions. The experimental HSA-SPME method can be used to perform rapid, non-equilibrium field sampling and demonstrates linearity in the

ppb range.[24]

1.2.3 Calibration in SPME

To date, there are several calibration approaches developed to address the need for rapid sampling and sample preparation, both in the laboratory and on site where the investigated system is located.

1.2.3.1 Equilibrium Extraction

The most well-established and widely used quantification method using SPME is the equilibrium extraction method, where a fiber, coated with a liquid polymeric film, is exposed to a sample matrix until equilibrium is reached.[25-27] The equilibrium conditions can be described by equation 1.4, if only two phases are considered.[28]

$$n_e = \frac{K_{es}V_sC_sV_e}{K_{es}V_e + V_s} \qquad\qquad \text{Equation1.4}$$

where V_s is the sample volume.

Equation 1.4 indicates that the amount of analyte extracted onto the coating (n) is linearly proportional to the analyte concentration in the sample, which is the analytical basis for quantification using SPME.

When the sample volume is large, the amount of analyte extracted becomes independent of the sample volume, and can be described using equation 1.1, previously described. On site sampling can take advantage of this equation. Practically speaking, this is because there is no need to collect a defined sample prior to analysis, since the fiber can be exposed directly to the sample system. When the sampling step is eliminated, the whole

analytical process can be accelerated, and errors associated with analyte loss through the decomposition or adsorption on the sampling container walls will be prevented. Furthermore, the concentration of the analyte can be determined by using the partition coefficient of analyte between fiber coating and sample matrix, which can be found in the literature or determined by experimentation.[29-30] This method eliminates the need for conventional calibration methods (such as external calibration curve), and simplifies the analytical procedure.

1.2.3.2 Exhaustive Extraction

In most cases, SPME is not used for exhaustive extraction; however, if the term of $K_{es}V_e$ is much larger than V_s, the equation 1.4 can be simplified to:

$$n_e = V_s C_s \qquad\qquad\qquad \text{Equation 1.5}$$

There are three situations where $V_s << K_{es}V_e$: (1) the sample volume is very small; (2) the partition coefficient is very large; (3) the extraction phase is large. The large partition coefficient can be obtained by an internally cooling fiber device, in which the sample matrix would be heated and the fiber coating is cooled simultaneously.[31-32] Additionally, using special samplers with a large extraction phase, such as thin film extraction, could also potentially achieve exhaustive extraction.

Equation 1.5 implies that the analyte in the sample matrix is completely extracted onto the fiber coating and the concentration of the target analyte can be easily calculated. This calculation uses the amount of analyte extracted by the fiber coating and the volume of the sample.

1.2.3.3 Diffusion Based Calibration

The highest sensitivity in SPME is achieved when equilibrium conditions are reached and the extracted amount is at a maximum. However, the equilibrium time varies from minutes to months, depending on the diffusion coefficients of the analyte in the sample, the flow velocity of sample matrix and the characteristics of the extraction phase. Therefore, pre-equilibrium extraction is required when extraction time is the main concern and the method sensitivity is high enough for quantification. In the case of the pre-equilibrium extraction, SPME is a kinetic process.

In recent years, several diffusion-based calibration methods have been proposed for the quantification of SPME. These calibration methods are developed using Fick's first law of diffusion, the interface model, the cross-flow model and the kinetic processes of absorption and desorption. They are mainly used for on site sampling, including spot sampling, which is representative of analyte concentration at the moment of sampling, and time-weighted average (TWA) sampling, which integrates the analyte concentration over the long-term sampling period.

1.2.3.3.1 Fick's First Law of Diffusion

The fiber is retracted a known distance into its needle housing during the sampling period.[33] This geometric arrangement is very simple and capable of generating a response proportional to the integral of the analyte concentration over time and space.

The analyte molecules access the fiber coating only by diffusion through the static

air/water gap between the opening and fiber coating. This is why Fick's first law of diffusion is used for the calibration (Figure 1-8). For these types of samplers, the diffusion paths are well defined. The sampling rate, R_s, is proportional to the molecular diffusion coefficient and the ratio of the opening area (A) to the diffusion path length (Z). If the sorbent is "zero sink" for the target analyte, and the sampling is limited in the linear regime, the amount of analyte extracted by the fiber after sampling time (t) is described as:[34]

$$n = R_s \int C_s(t)dt = D_s \frac{A}{Z} \int C_s(t)dt \qquad\qquad \text{Equation 1.6}$$

where C_s is the concentration of the target analyte in air or water, A is the cross-sectional area of the needle, and D_s is the diffusion coefficient of the target analyte in air or water. Equation 1.6 can be simplified to:

$$\overline{C} = \frac{nZ}{AD_s t} \qquad\qquad \text{Equation 1.7}$$

where $\overline{C}$ is the time-weighted average (TWA) concentration of the target analyte in air or water. With the well-defined diffusion path, Fick's first law of diffusion can be directly used for calibration and the calculation of $\overline{C}$ is thus very simple. In this way the SPME device can be used as a passive sampler.[35-36]
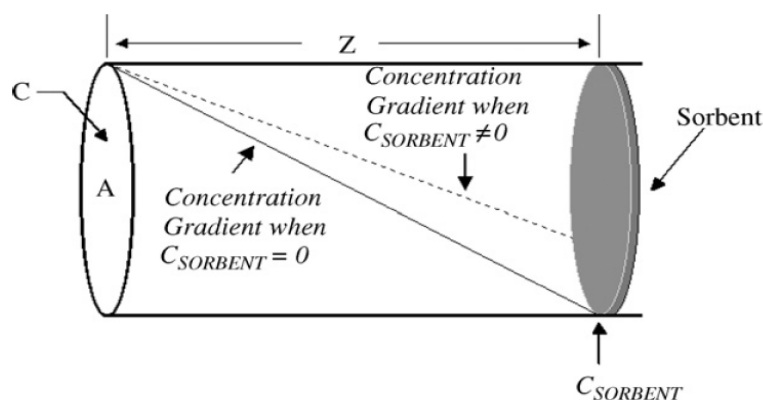
Figure 1-8 A fiber retracted SPME device and the concentration gradient.

An attractive feature of the samplers is that the performance of the device is independent of the face velocity, especially for field sampling, where the convection conditions of water are very difficult to measure and calibrate, due to the extremely small inner diameter of the diffusion path.[37-38]

1.2.3.3.2 Interface Model

Koziel *et al*. used adsorptive SPME coatings for rapid air sampling under controlled air convection conditions. A theoretical model for rapid extraction was formulated based on the diffusion through the interface surrounding the fiber.[39]

$$C_s = \frac{n \ln((b+\delta)/b)}{2\pi D_a L t}$$
Equation 1.8

where C_s is the analyte concentration in the bulk air; n is the amount of analyte extracted by the fiber coating during time, t; L is the length of the coated rod; D_a is the molecular diffusion coefficient in air; and b is the outside radius of the fiber coating.

The thickness of the boundary layer (δ) surrounding the fiber coating can be estimated using the following equation: [39]

$$\delta = 9.52(\frac{b}{Re^{0.62} Sc^{0.38}})$$
Equation 1.9

where Re is the Reynolds number ($Re = 2ub/v$); u is the linear air velocity; v is the kinetic viscosity for air; and Sc is the Schmidt number ($Sc = v/D_a$).

This model enabled the calibration of the extracted analyte mass as a function of the molecular diffusion coefficient, the analyte concentration, the sampling time, the air velocity, the air temperature and the fiber geometry. The use of short sampling times

minimized the effects of competitive adsorption for solid coating. This calibration method was not only used for rapid sampling of volatile organic compounds (VOCs) in air, but was also used in aqueous samples.[40-41]

1.2.3.3.3 Cross-flow Model

Another diffusion-based calibration method was proposed through a cross-flow model, as shown in Figure 1-9.[42] An empirical correlation to this model was used to predict the mass transfer coefficient. With this model, the target analyte concentration can be calculated as:

$$C_s = \frac{n}{\bar{h}At} = \frac{nd}{ERe^m Sc^{1/3}ADt} \qquad \text{Equation 1.10}$$

where A is the surface area of the fiber; n is the mass uptake onto the fiber during sampling time, t; D is the diffusion coefficient of the analyte molecule; $\bar{h}$ is the average mass-transfer coefficient; d is the outer diameter of the fiber; Re is the Reynolds number; and Sc is the Schmidt number. Constants E and m are dependent on the Reynolds number and are available in the literature.[42]
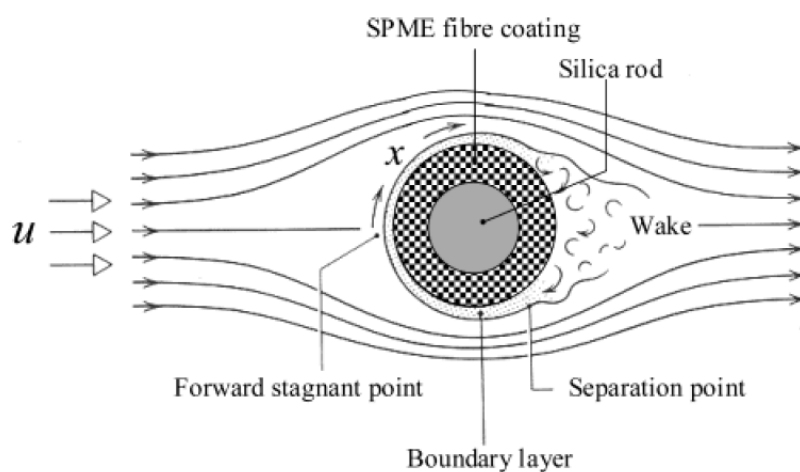
Figure 1-9 Rapid extraction with a SPME fiber in cross-flow.

Because the quantification of this method is diffusion-based, as in the interface model, the necessary constants (e.g., the diffusion coefficient) can be found in the literature or estimated with empirical equations. This means that no calibration curves or internal standards are needed. This characteristic makes this method especially suitable for on-site analysis where the construction of calibration curves or the addition of internal standards is very difficult. However, calibration with the interface or cross-flow model requires samples with a flowing medium. The sample velocity must be known or controlled and as such, additional equipment is needed.[42]

1.2.3.3.4 Kinetic Calibration

In 1997, Ai proposed a theoretical model based on a diffusion-controlled mass-transfer process to describe the kinetic process of SPME. The amount of analyte extracted in a fiber coating can be described in the equation 1.11.[43-44]

$$n = \left[1 - \exp(-at)\right] \frac{K_{es} V_e V_s}{K_{es} V_e + V_s} C_s \qquad \text{Equation 1.11}$$

Equation 1.11 can be changed to equation 1.12:

$$\frac{n}{n_e} = 1 - \exp(-at) \qquad \text{Equation 1.12}$$

where a is a rate constant that is dependent on the extraction phase, the sample volumes, the mass-transfer coefficients, the partition coefficients and the surface area of the extraction phase; and n_e is the amount of the extracted analyte at equilibrium.

Based on this theoretical model, two kinetic calibration methods were developed: the

standard in fiber technique and the standard-free technique.

1.2.3.3.4.1 Kinetic Calibration with the Standard in Fiber

The kinetic calibration method with the standard in fiber uses the desorption of the

standard, which are pre-loaded in the extraction phase, to calibrate the extraction of the

analyte. The desorption of the standard from a SPME fiber can be described by:[45-46]

$$\frac{Q}{q_0} = \exp(-at) \qquad\qquad \text{Equation 1.13}$$

where q_0 is the amount of pre-loaded standard in the extraction phase and Q is the amount

of the standard remaining in the extraction phase after exposure to the sample matrix for

the sampling time, t.

When the constant a has the same value for the absorption of target analytes and the

desorption of pre-loaded standards, the sum of q/q_0 and n/n_e should be 1 at any desorption/

absorption time:

$$\frac{n}{n_e} + \frac{Q}{q_0} = 1 \qquad\qquad \text{Equation 1.14}$$

Therefore, the initial concentrations of target analytes in the sample, C_s, can be calculated

with the following equation:

$$C_s = \frac{q_0 n}{K_{es}V_e(q_0 - Q)} \qquad\qquad \text{Equation 1.15}$$

A main advantage of this method is its feasibility for on-site sampling. The change of

environmental variables will affect the extraction of the analyte and the desorption of the

preloaded standard simultaneously, therefore, the effect of environmental factors, such as

biofouling, temperature or turbulence, can be calibrated with this approach.

This method requires that the physicochemical properties of the standard be similar to those of the analyte, so deuterated compounds are often used as the standards. However, deuterated compounds are expensive and sometimes not available, thus standard-free kinetic calibration was developed.

1.2.3.3.4.2 Standard-free Kinetic Calibration

When the extraction conditions are kept constant, e.g. fast sampling, equation 1.16 can be used for the calculation of n_e; the amount of analyte extracted at equilibrium.[47]

$$\frac{t_2}{t_1} \ln(1 - \frac{n_1}{n_e}) = \ln(1 - \frac{n_2}{n_e}) \qquad \text{Equation 1.16}$$

where n_1 and n_2 are the amounts of analyte extracted at sampling times t_1 and t_2, respectively. The concentration of the analyte in the sample can then be calculated.

The feasibility of this calibration method was validated in a standard aqueous solution flow-through system and a standard gas flow-through system.[47] This technique is particularly useful when a number of compounds are measured simultaneously; all the analytes can be calibrated with only two samplings.

1.3 Thesis Objective

The overall objective of this thesis is to develop thin film extraction technique, which is a SPME technique with enhanced sensitivity, without sacrificing analysis time due to the large surface area-to-volume ratio of the thin film. Thin film extraction was applied for both spot sampling and time weighted average (TWA) sampling in laboratory and on site.

Chapter 2 uses numerical simulation to validate and study the kinetic calibration method of SPME in aqueous samples.

Chapters 3 and 4 address spot sampling with thin film and compare its extraction performance to two conventional sample preparation methods: fiber SPME and stir bar sorptive extraction (SBSE), on the base of theoretical consideration and experimentations.

Chapter 5 discusses on site TWA sampling with thin film combined with the kinetic calibration method. The results from several sampling sites outside the laboratory demonstrate the feasibility of this technique.

Chapter 6 compares accumulation rates and partitions of the pollutants, in thin film and black worms during passive sampling. The thin film proved replaceable to live animals in aqueous samples for the analysis of contamination level.

Chapter 7 studies the application of thin film extraction on human skin and in human breath.

Chapter 8 summarizes the overall conclusion of the research work presented here, and makes recommendations for future considerations.

Chapter 2

Numerical Simulations for Kinetic Calibration Method in Solid

Phase Microextraction

2.1 Introduction

Polycyclic aromatic hydrocarbons (PAHs) can cause severe illness or death following direct consumption of a sufficient dose. Evaluation and monitoring of trace levels of these compounds from environmental waters is an important objective.

Solid-phase microextraction (SPME), a solventless sampling and sample preparation technique, was first invented over one decade ago.[1] SPME combines sample extraction, concentration, and introduction into one step. Since its conception, SPME has been widely applied to the sampling and analysis of various types of samples, including environmental, food, aromatic, forensic and pharmaceutical samples.[2]

In the SPME procedure, if convection and agitation of the samples are constant, the amount of analyte extracted depends on the extraction time. Quantification can be performed based on the timed accumulation of analytes in the coating. This pre-equilibrium dynamic SPME model is based on a diffusion-controlled mass-transfer process.[3-4] On the basis of this process, a new calibration method, called kinetic calibration, can be accomplished by investigating the kinetics of desorption/extraction processes.[5]

Absorption of an analyte onto a SPME liquid coating is theoretically described with equation 2.1.[5]

$$\frac{n}{n_e} = 1 - \exp(-at)$$
Equation 2.1

where n is the amount of analyte extracted by SPME coating at time t; n_e is the amount of analyte extracted by the SPME coating at equilibrium; and a is a constant that is dependent on the volumes of the fiber coating and sample, mass transfer coefficients, partition coefficients and the surface area of the extraction phase.

The extraction phase could be loaded with the standard, prior to sample extraction, thus eliminating the need for the standard spiking step. The standard can be introduced to the coating by exposing the fiber to a vial containing the standard.

Desorption kinetics of the standard can be expressed as:[5]

$$\frac{Q}{q_0} = \exp(-at)$$
Equation 2.2

where Q is the amount of standard remaining in the extraction phase after sampling time (t) and q_0 is the amount of pre-added standard in the extraction phase. The mirror reflection characteristic of the absorption and desorption can be demonstrated using:

$$\frac{n}{n_e} + \frac{Q}{q_0} = 1$$
Equation 2.3

In the sampling process, desorption and re-equilibration of the standard with the matrix occurs simultaneously with the absorption and equilibration of the target analytes from the matrix into the extraction phase. The standard delivery process is not expected to substantially increase the extraction time. Mass transfer through the boundary layer controls the rate of extraction. Therefore, the desorption rate of the standard can be used to give an indication of the extent that this layer and this information, could be used for calibration of the target analytes.[6]

This kinetic calibration method was successfully used for both in-vial SPME and LPME investigations.[7-8] Two passive samplers (the SPME rod and the SPME thin film), were developed based on this standardization technique for field time-weighted average (TWA) water sampling.[9-10] Moreover, the concept of calibrants in the extraction phase was extended to solid-coated SPME and directly determined the concentration of analytes in animal veins, illustrating the feasibility of this approach for in vivo studies.[11-12]

COMSOL is a finite element modeling program. It provides a complete environment to model a wide range of physical phenomena that can be described by partial differential equations (PDEs). COMSOL was formerly called FEMLAB, and was initially developed by Professor Germund Dahlquist at the Royal Institute of Technology (KTH) in Stockholm, Sweden. COMSOL is developed by the Swedish software developers, COMSOL AB.[13]

The numerical engine in COMSOL is able to handle the arbitrary coupling of systems of nonlinear partial differential equations; i.e. the equation which describes transport phenomena in space and time. The package solves the governing equations by dividing the geometry of the studied equipment into elements within a one-dimensional, two-dimensional or three-dimensional space. Applications of COMSOL in physics and engineering fields range from acoustics to fluid flow.[14-17] Flexibility within the software allows users to couple multiple PDEs within a single model domain, in addition to coupling multi-physical problems within adjoining model domains. COMSOL comes with a basic library of predefined PDEs for specific applications (Heat transfer, Convection/ Diffusion, Fluid Dynamics, etc.).[18-20] It has become the industry standard for

multi-physical modeling, researching, designing, and development. The software package is supported by most platforms, including Windows, Mac, Unix and Linux.

Modeling offers excellent methods for quantitative and qualitative studies of engineering processes. The costs associated with experiments can be substantially reduced if they are combined with theoretical modeling investigations. Moreover, these investigations provide a better understanding of the methodology required to breakdown a process into its fundamental physical phenomena. Modeling can be used successfully as a design tool for new experiments, or to optimize existing experiments.

In this modeling study, the absorption process of a PAH into SPME poly(dimethylsiloxane) (PDMS) extraction phase from a static aqueous solution, and the simultaneous desorption process of a calibrant into the solution from the extraction phase were simulated. The study provided the concentration distribution of PAH in both extraction phase and sample solution, and demonstrated the kinetic calibration method for both fiber extraction and thin film extraction by modeling. In addition, this study simulated the mass transport process of the PAH in a flow through system and a complex aqueous matrix, and also illustrated the symmetry of the absorption and desorption in both systems. Kinetic calibration method was used to calculate the total concentration of the analyte in the sample with the presence of binding matrix.

2.2 Modeling

2.2.1 Model Setup

Commercially available COMSOL version 3.4 includes 8 modules organized into a

unifying multiphysics simulation environment. The software was applied on a desktop computer under a Windows XP operating system with Intel Celeron processors 2.40 GHz and 1.25 GB RAM support. The software developer recommends that general system requirements are at least 1 GB of memory, Pentium III or later, and a graphics card with at least 32 MB of memory. The software installation went smoothly without any problems from DVD media. During the installation, a license file from the COMSOL was needed. The actual disk space used varied with the size of the partition and the optional installation of online help files. All the functions of COMSOL with Chemical Engineering (CE) Module were conducted under the aforementioned platform. The software was stable: it did not crash once while being used.

The model setup was tailored by defining a series of PDEs to describe the simulated physical phenomena. All the components of the constructed model can be accessed and edited in a panel (Model Tree). The COMSOL simulation environment facilitates all steps in the modeling process with a graphical user interface containing:

- Drawing tools (Computer-Aided Design (CAD) tools) for geometry definition;

- Equation formulations;

- Meshing tool for automatic meshing of the domain;

- Automatic solver;

- Post-processing tools for plotting and manipulation of the solution.

COMSOL supplies certain predefined Multiphysics-application templates (i.e., specialized PDE interfaces or problem type) to cover many common problems. There are options for different physics from the Multiphysics menu and opportunities to define the

interdependencies.

In this study, the Chemical Engineering Module was used. It can handle time-dependent and stationary problems for one-dimensional (1D), two-dimensional (2D), and three-dimensional (3D) systems with axis-symmetry for 1D and 2D. The predefined physics in the CE Module is well suited for chemical systems with respect to fluid flow, chemical composition, separation processes, chemical reactors and temperature as a function of space and time. It consists of a number of modeling interfaces for the modeling of laminar and turbulent fluid flows, multiphase flow, multicomponent mass transport, and energy transport in reacting systems. The Chemical Engineering (CE) Module is a popular tool for investigations in energy conversion (for example: fuel cells and combustion processes); applications such as microlaboratories in biotechnology; and in the development of sensors and equipment for analytical chemistry. In our research, mass transport and momentum transport were simulated using the CE Module to study the kinetics of SPME process.

During the solution, the solver is very stable. Both triangular and rectangular finite elements are supported, with a range of direct and indirect solver options, including geometric multi-grid techniques. The COMSOL modeling tool supports multicore processors and uses as many processor cores as are available in a computer, in order to decrease the time required to run a model. Our modeling supported a variety of postprocessing options, such as: plots of contours and streamlines; particle tracing; animations in GIF format; or, all of the results can be exported into text to postprocess in third-party software.

2.2.2 Geometry, Parameters and Mesh

Figure 2-1 shows the configuration for direct fiber extraction. Assuming that there are no angular gradients present in the SPME fiber, a two-dimensional axis-symmetric geometry approximation (instead of 3D geometry), was built to save the computational time. In the thin film extraction, because of the film's symmetry, the process was simulated using a 2D approximation as well (that is, assuming the concentrations are constant on the film surface and varied along the thickness). The rectangular thin film is 1 cm x 1 cm, with a thickness of 7 μm. Figure 2-2 describes the simplification from 3D to 2D, and Figure 2-3 shows the configuration used in the simulation of thin film extraction.
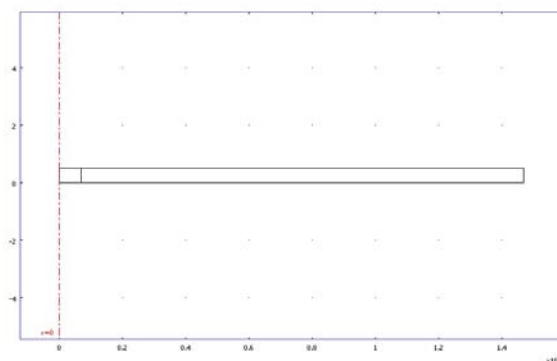
Figure 2-1 Configuration used in simulation of fiber SPME
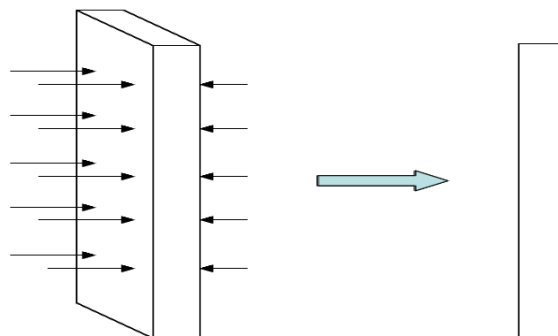
Figure 2-2 Model geometry reduction from 3D to 2D
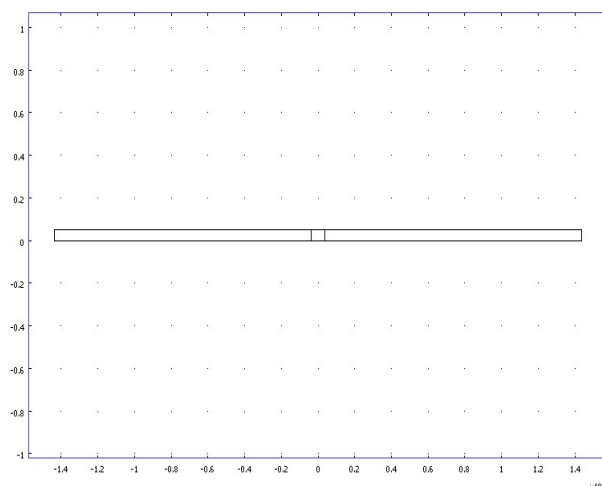
Figure 2-3 Configuration used in simulation of thin film extraction

In our study, the target analyte is the PAH compound, pyrene. As shown in Figure 2-1 and Figure 2-3, the sampling system is divided into two distinct sub-domains: (1) the extraction phase (PDMS fiber or thin film), which is completely surrounded by the target environment; (2) the large volume of aqueous solution environment. The surrounding environment is considered to be a square area that contains the main parts of the setup.

Table 2-1 describes the physicochemical properties of the extraction phase and sample. In the kinetic calibration method, the analyte and the calibrant preloaded in the extraction phase, have the same diffusion coefficient and partition coefficient values. In both fiber and thin film extraction, all the properties were set the same except for their geometries. For comparative purposes, this study used two thicknesses of thin film: 7 μm and 127 μm. The concentrations in the following table are the initial values; these parameters must be inputted before solving the problem.

Table 2-1 Physicochemical properties of extraction phase and sample

Name	Expression	Description
δ (μm)	7	Thickness
T	298	Temperature
K	44668	Partition coefficient
D_f (m^2/s)	1.5e-11	Diffusion coefficient in fiber
D_s (m^2/s)	6.6e-10	Diffusion coefficient in sample
C_s (mol/ m^3)	1.5e-4	Concentration of analyte in sample
C_c (mol/ m^3)	0.75	Concentration of calibrant in fiber
M	10000	Stiff-spring velocity

Free mesh parameters were set as the following: In the static sample system, the maximum element size is 8×10^{-6} m; the number of elements in base mesh is 105; the number of boundary elements is 51. In the flow through system, the maximum element size is 1.6×10^{-3} m; the number of elements in base mesh is 1566; the number of boundary elements is 94. After meshing based on these parameters, the elements were refined once.

2.2.3 Governing Modes and Equations

In the aqueous phase, the analyte (or calibrant) is transported by diffusion and convection, whereas in the extraction phase, diffusion is the only transport mechanism. Therefore, the fundamental governing modes and equations used to calculate the concentration distribution numerically are: convection and diffusion of the analyte (or

calibrant) in the sample; diffusion of the analyte (or calibrant) in extraction phase; and

Brinkman equation mode for modeling flows in porous media.

2.2.3.1 Convection and Diffusion Mode

In the Diffusion application mode as well as the Convection and Diffusion application

mode, Fick's law describes the diffusive transport in the flux vector. Fick's law is adequate

when the diffusing species is dilute with respect to a solvent. Assuming a binary mixture

of solute A in solvent B, concentrations of up to 10 mol% of A can be considered dilute.

The mass balance equation used in the Convection and Diffusion application mode is

given by:

$$\frac{\partial C_s}{\partial t} + \nabla \cdot (-D_s \nabla C_s) = -\mathbf{u} \nabla \cdot C_s \qquad \text{Equation 2.4}$$

where C_s is the concentration of analyte (or calibrant) in the aqueous sample (mol/m^3), D_s

is its diffusion coefficient in the sample (m^2/s), and $\mathbf{u}$ is the velocity vector (m/s).

The first term on the left-hand side of the equation corresponds to the accumulation of

species in the system. The second term describes the diffusional transport, accounting for

interaction between the dilute species and the solvent. The term on the right side

corresponds to transport due to convection, due to a velocity field $\mathbf{u}$.

2.2.3.2 Diffusion Mode

The Diffusion application mode is appropriate when convection does not contribute to

mass transport. The application mode sets up the following equation:

$$\frac{\partial C_f}{\partial t} + \nabla \cdot (-D_f \nabla C_f) = 0 \qquad \text{Equation 2.5}$$

where C_f is the concentration of analyte (or calibrant) in the extraction phase (mol/m³),

and D_f is its diffusion coefficient (m²/s).

2.2.3.3 Brinkman Equation Mode

The Brinkman equations describe flows in porous media, for which the momentum

transport within the fluid due to shear stresses is important. This mathematical model

extends Darcy's law to include a term that accounts for the viscous transport in the

momentum balance, and it treats both the pressure and the flow velocity vector as

independent variables. They can be expressed as:

$$\frac{\rho}{\varepsilon}\frac{\partial \mathbf{u}}{\partial t} + \frac{\eta}{\kappa}\mathbf{u} = \nabla \cdot \left[-p\mathbf{I} + \frac{1}{\varepsilon}\left\{ \eta(\nabla \mathbf{u} + (\nabla \mathbf{u})^T) - (\frac{2}{3}\eta - \kappa_{dv})(\nabla \cdot \mathbf{u})\mathbf{I} \right\} \right] + \mathbf{F} \quad \text{Equation 2.6 (a)}$$

$$\frac{\partial}{\partial t}(\varepsilon\rho) + \nabla \cdot (\rho\mathbf{u}) = 0 \quad \text{Equation 2.6 (b)}$$

where η and κ_{dv} denote, respectively, the dynamic and dilatational viscosities of the fluid

(both in M L⁻¹ T⁻¹), ε is the porosity, and κ is the permeability of the porous medium (L²).

2.2.4 Boundary Conditions

The interface conditions between the liquid and extraction phases for the analyte

concentration are described by the dimensionless partition coefficient, *K*. There are

discontinuities in the concentration profile at the boundaries between the liquid and

extraction phases. To acheive continuous flux over the phase boundaries, a special type of

boundary condition using the stiff-spring method was applied. Instead of defining

Dirichlet concentration conditions according to the partition coefficient *K* (which would

destroy the continuity of the flux), continuous flux conditions were defined at the same

time, to force the concentrations to the desired values:

$$(-D_s \nabla C_s + C_s \mathbf{u}) \cdot n = M(C_f - K_{fs}C_s) \quad \text{at} \quad \partial\Omega s / f \qquad \text{Equation 2.7}$$

$$(D_f \nabla C_f) \cdot n = M(K_{fs}C_s - C_f) \qquad \text{at} \quad \partial\Omega f / s \qquad \text{Equation 2.8}$$

Here, M is a (nonphysical) velocity large enough to let the concentration differences in the brackets approach zero. These boundary conditions also give a continuous flux across the interfaces; provided that M is sufficiently large.

2.3 Results and Discussion

2.3.1 Static Aqueous Solution

2.3.1.1 Kinetic Calibration in Fiber SPME

2.3.1.1.1 Desorption

In equations 2.1 to 2.3, the amount of an analyte remaining on the fiber decreases exponentially with time during the desorption process. The desorption rate is determined by the parameter a. To validate the theoretical description of the desorption of an analyte from a SPME fiber by simulation, a 7 μm PDMS fiber (7 μm PDMS fibers were used throughout the experiments, unless otherwise specified) was loaded with pyrene and then exposed to the aqueous solution to determine the desorption time profile. According to equation 2.2, ln (Q) changes with desorption time linearly and the slope is ($-a$). Figure 2-4 shows the desorption time profile where log (Q) is used as the y-axis; in this profile, log (Q) is linearly correlated to the desorption time. Thus ln (Q), expressed as log (Q)/log e was also linear to the desorption time, which demonstrates that equation 2.2 is suitable to describe the kinetics of the SPME desorption process.
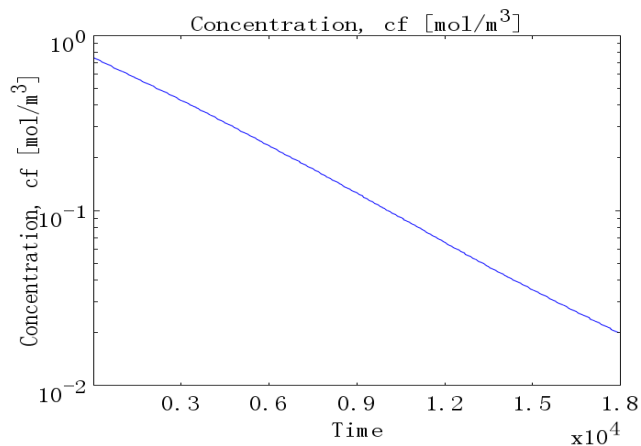
Figure 2-4 Desorption time profile of analyte.

2.3.1.1.2 Absorption versus Desorption

According to equation 2.3, when the constant a, has the same value for the absorption and the desorption, the sum of Q/q_0 (desorption) and n/n_e (absorption) should be 1 at any desorption/absorption time. This model involved the simultaneous determination of the desorption time profile of the calibrant and the absorption time profile of pyrene. A PDMS fiber was loaded with the calibrant, and the fiber was then exposed to a standard pyrene aqueous solution for different extraction times.
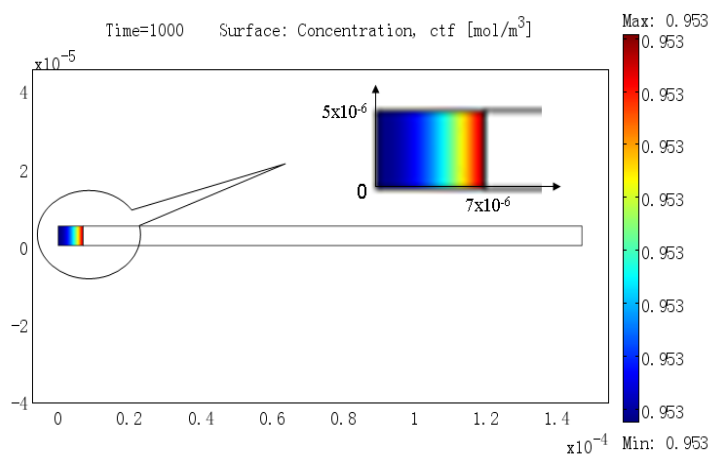
Figure 2-5 (A) Concentration profile of analyte in the fiber coating at t= 1000s.
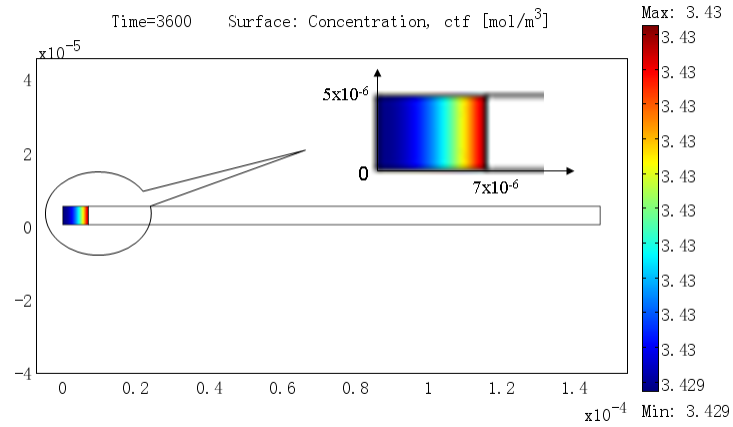
Figure 2-5 (B) Concentration profile of analyte in the fiber coating at t= 3600s.
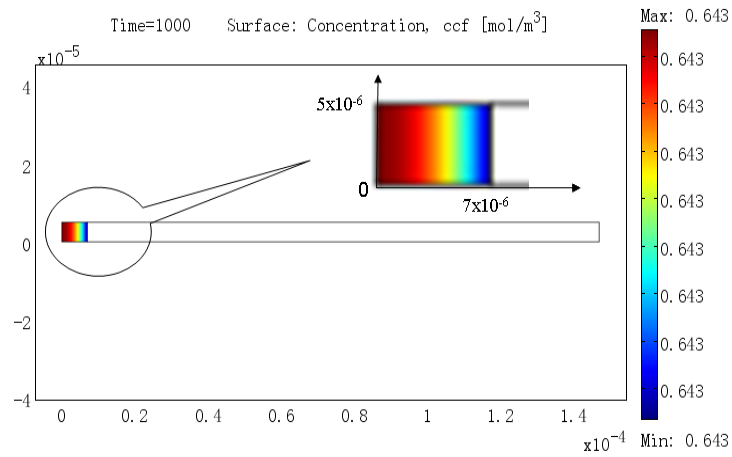
Figure 2-6 (A) Concentration profile of calibrant in the fiber coating at t= 1000s.
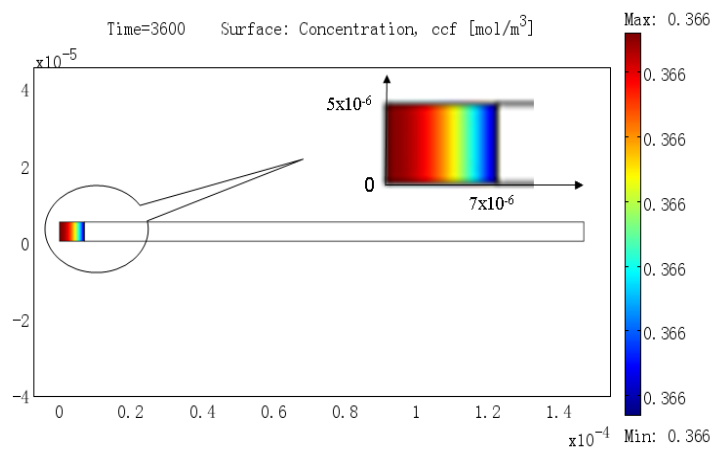
Figure 2-6 (B) Concentration profile of calibrant in the fiber coating at t= 3600s.

Figure 2-5 (A) and (B) display the simulated surface concentration profiles of analyte in the fiber coating at two different extraction time points: 1000 seconds and 3600 seconds. The figures clearly indicate that when the extraction time was longer, more analyte was extracted into the fiber coating. Figure 2-6 (A) and (B) display the concentration profiles of calibrant in the fiber coating at 1000 seconds and 3600 seconds. It is observed along the timeline, that more calibrant was desorbed from the coating into the aqueous phase and less calibrant remained in the coating.

Figure 2-7 presents the values of Q/q_0 (calculated from the resulting desorption time profile of the calibrant), the values of n/n_e (calculated from the resulting absorption time profile of the analyte), and the sum of Q/q_0 and n/n_e. The sum of Q/q_0 and n/n_e at any time was 1.00. It is noted that in the real laboratory, the experimental results of this sum are usually slightly smaller or larger than 1. We ascribed this phenomenon to the slight difference of physicochemical properties between the real calibrant and the analyte. In the simulation by software, the physicochemical properties of the calibrant were set the same as the analyte. However, in the real world, it is very difficult to find a calibrant that has exactly the same physicochemical properties as the analyte. The most frequently used calibrant in the laboratory is a deuterated compound of the target analyte. However, the constant (a) of this deuterated compound was also about 10% larger than that of the analyte. Usually this difference can be corrected by knowing the differences in physicochemical properties between calibrant and target analyte.
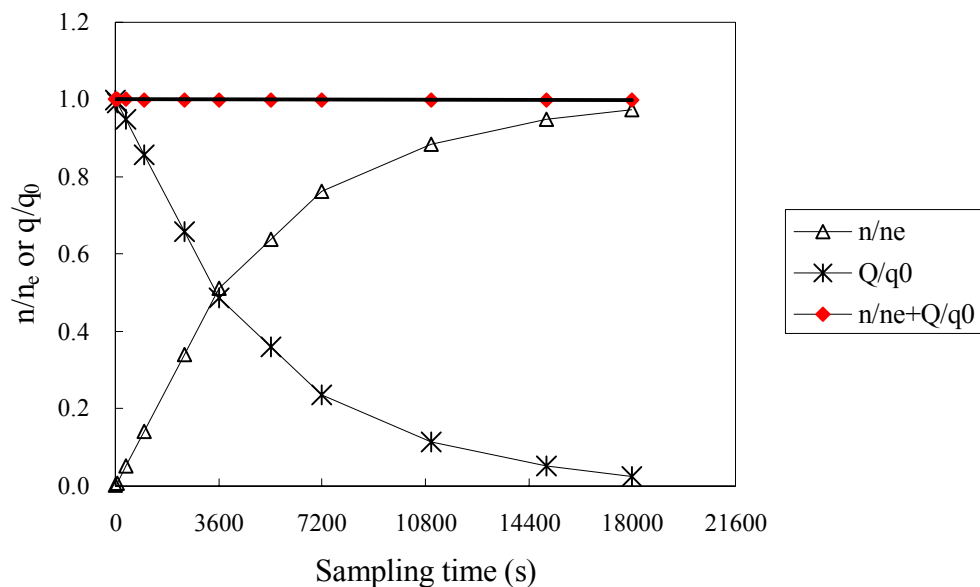
Figure 2-7 Symmetry of absorption and desorption in fiber SPME.

2.3.1.2 Thin Film Extraction

2.3.1.2.1 Kinetic Calibration in Thin Film Extraction

The aforementioned modeling proved the symmetry of the absorption of an analyte onto a fiber and the desorption of a calibrant from the fiber. By knowing the behavior of either the absorption or the desorption, the opposite one can also be understood. The geometry of thin film and fiber is different. A PDMS thin film possessed a high surface to volume ratio, which resulted in the extraction of large amounts of analyte within a short period. A 7 μm PDMS thin film was loaded with the calibrant, and the thin film was then exposed to a standard pyrene aqueous solution for different experimental times.
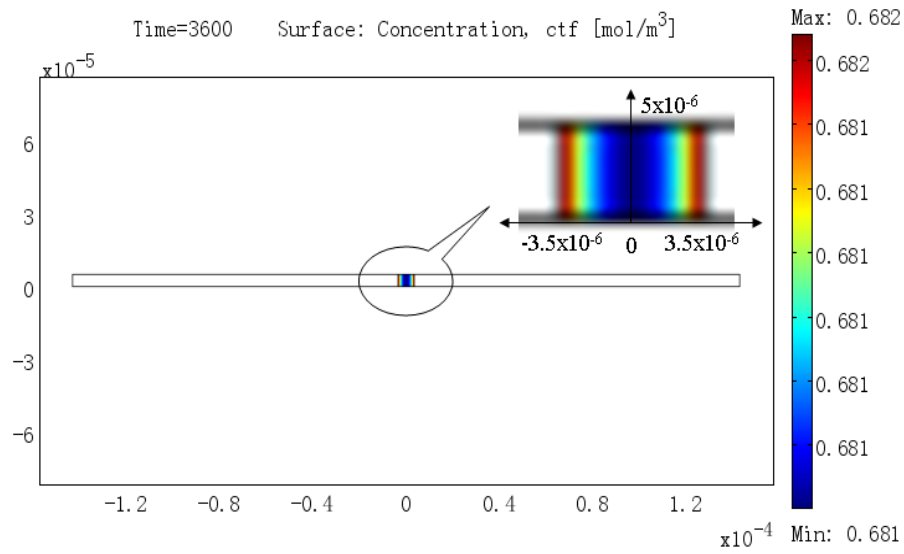
Figure 2-8 (A) Concentration profile of analyte in the thin film at t= 3600 s.
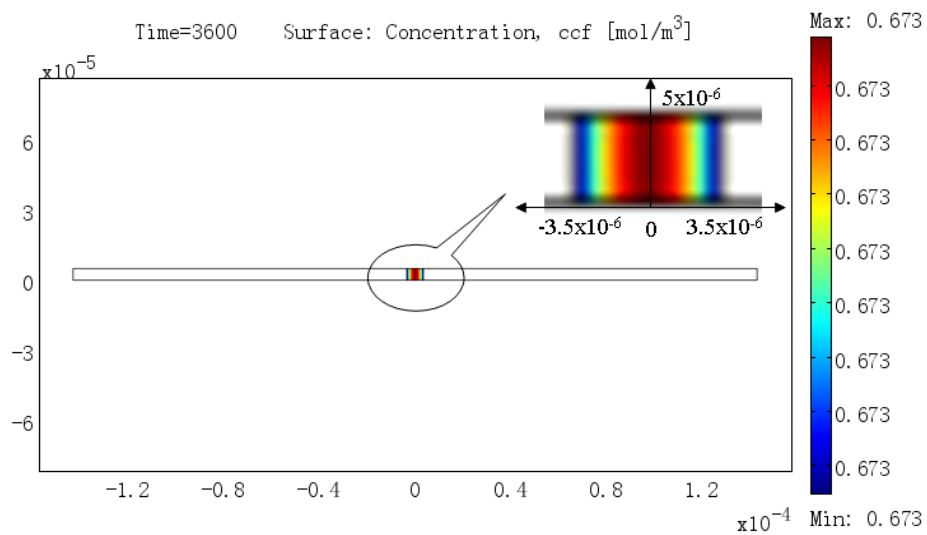
Figure 2-8 (B) Concentration profile of calibrant in the thin film at t= 3600 s.

Figure 2-8 (A) and (B) show the concentration profiles of the analyte and the calibrant in the thin film, when extraction was 3600 seconds. It can be seen at that time, that a part of the calibrant was desorbed from the thin film and a certain amount of the analyte was absorbed onto the thin film. The thin film has two flat sides capable of

accessing the sample solution, rather than a circular surface accessing the solution like in fiber SPME. The result shows that the concentration profiles of the analyte and calibrant in the thin film were bilaterally symmetric.

Figure 2-9 presents the simulated values of Q/q_0 calculated from the desorption time profile of the calibrant, and the values of n/n_e calculated from the absorption time profile of the analyte. The desorption and extraction reached equilibrium at the same time. From the beginning of the extraction until equilibrium, the sum of Q/q_0 and n/n_e at any time was 1.00. These findings demonstrate that the kinetic calibration method is suitable for the thin film extraction. Similarly, as in fiber SPME, the laboratory results of the sum of Q/q_0 and n/n_e in thin film extraction were usually slightly different from 1. It is expected that the deviation would be smaller if an isotopically labeled calibrant with more similar physicochemical properties to the analyte, were used.
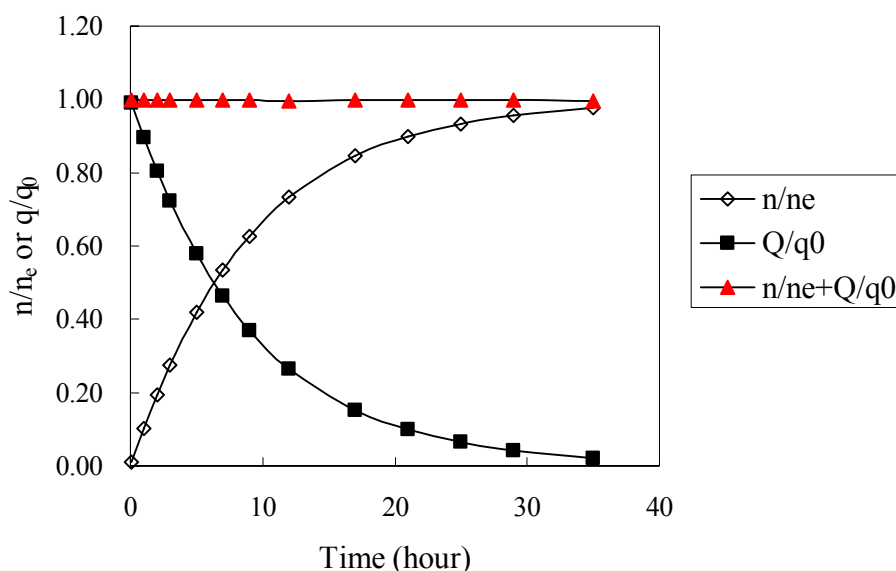
Figure 2-9 Symmetry of absorption and desorption in thin film extraction.

2.3.1.2.2 Effect of Thin Film Thickness on Extraction

In SPME, the time required to reach equilibrium can be estimated by the following equation.[1]

$$t_e = t_{95\%} = B \frac{\delta K_{es}(b-a)}{D_s}$$ Equation 2.9

where δ and (b-a) are the respective thickness of boundary layer and extraction phase; B is a geometric factor; D_s is the diffusion coefficient of analyte in the sample; and K_{es} is the partition coefficient of analyte between the extraction phase and sample.

In equation 2.9, the geometry of the supporting material on which the extracting phase is dispersed affects the equilibration time of extraction. This could be the reason for the difference in equilibrium times for fiber SPME and thin film extraction, with the same thick extraction phase.

It can also be inferred from the above equation, that the equilibrium time depends on the thickness of the extraction phase when the geometry of extraction phase keeps fixed. The effect of the thickness on the extraction performance was simulated by COMSOL. Figure 2-10 (A) and (B) compares the simulated extraction time profiles for pyrene, characterized by two thicknesses of thin film extraction phase as 7 μm and 127 μm from a standard pyrene aqueous solution. After 35 hours, equilibrium was reached for the extraction with the 7 μm thick film. At the same time, the extraction was still in the initial linear extraction region for the 127 μm thick film, which illustrated that the equilibrium time in this case was much longer than 35 hours. The thicker thin film resulted in slower equilibrium, since the analyte needed more time to be transported into the extraction phase.
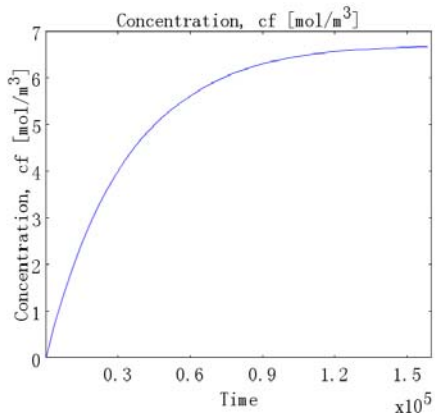
(A)   (B)
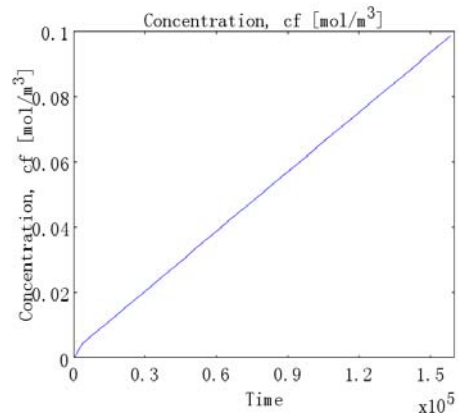
Figure 2-10 Extraction time profiles of analyte in thin film extraction with a thickness of
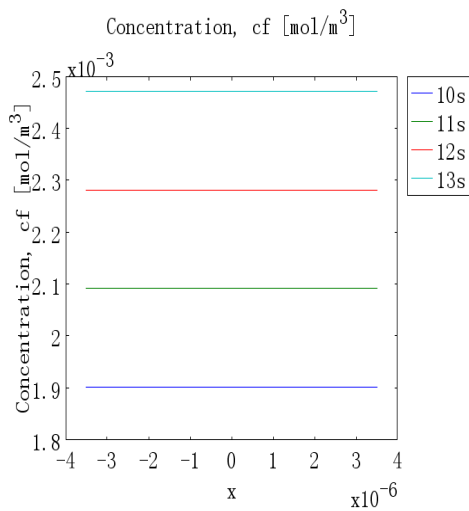
7μm (A) and 127 μm (B).

(A)   (B)
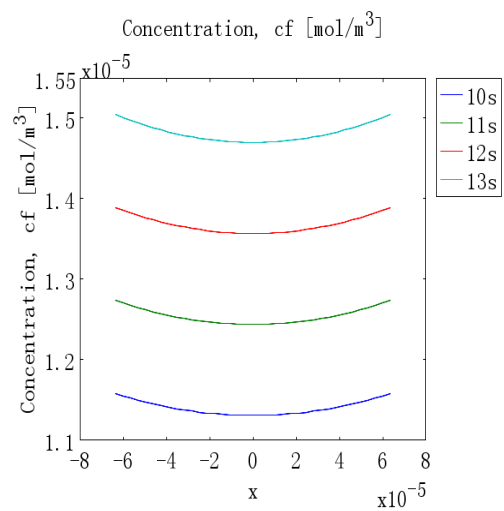
Figure 2-11 Concentration distribution profiles of analyte in thin film with a thickness of

7 μm (A) and 127 μm (B) at different extraction times from 10 s to 13 s.

Figure 2-11 (A) and (B) compares the concentration distribution in thin film with two

different thicknesses at different extraction times at the beginning of extraction. The figure

clearly indicates the process of diffusion of the analyte into the thin film along with the timeline. As expected, there was no concentration gradient in the thin extraction phase, compared to an obvious gradient in the thick extraction phase. For the latter, the concentration of analyte close to thin film/sample interfaces were higher than the concentration in the interior of thin film.

2.3.2 Flow through System

Although the symmetry of the absorption and desorption for static aqueous solution was demonstrated by modeling, there is still a problem associated with using the kinetic calibration method to calibrate the flowing system in practice. Therefore, the SPME extraction in a flow through aqueous system was investigated. The flow was introduced from the left side and exited from the right side. The extraction phase was a 100 μm thick fiber coating, which was coated onto an inner-fused silica fiber. The initial concentration in the flow through system was 9.9×10^{-6} mol/m^3. The other physicochemical properties of analyte (pyrene), calibrant and sample matrix were the same as in the model discussed before.

Figure 2-12 shows the concentration distribution around the fiber coating in the flow through system when extraction time is at 24 hours. In the profile, a SPME fiber is exposed to a fluid sample whose motion is normal to the axis of the fiber. The fluid is brought to rest at the forward stagnation point, from which the boundary layer develops along the surface of coating. The thickness of the boundary layer is at a minimum at the forward stagnation point. A wake is formed downstream, where flow is highly irregular

and can be characterized by vortex formation.
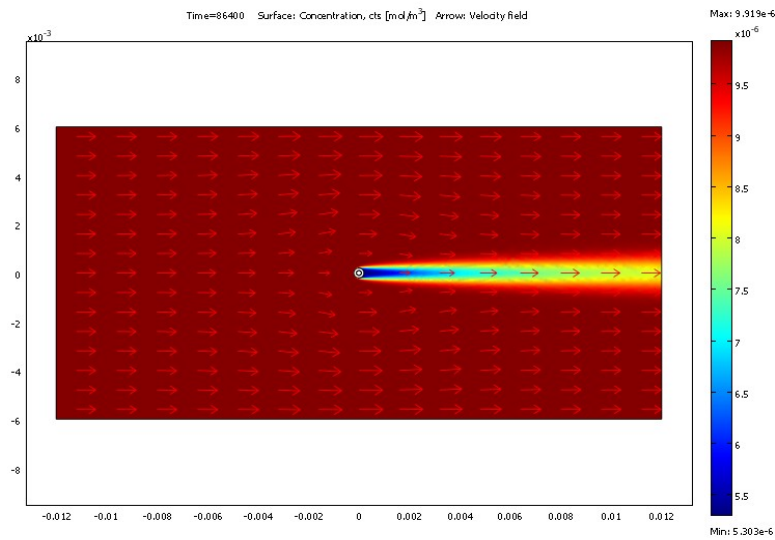
Figure 2-12 Concentration distribution profile of analyte around the fiber coating in the flow through system at t= 24 hour. Arrows symbolize the flow velocity vector.
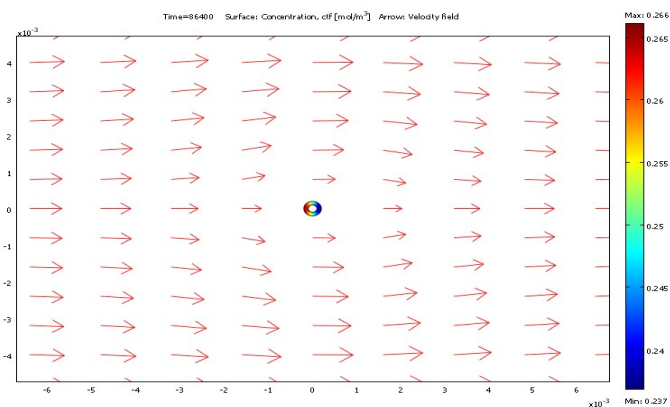
Figure 2-13 Concentration distribution profile of analyte in the fiber coating in the flow through system at t= 24 hour.

Figure 2-13 shows a concentration gradient in the fiber coating developed from the left side to the right side along the flow direction of the sample solution. Because the

thickness of boundary layer was lower at the forward stagnation point than in the wake, the mass transfer rate was reduced along the surface of the coating, resulting in lower concentration in the right side than in the left side. Figure 2-14 illustrates symmetry of absorption and desorption in a flow through system. The concentration in the fiber coating was calculated as the average concentration across the coating. The sum of Q/q_0 and n/n_e at any time was 1.00.
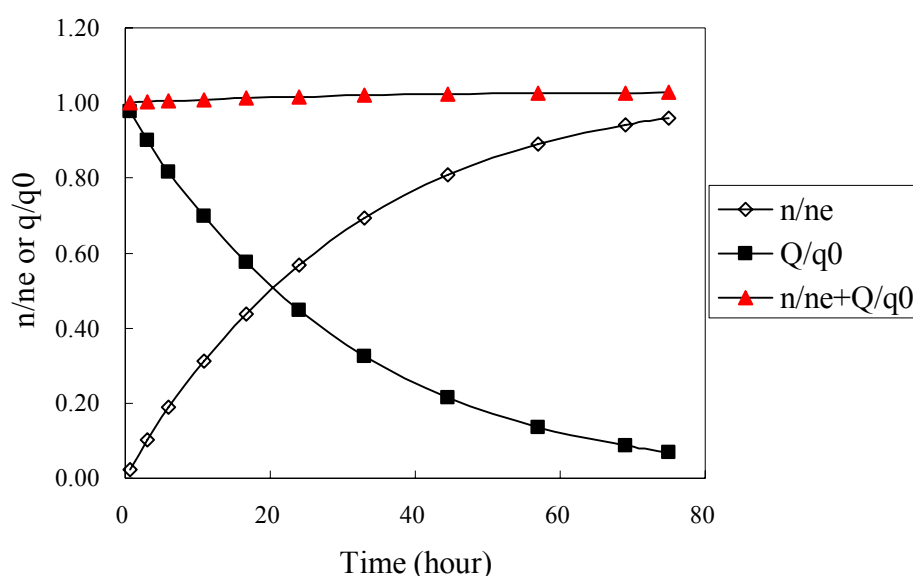
Figure 2-14 Symmetry of absorption and desorption in fiber SPME in flow through system.

2.3.3 Complex Aqueous Matrix

2.3.3.1 Simulation for Kinetic Calibration

Humic organic matters (HOM) comprise complex amorphous mixtures of highly heterogeneous, chemically reactive yet refractory molecules. The measurement of organic pollutant concentrations in solution with the presence of HOM is complex, because the

pollutants and HOM interact. The association and dissociation between the freely dissolved analyte and the binding matrix in the sample is expressed as:

$$S + B \rightleftarrows SB$$
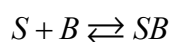
where S is freely dissolved analyte, B is binding matrix, SB is bound species.

A 7 μm PDMS fiber was preloaded with calibrant and then exposed to a sample matrix with the presence of HOM. The concentration of binding matrix was much higher than the pyrene concentration. Presence of a binding matrix could affect extraction kinetics of SPME. The symmetry of the absorption of analyte from the sample matrix and the desorption of calibrant from the fiber coating was investigated and it was further applied to calculate the total concentration of analyte in the system.
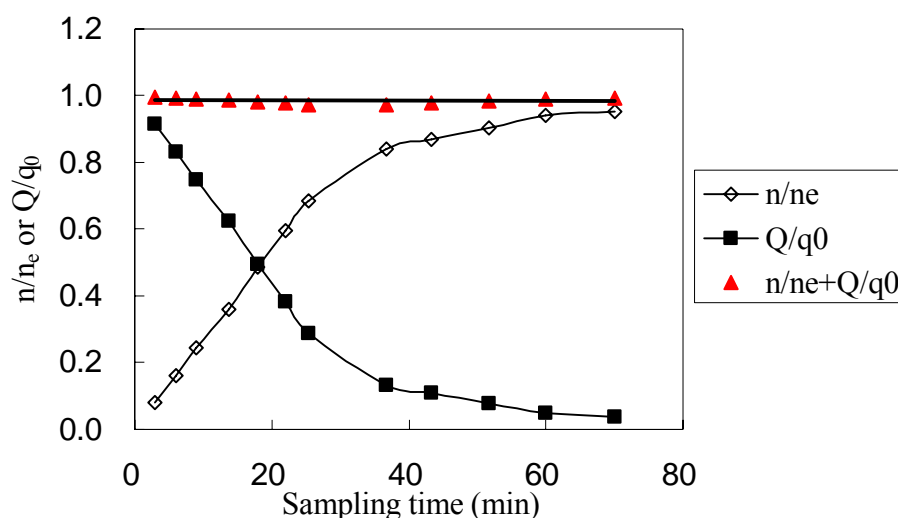
Figure 2-15 Symmetry of absorption and desorption in fiber SPME in complex sample matrix.

Figure 2-15 validates the symmetry of absorption and desorption in the sample with the presence of binding matrix. The sums of Q/q_0 and n/n_e were 1.0 at different extraction

times. Partition coefficient (K_e) in this complex sample matrix was determined based on external calibration method and proved much lower than the partition coefficient in pure sample. Combining the kinetic calibration method and determined partition coefficient, the total concentration of pyrene rather than free concentration of pyrene was calculated.

2.3.3.2 Comparison with Experimental Results

The laboratory experiment was completed by exposing a PDMS fiber loaded with deuterated pyrene to a pyrene solution with the presence of humic acid. Although the sums of Q/q_0 and n/n_e were close to 1, deviation of the sum from 1 could be ascribed to not only the difference of physicochemical properties between deuterated pyrene and pyrene, but also the experimental errors introduced by the complex sample matrix. The spiked pyrene concentration in the sample matrix is 30 ppb. The predicted total concentration of pyrene using kinetic calibration method was 26.8 ppb. It is quite comparable to the spiked concentration considering the complexity of the sample matrix.
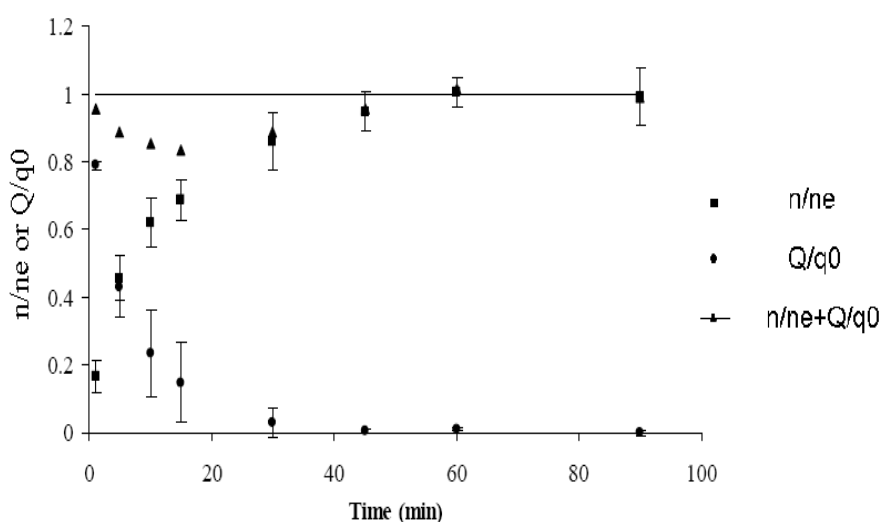
Figure 2-16 Experimental results: absorption and desorption in fiber SPME in complex sample matrix.

48

2.4 Conclusion

This study shows the applicability of modeling and simulation in the area of calibration of SPME processes. The kinetics of fiber SPME and thin film extraction in static aqueous solution and flow through system were simulated by COMSOL Multiphysics. The symmetry of absorption of analyte onto the fiber (or thin film) and desorption of calibrant from the fiber was demonstrated by modeling. The kinetic calibration method illustrated feasibility in both fiber SPME as well as thin film extraction. Furthermore, the symmetry of absorption and desorption in SPME was demonstrated in the sample with the presence of binding matrix, which allows for successful calibration of total concentration of analyte in complex sample matrix.

Chapter 3

Rapid Spot Water Sampling Using Thin Film

3.1 Introduction

Solid phase microextraction (SPME) has become suitable for different types of analytes and samples in both laboratory and field applications. [1-6] In the SPME process, the movement of analytes follows a concentration gradient according to Fick's first law of diffusion. The fluid contacting the extraction phase's surface is always stationary. To model mass transport, the gradation in fluid motion and convection of molecules in the space surrounding the extraction phase can be simplified by Prandtl boundary layer. [1] Thin film is a new format of SPME that differs from the coated fiber format. [7] PDMS thin films have a high surface-to-volume ratio, which gives them a high extraction efficiency and sensitivity without sacrificing analysis time. [7]

Significant analytical chemistry effort is currently directed at developing suitable methods to facilitate on-site analysis. [8-10] Performing sample preparation on site has some advantages, since analytes are more stable in the extraction phase compared to the natural matrix. [10] As a sampling technique used to load samples on site, passive sampling is based on the free flow of analyte molecules from the sampled medium to a collecting medium as a result of a difference in chemical potential. [11] Passive sampling devices allow long-term monitoring of pollutant levels in aquatic systems. [12-14] An alternative approach to environmental analysis involves performing spot sampling to measure contaminant levels in water at the moment of sampling. [10] Rapid sampling and sample preparation is therefore

necessary. When rapid spot sampling is performed, the amount collected by the sampler depends on both sampling rate and exposure time. [11] If exposure time is short (in contrast with one week or one month in long-term monitoring), the sampling rate should be fast enough to achieve high sensitivity for analysis. In passive sampling, because the flow of analytes from the sample into the trap is completely free and follows Fick's first law of diffusion, the sampling rate is controlled by the molecular diffusion coefficient of the analyte and the parameters of the sampler device. [15, 16] Compared with passive sampling, active sampling uses electrically powered equipment and thus requires an energy source. Although an active sampler is more complicated and costly, it is an attractive option because it allows for better control of the sampling rate and is more suitable for rapid sampling.

In the initial phase of sampler exposure, the rate of desorption of analytes from the receiving phase into water is negligible, and the sampler works in the linear uptake regime. [17-20] Rapid sampling happens in this regime. The mass of analyte accumulated in the extraction phase after an exposure time (t) is in direct proportion to the bulk analyte concentration and can be calculated as [17]

$$n(t) = C_s R_s t \hspace{4cm} \text{Equation 3.1}$$

where C_s is the concentration of analyte in the water phase, and R_s is the proportionality constant (sampling rate) and may be interpreted as the volume of water cleared of analyte per unit of exposure time by the sampler. When the sampler is used for on-site sampling, the sampling rate can be determined in the laboratory. If R_s is known, C_s can be calculated from the sampling rate (R_s), the exposure time (t) and the amount (n (t)) of the analyte

trapped by the receiving phase.

This study investigates, both theoretically and experimentally, the application of coupling an electric drill with thin film or SPME fiber as active samplers. The present study aims to design a convenient and effective SPME device as an active sampler for rapid and low-cost on-site sampling.

3.2 Theory

3.2.1 Mass Transfer Associated with SPME Fiber Extraction

3.2.1.1 Cross flow Model

When the motion of the fluid sample is normal in relation to the fiber axis, heat transfer can be translated into a mass transfer solution by replacing temperatures with concentrations, heat with the flux of mass, and thermal conductivity with diffusion coefficient. [21, 22]

The average Nusselt number Nu can be calculated with equation 3.2. [23, 24]

$$\overline{Nu} \equiv \overline{h}d / D_s = ERe^m Pr^{1/3} \qquad \text{Equation 3.2}$$

where $\overline{h}$ is the average mass-transfer coefficient, d is the outside diameter of the fiber, and D_s is the diffusion coefficient. Re is Reynolds number ($Re= ud/ v$), u is the linear velocity of the sample, and v is the kinematic viscosity of the matrix media at the extraction temperature. The fluid's linear speed is calculated as the angle speed of the rotation $\omega \times$ rotating radius. Pr, the Prandtl number of the liquid, equals v/D_s. Constant E is 0.989 and constant m is 0.33 under the experimental conditions. [23, 24] Once $\overline{h}$ is known, the amount of extracted analytes n during sampling period t can be calculated by equation

3.3:

$$n = \bar{h} A C_s t$$ <div align="right">Equation 3.3</div>

where A is the surface area of fiber, C_s is the bulk analyte concentration. Equation 3.3 is used to calculate the theoretical values of the amount extracted by the fiber based on the cross flow model.

3.2.1.2 Boundary Layer Model

The agitation conditions and sample viscosity determine the boundary layer thickness:[1]

$$\delta = 2.64 \frac{b}{Pr^{0.43} \sqrt{Re}}$$ <div align="right">Equation 3.4</div>

where b is radius of the fiber.

The theoretical values of the initial extraction rate by fiber, based on the boundary layer model, can be estimated with

$$dn / dt = (D_s A / \delta) C_s$$ <div align="right">Equation 3.5</div>

3.2.2 Mass Transfer Associated with Thin Film Extraction

When the 5 cm^2 thin film is rotated around its axis vertically below the fluid surface (Figure 3-1 (A)), the relative motion of the thin film and fluid can be regarded as the composite result of both parallel and perpendicular directions.

(A)   (B)
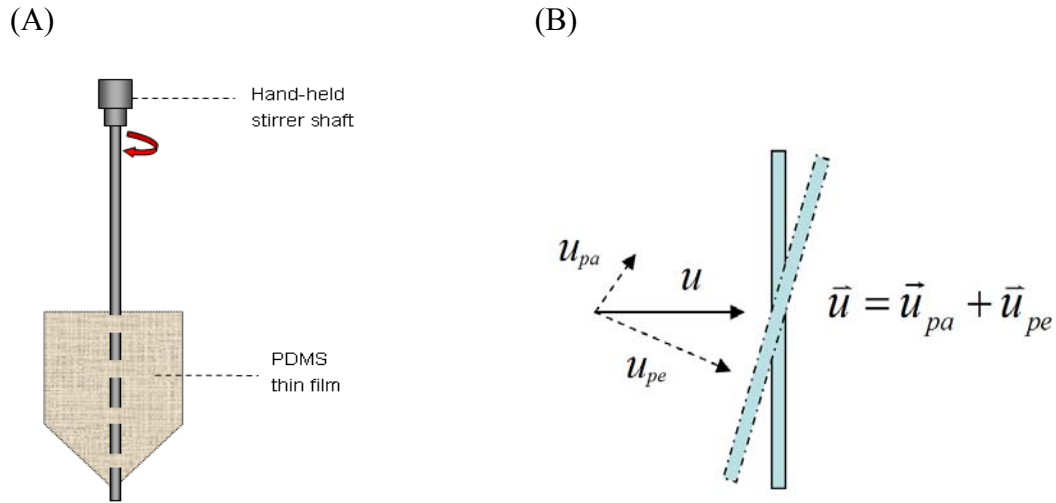
Figure 3-1 Rotated thin film sampling.

If a little portion of the thin film at any time t is considered, then the fluid flows past it

at a velocity vector $\vec{u}$. In Figure 3-1 (B), when thin film rotates a small angle,

$$\vec{u} = \vec{u}_{pa} + \vec{u}_{pe}$$ Equation 3.6

where $\vec{u}_{pa}$ is the velocity vector parallel to the thin film plane, and $\vec{u}_{pe}$ is the velocity

vector perpendicular to the thin film plane.

The mass transfer in the thin film extraction process is associated with the relative

motion of the thin film and the fluid. For this reason, at any time t, the mass loaded from

fluid to the little portion of film can be divided into parallel and perpendicular parts

(equation 3.7):

$$M = M_{pa} + M_{pe}$$ Equation 3.7

where M_{pa} is the mass loaded into the little portion of film by parallel motion of the

fluid to the thin film plane, and M_{pe} is the mass loaded into the little portion of film by

perpendicular motion of the fluid to the thin film plane. Therefore, the total mass uptake

from the fluid to the whole thin film can be expressed as:

$$\sum M = \sum M_{pa} + \sum M_{pe} \qquad\qquad \text{Equation 3.8}$$

In other words,

$$n = n_{pa} + n_{pe} \qquad\qquad \text{Equation 3.9}$$

where n is the amount extracted by the thin film after extraction time t, n_{pa} is the total

mass uptake by parallel mass transfer, and n_{pe} is the total mass uptake by perpendicular

mass transfer.

The theoretical descriptions of separate perpendicular mass transfer process and

parallel mass transfer process are complicated. However, empirical correlations are readily

available. [24] The mathematics of diffusion and heat transfer are equivalent because both

processes are described by Laplace's equation. The formula for heat transfer can be used

for mass transfer by substituting diffusion coefficients for thermal conductivity and

diffusivity constants. [25]

The relationships for predicting Nusselt numbers for laminar flow and turbulent flow

parallel to the film plane are described as follows. [24]

$$\overline{Nu}_{laminar} = 0.648 \, Re^{1/2} \, Pr^{1/3} \qquad\qquad \text{Equation 3.10}$$

$$\overline{Nu}_{turbulent} = 0.0366 \, Re^{4/5} \, Pr^{1/3} \qquad\qquad \text{Equation 3.11}$$

where Re is Reynolds number ($Re= ud/ v$), u is the linear velocity of the sample, and v is

the kinematic viscosity of the matrix media. Pr, the Prandtl number of the liquid, equals

v/D.

Substituting equation 3.2 into equation 3.3,

$$n = (\frac{\overline{Nu}D}{d}) AC_{bulk} t \qquad\qquad \text{Equation 3.12}$$

The above equation in combination with equation 3.10 and equation 3.11 can be used

to calculate the mass loaded into the thin film by parallel mass transfer process after extraction time t:

$$n_{pa} = \left[(0.648\,\mathrm{Re}^{1/2}\,\mathrm{Pr}^{1/3} + 0.0366\,\mathrm{Re}^{4/5}\,\mathrm{Pr}^{1/3}) \frac{D}{d} \right] AC_{bulk}t \quad \text{Equation 3.13}$$

The empirical result of the Nusselt number for perpendicular flow to the film plane is:[24]

$$\overline{Nu}_{pe} = 0.0921\,\mathrm{Re}^{0.675}\,\mathrm{Pr}^{1/3} \qquad\qquad\qquad \text{Equation 3.14}$$

Combining equations 3.12 and 3.14 gives equation 3.15:

$$n_{pe} = 0.0921\,\mathrm{Re}^{0.675}\,\mathrm{Pr}^{1/3} \frac{D}{d} AC_{bulk}t \qquad\qquad \text{Equation 3.15}$$

Using this expression along with equations 3.9 and 3.13, equation 3.9 then becomes equation 3.16

$$n = \left[(0.648\,\mathrm{Re}^{1/2}\,\mathrm{Pr}^{1/3} + 0.0366\,\mathrm{Re}^{4/5}\,\mathrm{Pr}^{1/3}) \frac{D}{d} \right] AC_{bulk}t + 0.0921\,\mathrm{Re}^{0.675}\,\mathrm{Pr}^{1/3} \frac{D}{d} AC_{bulk}t$$

Equation 3.16

Equation 3.16 was used to calculate the theoretical mass uptake by the rotated thin film immersed in the aqueous solution.

3.3 Experimental Section

3.3.1 Chemicals and Supplies

All chemicals were of analytical grade. Methanol (HPLC grade) was purchased from BDH (Toronto, ON, Canada). Polycyclic aromatic hydrocarbons (acenaphthene (Ace), fluorene (Fl), anthracene (Anth), fluoranthene (Fla) and pyrene (Pyr)) were purchased from Supelco (Oakville, ON, Canada). Praxair (Kitchener, ON, Canada) supplied helium

(99.9 %), nitrogen (99.9 %), liquid nitrogen, and compressed air for the analytical instruments. Nano-pure water from a Barnstead water system (Dubuque, IA) was used for all the experiments. The SPME fibers used in all experiments were 100 μm PDMS metal fibers from Supelco (Oakville, ON, Canada). These fibers were conditioned before use for 30 min at 250 °C in a fiber conditioner. PDMS thin films with a thickness of 127 μm were purchased from Specialty Silicone Products Inc (Ballston Spa, NY). A Mastercraft 10" bench drill was used at the 600 rpm setting in the following experiments. A portable 7.2 V Makita drill was applied with a constant agitation speed of 600 rpm. These two drills were purchased in Canadian Tire (Waterloo, ON, Canada). Portable cordless drills are more practical for sampling on site. The controlled speed drill was deemed suitable for field sampling because it is easier to maintain drill rotation at a constant speed.

3.3.2 Thin Film Sampler and SPME Fiber

Initial laboratory experiments in a 10 mL sample involved attaching the SPME fiber or thin film to the bench drill like a drill bit. The thin film was cut into the shape of a house (i.e., a 2 cm × 2 cm square with a 1-cm high triangle on top) and secured to the drill. The surface area for one side was 5 cm^2 and the volume of each thin film was 0.0635 cm^3. Such a thin film sampler was designed to be coiled and fitted inside the liner for injection, taking into consideration the length of the heat zone. Before use, the thin film was conditioned for 1 hour at 250 $^\circ$C in a GC injection port. After extraction, the thin film was removed from the solution, dried with a lint-free tissue, and inserted into the liner. The liner containing the thin film was inserted in the thermal desorption unit for automated

analysis by thermo-desorption.

For laboratory sampling in the 50 L sample, a special "drill bit" (Figure 3-2) was developed for attaching a fiber to the bench drill. Two Teflon disks (created by the University of Waterloo Science Shop, Waterloo, ON, Canada) were attached to a metal shaft using small screws. The fiber could be screwed into the top disk. A small hole in the bottom disk was used to secure the position of the fiber. The top disk was movable and could be adjusted to expose the fiber during sampling or to withdraw the fiber into the needle after use. When the drill was turned on, the fiber rotated and the water was agitated. The Teflon disks prevented the fiber from spinning outward during sampling.
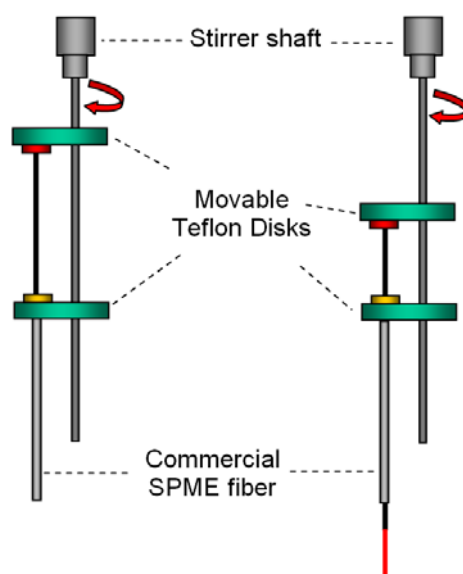
Figure 3-2 Fiber SPME sampler showing the protected position of the fiber before and after sampling and the exposed position during sampling.

3.3.3 Application of Thin Film Sampler for Rapid Sampling on Site

Laurel Creek, a small river located on the University of Waterloo campus (Waterloo, ON, Canada) was chosen to field test rapid sampling using the thin film sampler. The experimental site was about 1 m offshore.

Figure 3-3 On-site sampling of river water using the thin film sampler.

On site sampling with thin film sampler was illustrated in Figure 3-3. The thin film was positioned in the designed copper mesh pocket attached to the handling rod. The sampler was rotated with the portable drill at 600 rpm vertically 0.2-0.5 m below the surface of the water. An extraction time of 5 minutes, a short sampling time in the linear range of uptake by thin film, was used for sampling. After retrieval, the thin film was sealed in the liner and transported to the lab, and then analyzed using the methods described above. To validate the thin film measurement, a water sample from the river was collected separately in a bottle and carried to laboratory. This water sample was treated by SPME fiber direct extraction using standard addition approach. PAHs concentrations were determined by adding a series of known concentrations of PAHs (10 ppb, 20 ppb, 50 ppb) to 10 mL river samples. The original and spiked samples were agitated at 600 rpm (Gerstel Agitator). Extraction lasted 30 min, followed by fiber desorption in GC injector.

3.3.4 Instrument

3.3.4.1 Thin Film Analysis

Gas chromatography was performed on an Agilent 6890 GC and 5973 MSD equipped with a Multipurpose Sampler (MPS 2) system (Gerstel GmbH, Mullheim, Germany). A Thermal Desorption System (TDS-2) unit was mounted on the GC via the Cooled Injection System (CIS-4) inlet for thermal desorption of analytes. The thin film was placed into a liner 187 mm in length, 6 mm O.D., and 4 mm I.D.

A Thermal Desorption Unit (TDU) was used for large volume injection (LVI). The liner with sampler was heated to transfer the compounds of interest into the CIS-4. The CIS acts as cryogenic trapping, focusing and concentrating the compounds to be determined, and then is heated, transferring them to the capillary column. The temperature of the CIS was 0 $^{\circ}$C for the first 5 minutes, during which time the temperature of TDU was increased to 250 $^{\circ}$C and the analyte was desorbed. After desorption, the cooled liner with the thin film was removed from the TDU. At last the temperature of CIS was increased to transfer the analyte to the GC column.

An HR-1 capillary column (30 m, 0.25 mm i.d., 0.25 μm film thickness) (Shinwa, Kyoto, Japan) was used with helium as the carrier gas at a flow rate of 1 mL/min. For the analysis of the PDMS thin film, column temperature was maintained at 40 $^{\circ}$C for 2 minutes, then increased at a rate of 15 $^{\circ}$C/min to 280 $^{\circ}$C, and finally held constant for 2 minutes. Total run time was 20 min. The MS system was operated in electron ionization (EI) mode and tuned to perfluorotributylamine (PFTBA). A mass scan from 40 to 300 was

acquired, and the base peak of each compound was selected and integrated.

Absolute amounts of target analyte were calibrated by the injection of liquid standards. Liquid injection was completed daily. Peak shape quality, resolution, and retention times were carefully monitored to ensure all chromatography was within required specifications.

3.3.4.2 SPME Fiber Analysis

Commercial SPME fibers were analyzed using a Varian 3800 GC coupled with a Saturn 4000 ion trap-MS system. Separation was performed using a RTX-5 column (30 m, 0.25 mm i.d., 0.25 μm film thickness) (Restek, Bellefonte, PA, USA). The column was initially set at 40 °C, held constant for 2 min, then ramped at 15 °C/min to 250 °C, and finally held at this temperature for 4 min; total run time was 20 min.

3.4 Results and Discussion

3.4.1 Extraction by Thin Film and Fiber under Controlled Agitation Conditions in a 10 mL Sample

The PDMS thin films are very solid and reproducible when handled properly. Their lifetime has not yet been determined, but a single thin film can be used more than 20 times with no significant difference in the results. The cost of making each device is very small, so these thin films can even be used for single-use samplers.

Figures 3-4 (A) and (B) show the extraction time profiles determined using the bench drill with the thin film and fiber, respectively. For each direct extraction, 10 mL of PAHs aqueous solution (1 ppb) was added to a 10 mL vial, which immobilized with ring stands

and clamps. The fiber or the thin film was rotating with the bench drill at 600 rpm.

The time required to reach equilibrium increased with the thickness of the PDMS extraction phase. [1] The thickness of the thin film device is only 63.5 μm (thin film has two sides, so the extraction thickness is 127 μm/2 = 63.5 μm), and the fiber's extraction phase is 100 μm thick. The results show that the required length of equilibrium time was shorter for the thin film (10 min) than for the fiber (20 min).

(A)
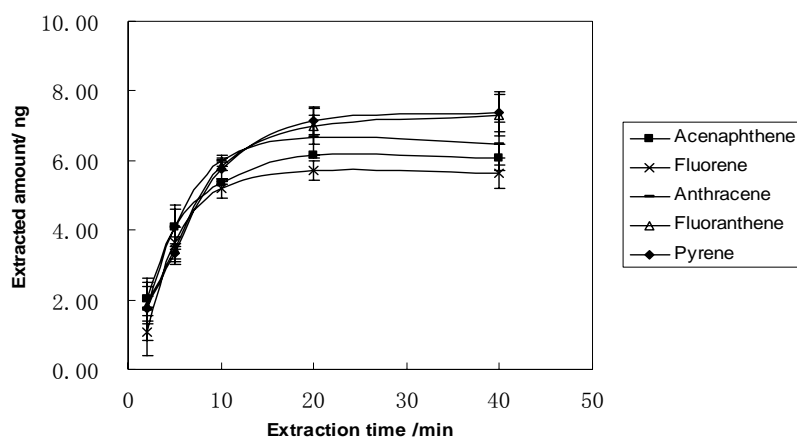
(B)
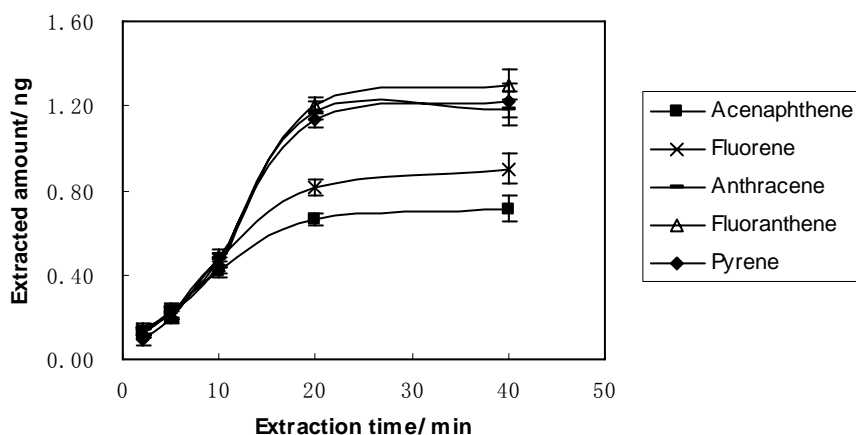
Figure 3-4 Extraction time profiles of PAHs in 10 mL samples using a bench drill coupled with (A) a thin film and (B) a fiber.

The amount of analyte extracted at equilibrium can be expressed by equation 3.17:

$$n = \frac{K_{es}V_sC_sV_e}{K_{es}V_e + V_s}$$ Equation 3.17

where n is the amount of analyte extracted, V_e is the volume of the extraction phase, V_s is the sample volume, K_{es} is the analyte's partition constant between the extraction phase and sample matrix, and C_s is the initial concentration of analyte in the matrix. The amount of analyte in the thin film extraction phase at equilibrium was much greater than that in the fiber (Figure 3-4). The thin film has a higher extraction phase volume than the fiber, and therefore the sensitivity of thin film was higher.

The volume of a thin film ($V_e = 63$ μL) is 100 times greater than that of a fiber ($V_e = 0.63$ μL). However, the amount of analyte extracted by the thin film was less than 100 times greater than that obtained by the fiber. This difference can be explained by the small sample volume and relatively large thin film volume used for extraction. According to equation 3.17, the extracted amount (n) is only directly proportional to the V_e when the $K_{es}V_e$ is negligibly smaller than V_s. Because of the larger extraction phase to sample volume ratio in this study, $K_{es}V_e$ in the denominator of equation 3.17 could not be ignored; thus, the amount (n) was not linearly proportional to the volume of the extraction phase. For the same reasons, analyte concentrations left in the vial during the thin film extraction decreased with extraction time. On the other hand, the fraction of extracted analytes increases with the ratio of $K_{es}V_e$ to V_s. Therefore most of the analytes in the system will be extracted in small sample volume when partition coefficient of the analyte is relatively high. This was observed in such a small system as the 10 mL sample: two PAHs with

higher K_{es} (fluoranthene and pyrene) were mostly extracted by the thin film.

Table 3-1 Theoretical calculations of fiber extraction of PAHs in a 10 mL sample (for 5 min extraction) and experimental results. n_1: Boundary layer model; n_2: Cross-flow model.

Analyte	Re	Pr	δ (cm)	$\bar{h}$ (cm/s)	n_1 (theoretical, ng)	n_2 (theoretical, ng)	n (experimental, ng)
Ace	3.533	1406	0.000989	0.00374	0.194	0.112	0.225±0.018
Fl	3.533	1475	0.000969	0.00362	0.189	0.109	0.221±0.0049
Anth	3.533	1525	0.000955	0.00354	0.185	0.106	0.220±0.010
Fla	3.533	1607	0.000934	0.00342	0.180	0.103	0.217±0.012
Pyr	3.533	1607	0.000934	0.00342	0.180	0.103	0.197±0.014

Table 3-1 shows theoretical mass uptake by the fiber based on the cross-flow model and boundary layer model in a 10 mL sample for 5 minutes. The surface area of the fiber is 10 mm^2. The results of boundary layer model were similar to the experimental values. However, the cross flow model underestimated the amount of extracted analytes. There are two possible reasons for this low prediction. Firstly, the fiber was vibrating, so a higher sampling rate may have resulted from faster relative movement between the fiber and water. Secondly, the model assumed that the motion of the fluid sample was normal in relation to the axis of the fiber, a condition not observed in the experiments. In the boundary layer model, the extraction rate of a compound is proportional to its diffusion coefficient. In Figure 3-4 (B), the fiber extracted a slight more amount of the low

molecular weight (M_w) PAHs than high melocular weight PAHs after 2 min. The higher

diffusion coefficient of the low M_w PAHs might explain this phenomenon.

Because analyte concentrations decreased during sampling, a 10 mL sample was not

sufficient for validating the proposed mass uptake model of the thin film.

3.4.2 Extraction by Thin Film and Fiber under Controlled Agitation Conditions in a 50 L Sample

To minimize depletion of analytes during extraction by thin film in a small sample

volume, a large spherical bottle filled with 50 L of PAHs aqueous solution was used. The

PAH concentrations in the 50 L sample were determined by SPME direct extraction. Ten

milliliters of the sample was collected and agitated at 500 rpm (Gerstel Agitator). The

extraction was lasted 30 min, followed by fiber desorption in the GC injector. External

calibration method was used and the average concentrations of acenaphthene, fluorene,

anthracene, fluoranthene and pyrene were 1.1, 1.7, 0.6, 5.7 and 5.6 µg/L, respectively.

Figure 3-5 shows the extraction time profiles for the thin film (A) and fiber (B). As

expected, at equilibrium the amounts of analytes extracted by the thin film are higher than

those extracted by the SPME fiber. This occurred because the thin film has a higher

extraction phase volume. The equilibration time by thin film extraction was more than 10

min, as with the 10 mL sample.

Sample volume has a significant effect on the extracted amount of the analytes. For

the compounds with relatively low K_{es} (acenaphthene, fluorene and anthracene), the thin

film extracted around 100 times more analytes at equilibrium than did the fiber. Using a 50 L sample volume instead of a 10 mL sample volume reduced depletion from 50-60 % to 0.2-0.4 %.

(A)
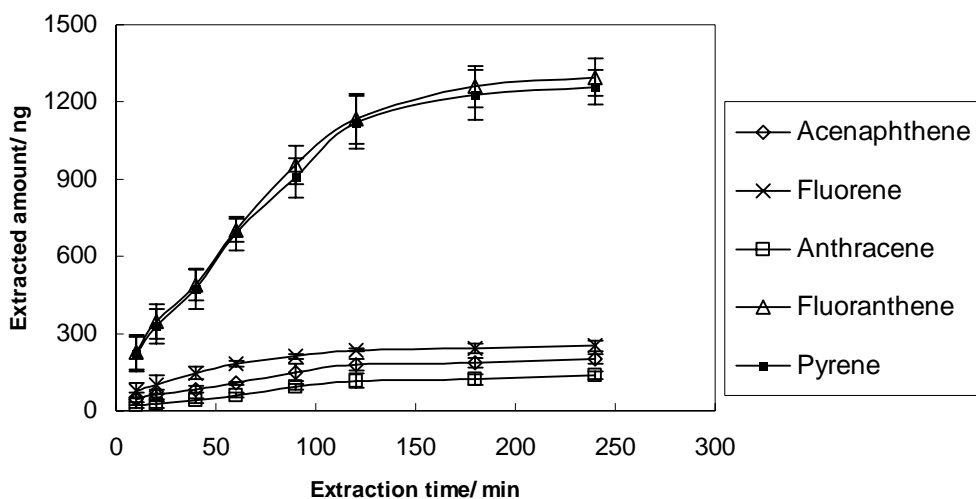
(B)
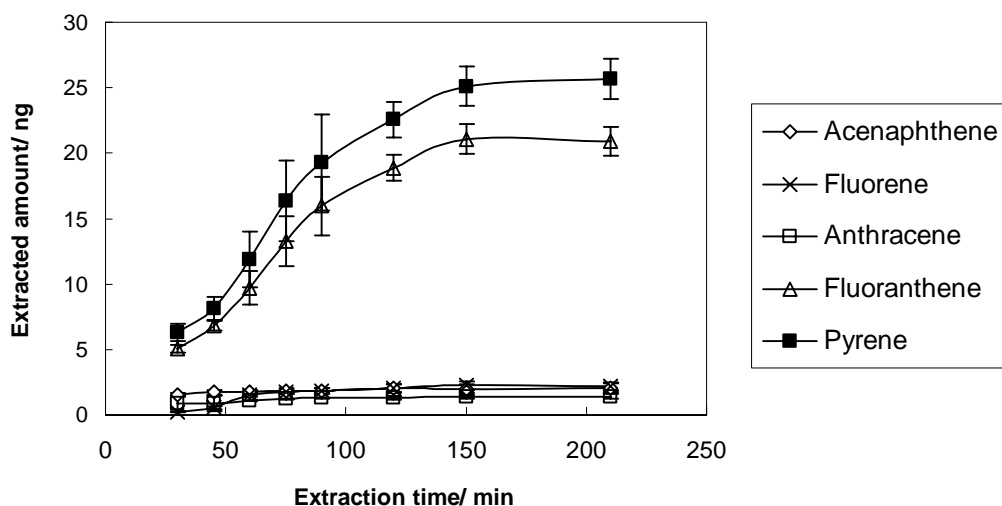
Figure 3-5 Extraction time profiles of PAHs in 50 L samples using a bench drill coupled with (A) a thin film and (B) a fiber.

Table 3-2 shows the theoretical and experimental results obtained by rotating thin film sampling in a 50 L sample after a 5 min extraction. Reynolds number (*Re*) and Prandtl number (*Pr*) of extraction by thin film were calculated and listed in the table. The predicted mass uptakes were obtained based on *Re*, *Pr* and equation 3.16. The theoretical values agree well with the observed experimental uptake. This suggests the model can be used for rotated thin film sampling in a fluid sample. Similar to the boundary layer model in fiber extraction, this thin film model also predicts the higher diffusion coefficients of low M_w PAHs results in their higher concentration rates in the thin film. This prediction was proven in the experiment.

Table 3-2 Theoretical calculations for rotated thin film extraction of PAHs in a 50 L sample (for 5 min extraction) and experimental results.

Analyte	D (cm^2/s)	Re	Pr	n_{pa} (ng)	n_{pe} (ng)	n (theoretical, ng)	n (experimental, ng)
Ace	0.0000064	13956	1406	17.8	6.7	24.5	23.2±2.04
Fl	0.0000061	13956	1475	27.7	10.5	38.2	39.7±3.52
Anth	0.0000059	13956	1525	9.1	3.4	12.5	11.1±0.86
Fla	0.0000056	13956	1607	85.3	32.4	117.7	113.6±7.71
Pyr	0.0000056	13956	1607	84.1	31.9	116.0	109.8±5.90

3.4.3 Design of a Novel Thin Film Sampler for Rapid Sampling

Because of its higher extraction efficiency, the thin film is more suitable than the fiber for rapid sampling on site. A copper mesh pocket and handling rod for attaching a drill was designed and manufactured for field-deployed thin film. The thin film was flattened and clamped tightly in the copper mesh pocket. The copper mesh was not prone to clogging by algae or sediment.
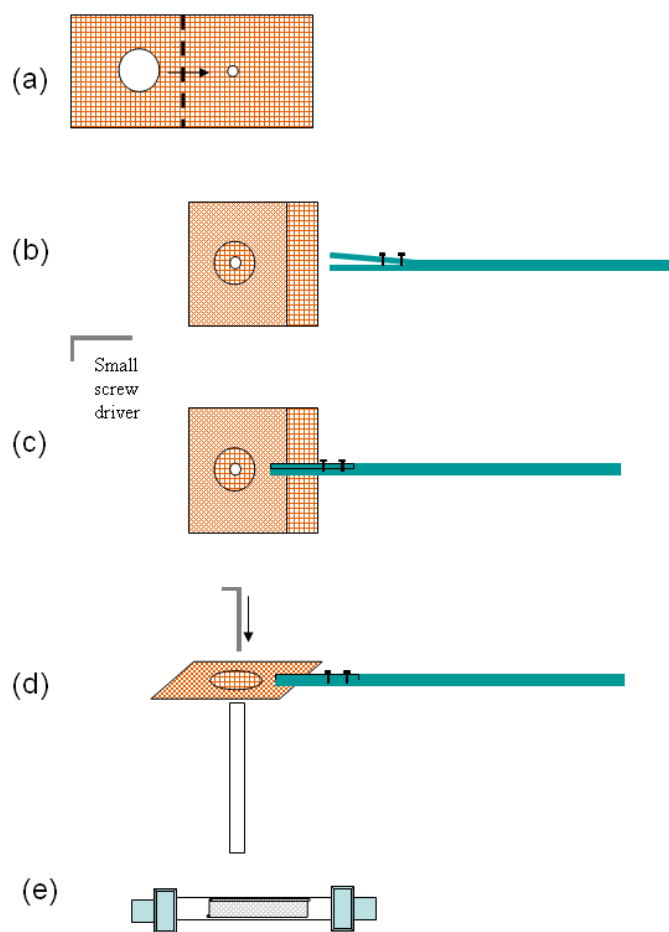
Figure 3-6 Schema of a thin film copper mesh sampler. (a) fold (b, c) fix on a rod (d) push into a liner (e) seal the liner for transportation.

Figure 3-6 depicts the new thin film sampler. A window was milled in the left part of a piece of copper mesh and another smaller window was milled in the right part. The left

window was used to permit analytes access to the thin film for extraction and to allow the thin film to go into the liner after extraction. The smaller window is just big enough to allow the passage of a small screw driver. It is smaller because it needs to support the thin film to prevent it from falling off during rotation and sampling. Step (b) involved folding the copper mesh along the dashed line and sealing the two edges by soldering. A pocket with one opening and two differently sized windows on two sides was thus formed. After placing the thin film in the pocket, the pocket was connected to a metal rod by two small screws. The rod could be extended or shortened depending on the specific requirements for on-site sampling. Step (c) represents the final thin film field sampler, which resembles a small racket. When the extraction was completed, the thin film could be pushed from the small window through the big window into the liner by the small screw driver as in step (d). Finally, in step (e), capping two ends of the liner to seal the thin film provided an effective mechanism for preserving the integrity of the sample and for preventing contamination.

3.4.4 Application of Novel Thin Film Sampler in Laboratory and on Site

The uptake experiment was conducted in the laboratory in a 50 L aqueous PAHs solution, using the new thin film sampler coupled with a portable drill. Extraction times were 2 min, 4 min, 6 min and 8 min. Replicate extractions ($n = 3$) were sampled for each extraction period of exposure. Short exposure times reduced the accumulation of chemicals, so detection sensitivity and variability at lower amounts are important. With the PAHs studied here, a 2-minute exposure provided sufficient mass to yield reproducible

measurements. The longest extraction time was 8 minutes.
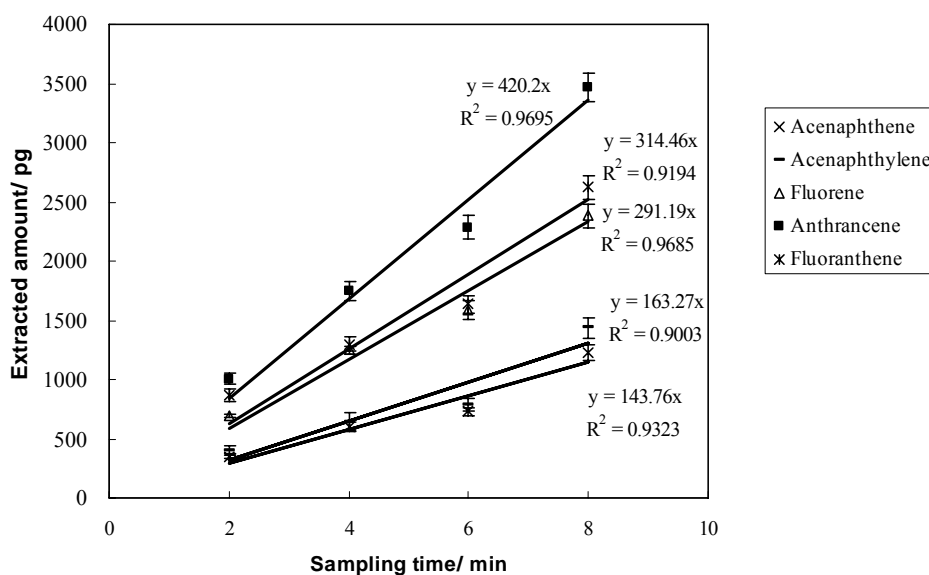
Figure 3-7 Uptake by the novel thin film sampler over 8 minutes in a 50 L sample.

The uptake curve for the PAHs shown in Figure 3-7 used linear regression analysis. Because the regression coefficients (R^2) range from 0.9003 to 0.9695, all PAHs remained in the linear uptake phase for the full 8 minutes. These findings obey first-order uptake kinetics. This is an important verification of the appropriateness of a linear model (equation 3.1) for deriving thin film sampling rates for all the PAHs. R_s values were determined by rearranging equation 3.1 to solve for R_s (at a fixed C_s) (Table 3-3).

$$R_s = M_s(t) / C_s t \qquad\qquad \text{Equation 3.18}$$

These calibration data were used to estimate analyte concentrations in the ambient environment.

The results of field sampling in the campus river are shown in Table 3-3. There was no significant difference in the concentrations measured by the thin film and by the fiber. The approach based on rapid sampling by thin film proved successful.

70

Table 3-3 Sampling rates of PAHs using the novel thin film sampler coupled with a portable drill (operated at 600 rpm) and results of field sampling.

Compounds	Sampling rate R_s (mL/min)	Concentration	
		Thin film on-site sampling (ng/L)	SPME off-site sampling (ng/L)
Acenaphthene	1.44	2.0±0.18	2.3±0.15
Acenaphthylene	1.64	5.0±0.57	6.1±0.38
Fluorene	2.91	5.7±0.32	4.9±0.39
Anthracene	4.20	4.2±0.37	3.4±0.22
Fluoranthene	3.14	26.9±2.11	21.8±1.06

3.5 Conclusion

This study demonstrates the advantages and promising applications of a rotated thin PDMS film for rapid analysis of semivolatile compounds in water samples. Unlike the SPME PDMS fiber, the rotated thin film coupled with an electric drill achieved high extraction sensitivity without sacrificing equilibrium time. This is due to its larger surface area to extraction phase volume ratio. We proposed a mass transfer model to quantitatively describe rapid and direct extraction of PAHs with rotated thin film extraction. The mass uptake predicted by the model compares well with experimental mass uptake. Therefore this method would be appropriate for situations in which calibration curves or internal standards are difficult to determine. For SPME fiber extraction, the theoretical prediction

based on the boundary layer model is close to the experimental results.

To quantify rapid water sampling with thin film on site, mass loading rates in the linear uptake regime over 8 min were obtained in the laboratory. A novel and simple copper mesh sampler was used during the rotation of the thin film, thus integrating sampling, sample preparation, storage and transport. This characteristic of the sampler makes it suitable for field sampling. The entire sampling period on site is only 5 min, which meets the requirement of rapid sampling and shows great potential for future applications. The comparable results using this sampler and the regular SPME fiber prove that this technique is an accurate and reliable method for rapid on-site sampling of organic pollutants in water. Plausible modifications to the thin film sampler could avail it to automation and miniaturization.

Chapter 4

Comparison of Thin Film Extraction and Twister Extraction for Spot Water Sampling

4.1 Introduction

Water pollution by organic compounds, many of which are toxic, has caused considerable concern worldwide. The evaluation and monitoring of trace levels of the contaminants in environmental samples is an important objective. Polycyclic aromatic hydrocarbons (PAHs) represent a complex mixture of compounds originating from the incomplete combustion of organic matter. Environmental exposure to PAHs occurs primarily from inhalation of engine exhaust and tobacco smoke, and from ingestion of smoked and barbecued foods. [1, 2] Due to their potential or proven carcinogenic effects, the US Environmental Protection Agency (EPA) has promulgated 16 unsubstantiated PAHs in their list of 129 priority pollutants. [3]

The technology employed for the extraction of PAHs from aqueous samples includes liquid-liquid extraction, [4, 5] solid-phase extraction (SPE), [6, 7] semipermeable membrane device (SPMD), [8, 9] solid-phase microextraction (SPME), [10] and stir bar sorptive extraction (SBSE).[11]

Solid phase microextraction (SPME) is a simple, fast, solvent-free and inexpensive sample-preparation technique introduced in 1990. [10] It can be also regarded as a combination of sampling, extraction, pre-concentration, matrix removal, and chromatographic introduction technique. It is composed of a quartz fiber coated with a

polymeric layer, such as PDMS, retractable inside the needle of syringe-like device. This easily-handled device allows on-line coupling with Gas Chromatography (GC). Since its conception, SPME has been successfully applied in the analysis of fragrances, and in environmental and clinical sampling. [12-15]

There are some limitations in terms of efficiency for SPME fiber, due to the small volume of extraction phase. For this reason, a polydimethylsiloxane (PDMS) rod was developed based on the SPME technique. [16, 17] The rod is 1 cm long with a 1-mm diameter, corresponding to about 7.85 µL of PDMS, which is much larger than the PDMS volume of the SPME fiber. By shaking the sample solution containing the rod, the analytes are enriched in the PDMS phase. Other advantages of this approach are simplicity and low cost. [18]

Bruheim *et al.* adopted a thin-sheet PDMS membrane as an extraction phase and compared it to a SPME PDMS fiber in the analysis of semi-volatile analytes in direct and headspace modes. [19] This extraction approach exhibited much higher extraction rates than SPME fiber due to the higher surface area to extraction-phase volume ratio of the thin-film. Unlike the coated rod formats of SPME with thick coatings, the high extraction rate of the thin-film SPME technique allows for the extraction of larger amounts of analyte within a shorter period. Therefore, a higher extraction efficiency and sensitivity can be achieved without sacrificing analysis time.

Apart from SPME, sorptive techniques have been performed for sample enrichment. An open-tubular capillary column with cross-linked PDMS coating was employed to trap the analytes. [20-22] Another sorptive technique consists of a short bed packed with PDMS

particles.[23] Higher sensitivity was achieved when compared to PDMS-SPME, because it contained 300 uL of PDMS. A disadvantage of this technique was the drying step under a gas stream after enriching aqueous samples, which led to loss of analytes.

Recently, a procedure for the sorptive enrichment of water samples with the sensitivity of packed PDMS, called stir bar sorptive extraction (SBSE), was developed and commercialized by Gerstel under the trade name Twister. [11, 24] It consists of a magnetic rod incorporated into a glass jacket coated with a 0.5-mm layer of PDMS. Twister is placed in the sample, where it performs extraction during stirring followed by thermal desorption. The theory of SBSE is similar to that of SPME. The extraction is controlled by the partitioning coefficient of the solutes between the polymer coating and the sample matrix, and by the phase ratio between the polymer coating and the sample volume. Compared to SPME, a larger amount of sorptive material is used and consequently extremely high sensitivities can be obtained, as illustrated by several applications in trace analysis in environmental, [25, 26] food, [27, 28] and biomedical fields. [29, 30]

In this study, the performance of thin-film and stir-bar extraction, including extraction rate, equilibration time, and sensitivity, were investigated and compared in the analysis of PAHs in water. Magnetic stirring was used for stir bar extraction. For thin film extraction, an electric bench-drill and a hand-held battery-operated drill were used for off-site and on-site sampling, respectively.

4.2 Theory

Independently of agitation level, the fluid contacting the surface of the extraction

phase is always stationary. This static layer of defined thickness is the Prandtl boundary layer, which determines the equilibration time and extraction rate, as extraction rate is controlled by diffusion from the sample matrix through the boundary layer to the extraction phase. [31] The thickness of the boundary layer depends on agitation conditions and the viscosity of the fluid. Therefore, agitation is controlled to facilitate mass transport between the bulk of the aqueous sample and the extraction phase.

For Twister, the effective thickness of a boundary layer can be estimated from empirical formulae of fluid mechanics: [31]

$$\delta = 2.64 \frac{b}{Pr^{0.43}\sqrt{R_e}} \qquad\qquad \text{Equation 4.1}$$

where b is radius of the Twister, and R_e is Reynolds number. $R_e = 2ub/v$, where u and v are the fluid's linear speed and kinematic viscosity (for water at 25 °C kinematic viscosity is 0.009 cm^2/s). The fluid's linear speed is calculated as the angle speed of the rotation $\omega \times$ half of the rotating radius. Pr, the Prandtl number of the liquid, equals v/D_s, where D_s is the diffusion coefficient of the analyte in the liquid.

The initial rate of SPME extraction is proportional to the surface area of the extraction phase: [19]

$$dn/dt = (D_s A/\delta)C_s \qquad\qquad \text{Equation 4.2}$$

The time required to reach equilibrium can be estimated by: [19]

$$t_e = t_{95\%} = 3\frac{\delta K_{es}(b-a)}{D_s} \qquad\qquad \text{Equation 4.3}$$

where (b-a) = thickness of PDMS extraction phase, D_s is the analyte's diffusion coefficient in the sample fluid, and K_{es} is the analyte's partition coefficient between extraction phase

and sample.

4.3 Experimental Section

4.3.1 Chemicals and Supplies

The solvent methanol was obtained from BDH (Toronto, ON, Canada) at HPLC grade. The 100 ppm stock solution in methanol was prepared with pure solid standard of Acenaphthene, Fluorene, Anthracene, Fluoranthene, Pyrene, d_{10}-pyrene and d_{10}-fluoranthene purchased from Sigma-Aldrich (US). Deionized water was obtained using a Barnstead/Thermodyne NANO-pure ultrapure water system (Dubuque, IA, USA). The PDMS thin film, 127 μm thick, was purchased from Specialty Silicone Products Inc (Ballston Spa, NY). Ultrahigh-purity helium was purchased from Praxair (Kitchener, ON, Canada). The commercial Twister™ stir bar for sorptive extraction was obtained from Gerstel (Mullheim, Germany). A Mastercraft 10" bench drill press with 3 speeds (600, 900, 1400 rpm) and a portable 7.2 V Makita drill with a constant agitation speed of 600 rpm were used.

4.3.2 Thin Film Sampler and Twister Sampler

The PDMS thin-film was cut into a house-like shape using a special cutter made by the University of Waterloo Machine Shop (Waterloo, ON, Canada). The dimensions of the thin-films were 2 cm × 2 cm square with a 1-cm high triangle on top. The surface area for one side was 5 cm^2 and the volume of each thin-film was 0.0635 cm^3. A piece of stainless steel wire was used to hold the thin film for easier movement. Such a thin-film

micoextraction device was designed to be coiled and fitted inside the glass tube for injection, taking into consideration the heat zone length. Before use, the thin film was conditioned for 1 hour at 250 $^{\circ}$C in a GC injection port. Between consecutive extractions, a blank run of the same PDMS thin film was analyzed, proving that there was no carryover of the target analyte on the thin film from the previous desorption.

Some traditional agitation methods have been used for SPME, presenting various advantages and disadvantages. Magnetic stirring is the most common method for both fiber SPME and thin-film extraction because it is available in most analytical laboratories.[19, 32] However it requires a stir bar in the vial, which may result in loss of analyte by absorption into the bar. Sonication is another efficient agitation method; however, it introduces a large amount of energy into the system, which heats up and may even destroy the sample. [33] The shaking of the sample-containing vial during extraction can provide good performance, [34] but the consequent stress placed on the needle and fiber requires the fiber to be very flexible, which increases expense.

In our study, we use an electric drill coupled with a thin film to control the movement of the extraction phase when the sample solution is static. With this new technique, most of the disadvantages listed above can be eliminated. This technique can also be extended to on-site spot sampling.

The need for fast on-site analysis of environmental sample is increasing. On-site analysis can minimize loss and degradation of analytes during the collection, transportation and storage of the sample, thus providing more representative quantitative results of the original sample characteristics. In this study, thin film extraction was applied

for spot sampling in the field. To reduce on-site sampling time, the SPME active sampling device, which couples the thin film with the hand-held battery-operated drill, was used.

The magnet of a 1.5-cm stir bar was enveloped by a glass tube, and then by PDMS. The PDMS coating was 0.5 mm thick and 1 cm long. The effective extraction phase volume was 24 μL with a surface area of 1.0 cm^2.

4.3.3 Extraction in 1 L Sample and Flow through System

To perform the thin film extraction, a 0.2 ppb standard aqueous solution was prepared. The thin film was attached to the bench drill and introduced into a 1 L sample solution. The thin film was placed in the middle of the beaker, which was covered with aluminum foil to prevent analyte loss by evaporation. Blank test with the foil was performed prior to extraction and no PAH was detected. The drill's rotational speed could be easily adjusted between 600 rpm, 900 rpm, and 1400 rpm, as required. Once the drill stirrer was turned on, the thin-film rotated and extraction began. After extraction, the thin film was removed from the solution, dried with a lint-free tissue, and inserted into the glass tube. The tube containing the thin-film was inserted in the thermal desorption unit for automated analysis by thermo-desorption GC-MS.

To perform the stir bar extraction, the same solution of fluoranthene and pyrene used in the thin film extraction was prepared. The stir bar was introduced into the sample and stirred on a magnetic stirrer for a predetermined length of time at the same rotational speeds used in the thin film extraction. Next, the stir bar was removed with a magnetic rod, dried with a lint-free tissue, and inserted into Gerstel glass tube for analysis.

The flow-through system for the generation of a standard PAHs aqueous solution has been previously described. [35] PAH concentrations in the flow-through system were determined by SPME direct extraction. Ten milliliters of the effluent was collected in a 10 mL vial and agitated at 500 rpm (Gerstel Agitator). The extraction lasted 30 min, followed by fiber desorption in the GC injector. The average concentrations of Acenaphthene, Fluorene, Anthracene, Fluoranthene, Pyrene were 3.5 μg/L, 1.0 μg/L, 0.4 μg/L, 0.4 μg/L, 0.3 μg/L, respectively.

A 1 L sampling chamber with an inlet close to its bottom and a waste outlet near its top was used to collect the effluent after the sampling cylinder. The extraction of thin-film and Twister were performed in this chamber.

4.3.4 Field Spot Sampling at a Campus River

The thin film coupled with the portable drill was applied in Laurel Creek, a small river located on the University of Waterloo campus (Waterloo, ON, Canada.). The drill was set at 600 rpm and kept constant during extraction. The thin-film was exposed on the river bank for easy operation. After 2 hours of extraction, the thin-film was sealed in the vial and transported to the laboratory. The thin film was analyzed immediately to minimize analyte loss. To evaluate the feasibility of on-site thin-film sampling, a bottle of the river water was transported to the lab and analyzed by direct SPME method.

4.3.5 Instrument

Gas chromatography was performed on an Agilent 6890 GC and 5973 MSD equipped

with a Multipurpose Sampler (MPS 2) (Gerstel GmbH, Mullheim, Germany) system. The Thermal Desorption System (TDS-2) unit was mounted on the GC via the Cooled Injection System (CIS-4) inlet for the thermal desorption of analytes. The thin-film or stir bar was placed in a glass tube of 187 mm length, 6 mm O.D. and 4 mm I.D.

The temperature of the CIS was 0 ^{o}C for the first 5 minutes, during which time the temperature of TDU was increased to 280 ^{o}C and the analyte was desorbed. After desorption, the cooled liner with the thin film or Twister was removed from the TDU, followed by temperature increase of the CIS to transfer the analyte to the GC column. The transfer line situated between the thermodesorption device and the CIS was set at 300 ^{o}C.

An HR-1 capillary column (30 m, 0.25 mm i.d., 0.25 μm film thickness) (Shinwa, Kyoto, Japan) was used with helium as the carrier gas at a flow rate of 1 mL/min. For the analysis of both the PDMS thin film and the Twister, column temperature was maintained at 40 ^{o}C for 2 minutes, then programmed to increase at a rate of 15 ^{o}C/min to 280 ^{o}C, and then held constant for 2 minutes. The total run time was 20 min. The MS system was operated in the electron ionization (EI) mode, and tuned to perfluorotributylamine (PFTBA).

4.4 Results and Discussion

4.4.1 Extraction by Thin Film and Twister in a 1 L PAH Sample

Extraction efficiency is determined by several parameters, including the extraction phase/sample matrix partition coefficient, the extraction phase volume, the sample volume, and the initial concentration of the analyte in the sample.

(A)
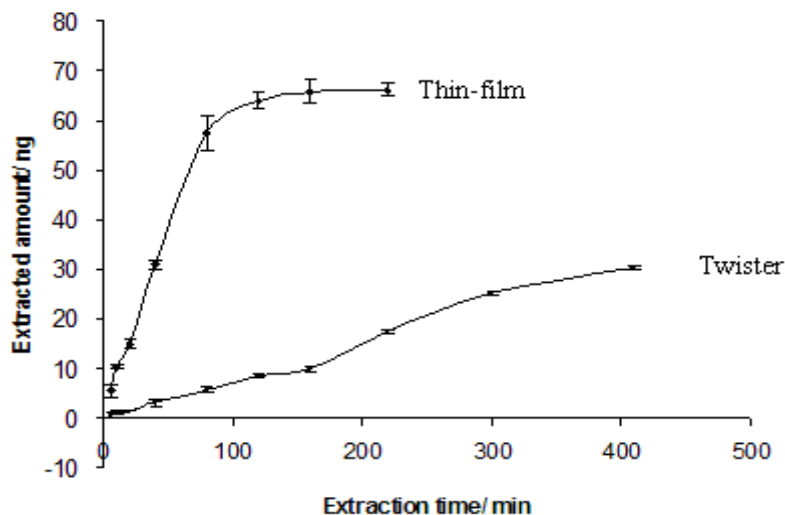
(B)
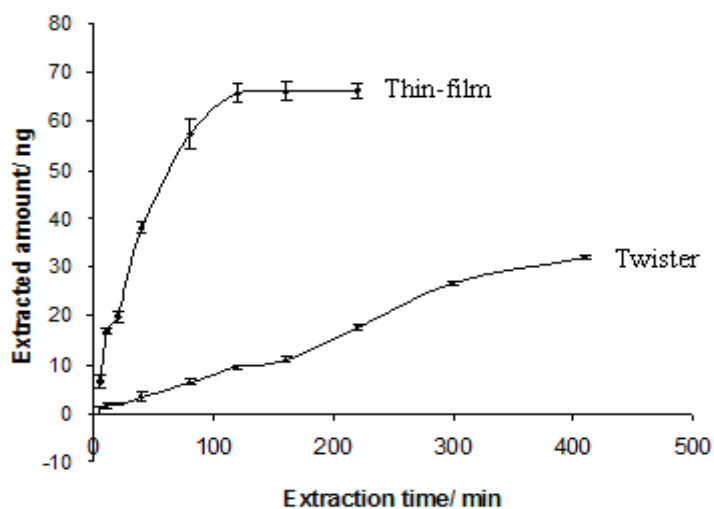
Figure 4-1 Extraction time profile of (A) fluoranthene and (B) pyrene by Twister and thin-film coupled to drill in 1 L sample.

Extraction time profiles of fluoranthene and pyrene by enrichment of thin-film (rotating) and Twister (stirring) at 600 rpm were investigated for extraction times varying between 10 minutes to several hours. These profiles are presented in Figure 4-1 (A) and

(B). The extracted amount increased progressively but extraction rate slowed down for both thin film and stir bar. Three replicates, whose RSD were below 10%, were performed for each extraction time. Reproducibility increased with extraction time, and RSD reached below 3 % when extraction time exceeded 2 hours. It is believed that better reproducibility can be obtained when the system is closer to equilibrium.

Equation 4.3 indicates that the equilibrium time depends on the thickness of the extraction phase. [19] The thickness of thin-film device is only 0.127 mm, but the extraction phase of Twister is much thicker (0.5 mm); therefore the equilibration time of Twister is expected to be longer. The experimental measurements showed that, after 2 hours, the thin-film extraction reached equilibrium; by contrast, the extracted amount by Twister was still progressively increasing, demonstrating its much longer equilibration time.

Table 4-1 Ratio of extracted amount of fluoranthene and pyrene by thin-film (n_f) and Twister (n_T) in 1 L sample.

Extraction time (min)	n_f/n_T	
	Fluoranthene	Pyrene
5	10.6	10.7
10	9.4	10.2
20	9.6	9.6

In addition, referring to equation 4.2, the initial rate of SPME extraction is proportional to the surface area of the extraction phase. The surface area of the thin-film is 2×5 cm^2 = 10 cm^2, which is 10 times that of a 1.5 cm long Twister (A = 1.0 cm^2).

Table4-1 shows the experimental ratio of the amounts of fluoranthene and pyrene extracted by thin-film to the amount extracted by the Twister. After extraction times of 5, 10, and 20 minutes the amounts extracted by the thin-film were about 10 times higher than those extracted by the Twister. During the initial stage of the extraction process, a higher extraction rate was found for the thin-film than for the Twister, as expected. This finding gives opportunity to perform a faster extraction using thin-film. In summary, the advantage of the thin-film, compared with the Twister, is a shorter equilibration time and a higher extraction rate due to its thinner extraction phase and larger surface area.

Tables 4-2 and 4-3 present the results of the theoretical calculation of extraction rate and equilibrium time for Twister in the 1 L sample and the flow-through system. Theoretical calculation results are close to the experimental values.

Table 4-2 Theoretical calculation of Twister extraction rate of PAHs in (A) 1 L sample and (B) Flow through system.

(A)

Compounds	D_s ($\times 10^6$cm^2/s)	$Pr^{0.43}$	Thickness of boundary layer (cm)	dn/ dt (ng/ s)	Extracted amount after 5 min (ng)
Acenaphthene	0.0000064	22.58	0.000530	0.0026	0.79
Fluorene	0.0000061	23.05	0.000520	0.0026	0.77
Anthrancene	0.0000059	23.38	0.000516	0.0025	0.75
Fluoranthene	0.0000056	23.91	0.000504	0.0024	0.73
Pyrene	0.0000056	23.91	0.000504	0.0024	0.73

(B)

Compounds	Concentration (ppb)	D_s ($\times 10^6$cm^2/s)	Pr	Thickness of boundary layer (cm)	dn/ dt (ng/ s)	Extracted amount after 5 min (ng)
Acenaphthene	3.5	0.0000064	1406.3	0.000530	0.046	13.8
Fluorene	1.0	0.0000061	1475.4	0.000520	0.013	3.9
Anthrancene	0.4	0.0000059	1525.4	0.000515	0.005	1.5
Fluoranthene	0.4	0.0000056	1607.1	0.000504	0.005	1.4
Pyrene	0.3	0.0000056	1607.1	0.000504	0.004	1.1

Table 4-3 Theoretical calculation of Twister equilibrium time of PAHs in Flow through system

Compounds	K_{es}	D_s ($\times 10^6$cm^2/s)	t_e (s)	t_e (hour)
Acenaphthene	2512	0.0000064	31435	8.7
Fluorene	5129	0.0000061	65961	18.3
Anthrancene	20640	0.0000059	270549	75.2
Fluoranthene	28262	0.0000056	381653	106.0
Pyrene	31097	0.0000056	419937	116.6

To investigate the effect of rotation speed on extraction efficiency, a procedure involving thin-film and Twister extraction was performed at three different rotation speeds (600, 900, and 1400 rpm). A shorter extraction time compared to equilibrium time was used. From Figure 4-2 (A) and (B), it can be concluded that for both thin-film and Twister, after a 20-minute extraction, extracted mass of analytes increased with increasing rotation or stirring speeds. The results can be easily understood by considering the effect of the reduced thickness of the boundary layer at increasing linear speeds of the fluid. At 600 rpm, the extracted amount by the thin-film was about 10 times that extracted by the Twister, a result consistent with the ratio of their surface areas. However, at 900 and at 1400 rpm, the thin-film extracted much less than 10 times the amount extracted by the Twister. The reason for this change is that the effective extraction surface area of the thin-film decreased with rotating speed. The thin-film sampler is flexible and bends easily; therefore it cannot maintain an absolutely flat shape at high rotation speeds. Decrease of effective extraction surface area caused decreased extraction efficiency.

(A)
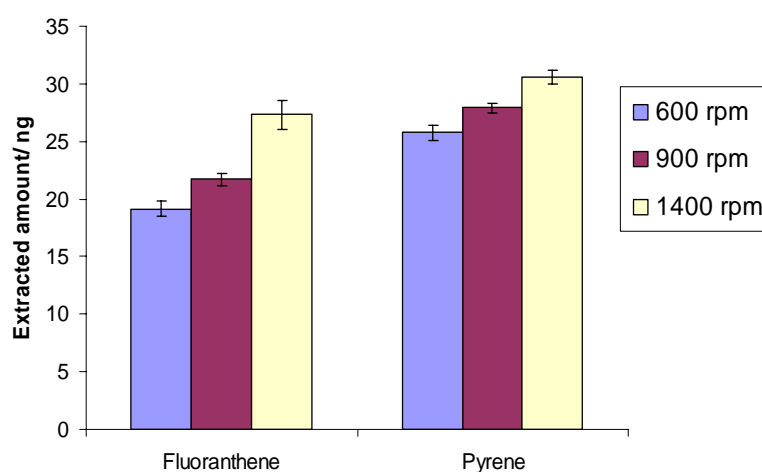
(B)
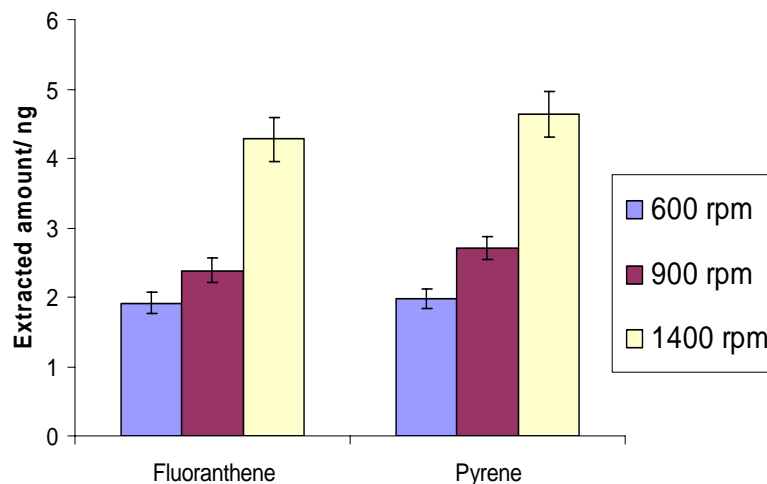
Figure 4-2 Extraction of (A) thin-film and (B) Twister at three different rotation speeds.

A special framed holder was built based on the design of the upper part of a snap pill jar in order to secure and flatten the thin-film. Figure 4-3 shows this holder. The thin-film was positioned and fixed to the holder by tightly fastening the cap and jar part. A round hole was cut in the cap, providing windows for analytes to access the thin-film. A rod was attached near the cap for handling. By controlling the movement of the rod, the thin-film could be rotated with the holder for extraction with very flat shape. After sampling, the thin-film can be easily removed from the holder by opening the cap and then pushed into the liner for desorption. Table 4-4 presents the extracted amount of analytes by the thin-film, with framed holder and regular thin-film sampler at 900 rpm and 1400 rpm. The results prove that the holder could improve the extraction efficiency at high rotation speeds, especially under vigorous agitation, such as 1400 rpm.
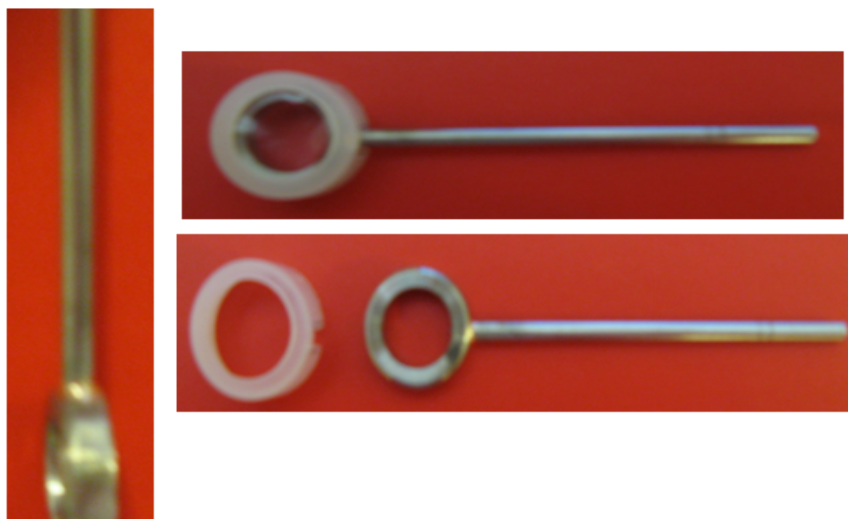
Figure 4-3 Specially designed thin-film framed holder.

Table 4-4 Comparison of thin-film performance with framed holder and regular thin-film sampler**.**

Compounds	Extracted Amount/ ng	
	With framed holder	With regular sampler
	900 rpm	
Fluoranthene	4.90	3.73
Pyrene	5.50	4.65
	1400 rpm	
Fluoranthene	7.30	4.59
Pyrene	8.66	5.09

4.4.2 Extraction by Thin Film and Twister in a Flow through System

The next demonstration of the advantages of thin-film extraction was completed in the

flow-through system. The extracted amounts of five PAHs (Acenaphthene, Fluorene, Anthracene, Fluoranthene, Pyrene) by both thin-film and Twister were compared.

(A)
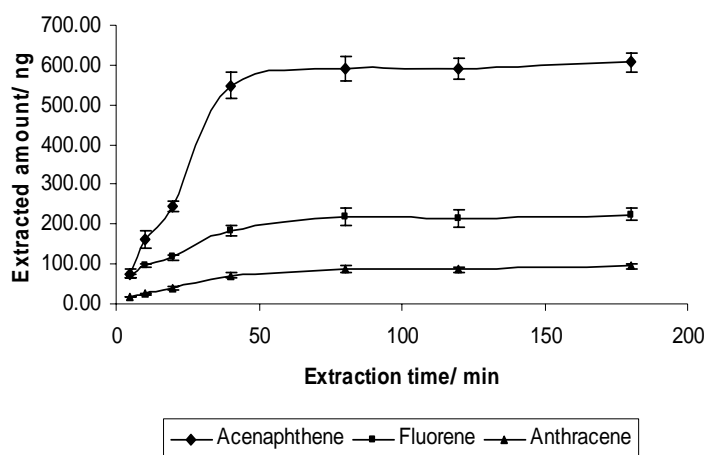
(B)
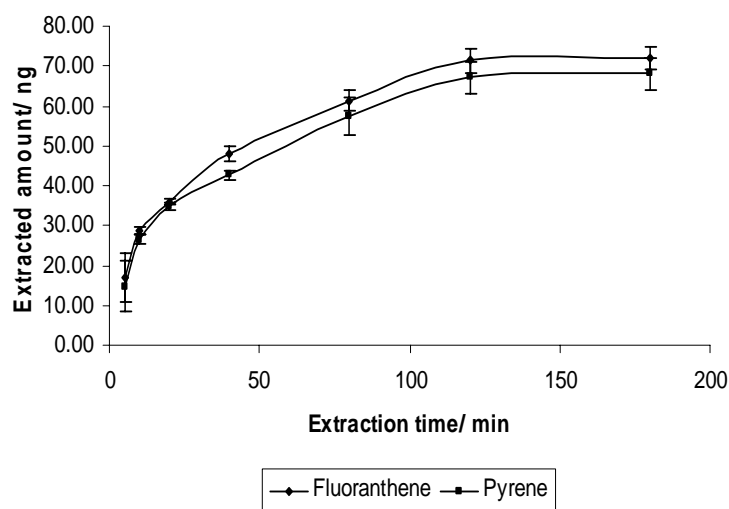
Figure 4-4 Extraction time profile of thin-film for (A) Acenaphthene, Fluorene, Anthrancene and (B) fluoranthene and pyrene in the flow through system.

Figure 4-4 (A) and (B) present the extraction time profiles of the 5 PAHs by the thin-film at a rotation speed of 600 rpm in the flow-through system. The thin-film extraction of Acenaphthene, Fluorene, and Anthracene reached equilibrium after 40

minutes, while Fluoranthene and Pyrene reached equilibrium after 120 minutes. It is observed from Figure 4-5 (A) and (B) that no PAHs reached equilibrium after 180 minutes of Twister extraction. The results strongly suggests a longer equilibrium time for analytes when the Twister is used in the flow-through system.

(A)
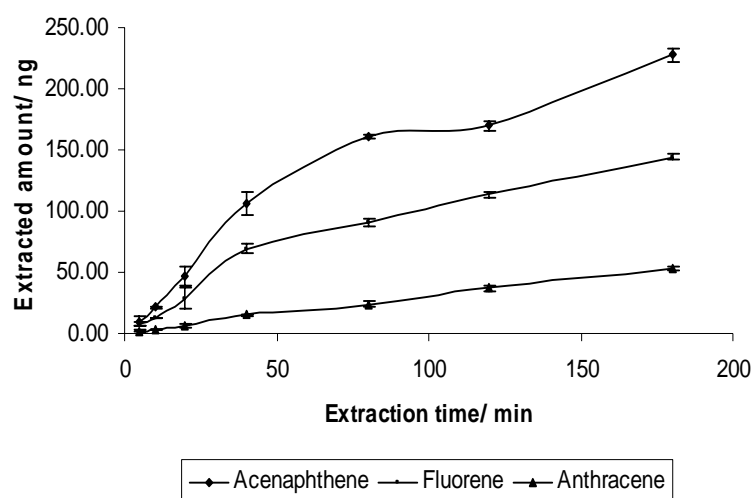
(B)
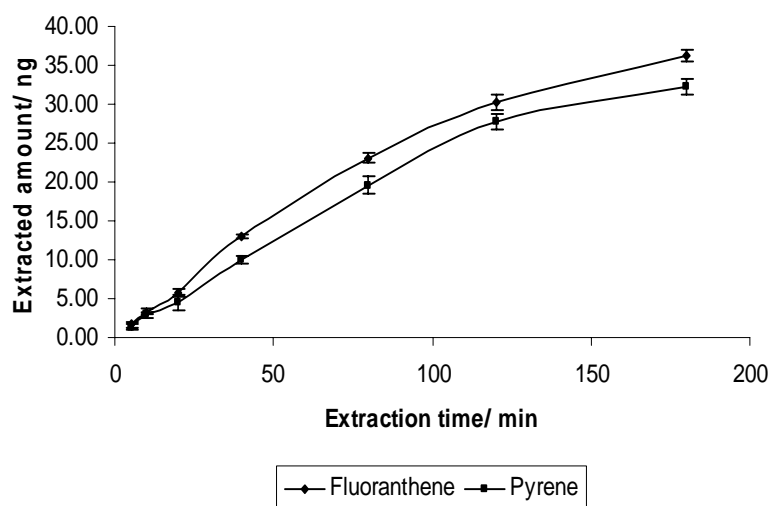
Figure 4-5 Extraction time profile of Twister for (A) Acenaphthene, Fluorene, Anthrancene and (B) fluoranthene and pyrene in the flow through system.

The thin-film extraction technique obtained, as it did in the 1 L sample, much higher extraction rates compared with the Twister extraction. The ratios of extracted amounts with the two extraction devices are shown in Table 4-5. In the initial stage of extraction, after 5 min, the amounts of fluoranthene and pyrene extracted by the thin-film were 10.1 and 10.8 times higher, respectively, than those extracted by the Twister. The ratios at this stage are approximately equal to the ratio of the two devices' surface areas. For the other PAHs, values varied from 7.6 to 9.0. When extraction time was increased to 40 minutes or longer, the ratios obviously decreased and more close to the ratio of extraction volumes ($63.5/24 = 2.6$), because some analytes have reached equilibrium with thin-film extraction.

Table 4-5 Ratio of extracted amounts of 5 PAHs by thin-film (n_f) and Twister (n_T) in flow through system.

Extraction	n_f/n_T				
time/ min	Acenaphthene	Fluorene	Anthracene	Fluoranthene	Pyrene
5	7.6	9.0	8.0	10.1	10.8
10	7.5	7.7	8.4	8.6	9.2
20	5.3	4.1	6.5	6.2	7.8
40	5.1	2.6	4.8	3.7	4.2
80	3.7	2.4	3.6	2.7	2.9
120	3.5	1.9	2.3	2.4	2.4
180	2.7	1.6	1.8	2.0	2.1

4.4.3 Field Sampling at a Campus River

The thin-film was deployed for analysis of Fluorene, Anthracene, Fluoranthene and Pyrene in Laurel Creek. To validate the feasibility of using the thin-film in field sampling, water samples were also collected from the sampling site. The water samples were analyzed by SPME direct extraction.

Table 4-6 presents the results of the thin-film and the direct fiber SPME extractions. PAH concentrations obtained by thin-film on-site sampling are similar to those determined by lab analysis, indicating a strong agreement between the two methods and demonstrating the feasibility of thin-film device for field sampling.

Table 4-6 Determination of PAHs in a campus river by thin-film extraction and fiber SPME.

Compounds	Concentration (ng/L)	
	thin-film extraction	fiber SPME
Fluorene	16±3.1	22±1.4
Anthracene	61±7.6	60±5.2
Fluoranthene	27±3.5	34±4.0
Pyrene	22±4.3	30±4.8

In contrast, field sampling with the Twister was not as easy as with the thin-film because the magnetic stirrer is not conveniently moved in the field. Moreover, coupling

the Twister to the hand drill is difficult. This shows another advantage of the thin-film sampler over the Twister.

4.5 Conclusion

In this study, the performance of a thin-film attached to an electric drill at a constant rotation speed was compared with the performance of a Twister coated with PDMS at a constant stirring rate. In both the 1 L beaker and the flow-through system, the thin-film achieved shorter equilibration times and greater extraction rates of PAHs from aqueous solutions than did the Twister. This is due to the thin-film's thinner extraction phase and larger surface area. Increasing rotation speeds improved extraction efficiency for both devices. At high rotation speeds, the thin-film sampler was found to bend, thus decreasing extraction efficiency. A specially-designed framed holder for securing the thin film solved this problem.

Chapter 5

Time-Weighted Average (TWA) Water Sampling Using Thin Film

5.1 Introduction

In time-weighted average (TWA) sampling, the analyte concentration is integrated over the time of sampling. [1] Compared to spot sampling at one particular time, TWA sampling is less sensitive to accidental extreme variations in organic pollutant concentration, thus giving more accurate information for the long-term monitoring of environmental pollutants.

There are two approaches for determination of TWA concentration. The first one needs collecting a large number of grab samples over the interval of interest, and averaging the concentrations, as shown in the following equation:

$$\overline{C} = \frac{C_1 t_1 + C_2 t_2 + C_3 t_3 + ... + C_n t_n}{t_1 + t_2 + t_3 + ... + t_n} = \frac{\sum_{i=1}^{n} C_i t_i}{\sum_{i=1}^{n} t_i} \qquad \text{Equation 5.1}$$

Where $\overline{C}$ is the TWA concentration, and C_i is the analyte concentration observed in time period t_i. However, this method is time-consuming and expensive, and sampling frequency needs to be increased for more accurate time integrated pollutant levels.

The second approach to obtain TWA concentration is using a single sampler if the mass loading of the analyte is directly proportional to the analyte concentration for the time period of interest. This approach is much simpler and less expensive than the first approach.

Both active and passive sampling can be used to determine the TWA concentration

with a single sampler. Active samplers are complicated and expensive, because usually flow meters, pumps and a power supply are usually required during monitoring. Therefore, for the long-term monitoring of organic pollutants in water, passive sampling techniques are more attractive, compared to active sampling approaches. [2-4] This technique utilizes the free flow of analytes from the sample into the receiving phase in a sampling device based on a difference in the chemical potentials between the two phases. The net flow of analyte molecules from one medium to the other continues until equilibrium is established in the system, or until the sampling period is stopped. Sampling proceeds without the need for any energy sources other than this chemical potential difference. [3]

There are many advantages to using passive sampling in the field. Because only a few samplers are required in a particular area, the analytical costs are very low, making these devices a cost-effective solution for field monitoring. [1] Additionally, passive samplers are both inexpensive to manufacture and inexpensive to analyze. These devices usually have a relatively simple construction and are easy to use. Often, deployment and removal of samplers is not conducted by scientifically trained personnel, so sampling devices are usually designed for easy deployment, and they are also small enough to be easily transported to the laboratory for further analyses. [1]

Calibration for many passive samplers is performed in the laboratory at known exposure concentrations. Extensive calibration studies are used to characterize the uptake of contaminants for different exposure conditions so that a TWA concentration of the chemicals can be determined. The uptake depends upon the properties of the sampler and, sampler design, and environmental variables, such as water turbulence, temperature, and

biofouling.[3] Passive samplers use information about sampling rates, exposure time, and the amount of analyte trapped in a receiving phase to determine the analyte concentration.[3]

There are several types of passive samplers currently available for water analyses, such as semipermeable membrane devices (SPMDs),[5-8] passive in-situ concentration extraction samplers,[9] supported liquid membrane techniques,[10] and sorbent-filled devices.[11] SPMDs are currently the most widely used type of passive samplers for field water analysis due to their ease of deployment, standardized character, and high sensitivity. However, the main disadvantage of SPMD technique is the time-consuming sample-treatment procedure.[12]

Solid-phase microextraction (SPME) was developed to address the need for rapid sampling and sample preparation, both in the laboratory and on-site.[13] It is a solvent-free sample preparation technique and combines sampling, extraction, and concentration into one step. Since its conception,[14] SPME has been widely applied to the sampling and analysis of environmental samples, food, and pharmaceuticals.[15-16] On-site sampling devices based on SPME integrate sampling with sample preparation and sample introduction. The design of these devices was based on different calibration methods, including traditional, equilibrium extraction and several diffusion-based approaches.[17]

Several diffusion-based SPME devices have been developed for passive TWA sampling, both in air and water.[18-22] These SPME passive samplers are unlike conventional sampling with SPME, in which the fiber is retracted a known distance into its needle housing during the sampling period. Analyte molecules access the fiber coating only by means of diffusion through the static air/water gap between the opening and the

fiber coating. Therefore, Fick's first law of diffusion can be used for the calibration. In 1997, Ai Jiu proposed a dynamic SPME model based on a diffusion-controlled mass transfer process. [23-24] Based on this model, Chen *et al*. demonstrated the isotropy of absorption and desorption in the SPME liquid coating fiber and a new calibration method, kinetic calibration, was proposed. [25-26] The kinetic calibration method, also referred to as the in-fiber standardization technique, uses the desorption of the standards, which are preloaded in the extraction phase, to calibrate the extraction of the analytes. [27]

In this study, the principles of kinetic calibration in the extraction phase initially developed for SPME fiber were used for extractions with a poly(dimethylsiloxane) (PDMS) thin-film. Polycyclic aromatic hydrocarbons (PAHs) were selected as the target analytes because of their widespread presence in the environment and their known affinity to PDMS. On site sampling and determination of TWA concentrations of PAHs in Hamilton Harbour, ON, Canada during September, October and November, 2005, were successfully completed using this type of thin film extraction. In addition, the thin film sampler, a modified fiber-retracted SPME field water sampler, and a SPME PDMS rod, were used simultaneously to determine the TWA concentrations of PAHs in Hamilton Harbour in July and August, 2006. The distinct features of the three types of samplers are also discussed and compared.

5.2 Theory

Absorption of an analyte onto a SPME liquid coating based on a diffusion-controlled mass transfer process is theoretically described with equation 5.2. [26]

$$\frac{n}{n_e} = 1 - \exp(-at) \hspace{4cm} \text{Equation 5.2}$$

where n is the amount of analyte extracted by SPME coating at time t, n_e is the amount of analyte extracted by the SPME coating at equilibrium, and a is a constant that is dependent on the volumes of the fiber coating and sample, mass transfer coefficients, partition coefficients and the surface area of the extraction phase.

The main challenge for this pre-equilibrium calibration method is to determine the value of constant a. The kinetic process of the desorption of the analyte from a SPME coating has been studied and it was found that the desorption of analytes from a SPME coating into the sample matrix is a mirror reflection process of the absorption of the analytes onto the extraction phase from the matrix under the same matrix conditions, and this allows for the calibration of absorption using desorption. [26]

In on site sampling analyses where the sample volume is large, the desorption kinetics can be expressed as: [26]

$$\frac{Q}{q_0} = \exp(-at) \hspace{4cm} \text{Equation 5.3}$$

where Q is the amount of standard remaining in the extraction phase after sampling time t and q_0 is the amount of pre-added standard in the extraction phase. The mirror reflection characteristic of the absorption and desorption can be demonstrated:

$$\frac{n}{n_e} + \frac{Q}{q_0} = 1 \hspace{4cm} \text{Equation 5.4}$$

Theoretically, n_e can be obtained by two methods: (1) performing the absorption and desorption alternatively under the same experimental conditions, time constant a can be calculated using equation 5.3 and substituted the constant into equation 5.2 to determine n_e;

(2) performing the desorption and absorption simultaneously and n_e can be directly calculated from equation 5.4.

For two-phase system, the initial concentration of the analyte in the sample matrix, C_s, can be determined in equation 5.5: [26]

$$C_s = \frac{q_0 n}{K_{es} V_e (q_0 - Q)}$$

Equation 5.5

After preloaded with a certain amount of standard q_0, onto the extraction phase, the extraction phase was exposed to the sample matrix for a defined period. n, the amount of analyte extracted by the sampler after exposure time t, and Q, the amount of standard remaining in the sampler, can be determined. Last the initial concentration of analyte in the sample matrix, C_s, can be calculated using equation 5.5.

If the sorbent is "zero sink" for the target analytes, the concentrations of analytes in the sample can be calculated with equation 5.6. [18]

$$\overline{C} = \frac{nZ}{A D_s t}$$

Equation 5.6

where $\overline{C}$ is the TWA concentration of the target analyte in water during the sampling time t, Z is the diffusion path length, A is the cross-sectional area of the needle, D_s is the diffusion coefficient of the target analyte in water, and n is the amount of analyte that is extracted by the fiber during time t.

The diffusion coefficients of the target analytes in water, D_s, were calculated with the following empirical equation. [28]

$$D_s = \frac{1.326 \times 10^{-4}}{v^{1.14} \overline{V}^{0.589}}$$

Equation 5.7

where v is the kinematic viscosity of water at the temperature of interest and $\overline{V}$ is the

molar volume of the analyte. The average temperatures at the three different depths were used as the approximate temperature for sampling.

5.3 Experimental Section

5.3.1 Chemicals and Supplies

HPLC grade methanol was purchased from BDH (Toronto, ON, Canada). Acenaphthene, fluorene, phenanthrene, anthracene, fluoranthene, d10-fluoranthene, pyrene, and d10-pyrene were purchased from Sigma-Aldrich (Mississauga, ON, Canada). Helium (99.999%), nitrogen (99.999%), liquid nitrogen, and compressed air that were used for the analytical instruments were obtained from Praxair (Kitchener, ON, Canada). Water used in these experiments was Nano-pure water from a Barnstead water system (Dubuque, IA). The PDMS thin film, with a thickness of 127 μm, was purchased from Specialty Silicone Products Inc (Ballston Spa, NY). The SPME holder, the 100 μm PDMS fibers and the PDMS rods, with a diameter of 1 mm, were also obtained from Supelco (Oakville, Canada). Silco steel-treated tubing (i.d. 0.76mm) was purchased from Restek (Bellefonte, PA). Copper wire mesh was purchased from Goodfellow (Devon, PA). All preparations that involved PAHs were carried out in a ventilated fume hood.

5.3.2 Thin Film Field Sampler

There were several challenges encountered during the development of a field sampler using PDMS thin-films. For example, the intended field application of this device, during which time the device would be placed in a body of water for a long period of time,

necessitated the design of a robust sampler that was not prone to clogging by algae or sediment. Thus, the number of parts in the system was kept to a minimum, both for ease of deployment and to minimize the risk of breakage. Copper caging was also used to prevent algal buildup on the device during field sampling. PDMS thin film was cut into a specific house-like shape using a special cutter, which was manufactured in-house by the University of Waterloo Machine Shop (Waterloo, ON, Canada), as illustrated in Figure 5-1 (A). The dimension of the thin-films was 2×2 cm with a 1 cm high triangle on the top of the square. The surface area for one side was 5 cm^2, and the total volume of each thin-film was 0.0635 cm^3. These dimensions were optimized for ease of analysis so that the device could be coiled and fit inside a gas chromatography (GC) liner for injection. A piece of stainless steel wire, shaped like the eye of a needle, was used to hold the thin-film for easier movement. The thin films were conditioned before use with a 2 h bake out period in the GC injector port at 250°C, with a helium flow rate of 1 mL/min.
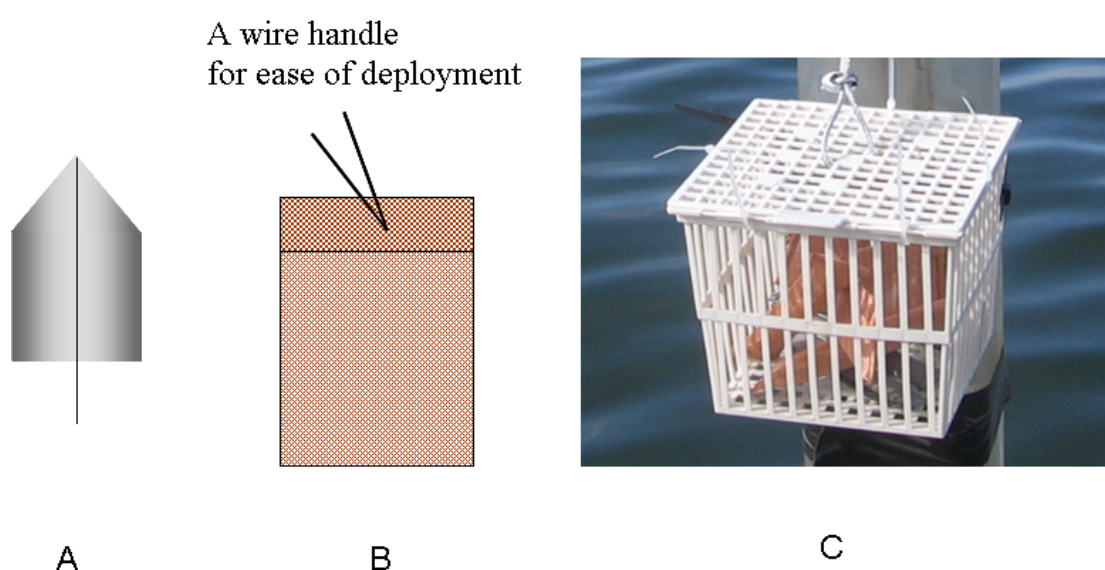
Figure 5-1 Thin film field sampler

Figure 5-1 (B) shows, for deployment in the field, the thin-films were then placed in small copper cages to help secure and protect them. This caging did not restrict the flow of analytes from the bulk water sample into the thin-film. A wire handle was placed on each cage for ease of deployment. Samplers were placed into plastic baskets and the handles of the copper cages were secured onto the top of the baskets (Figure 5-1 (C)). Several replicates of the samplers could be placed inside the same basket. The copper cages and baskets were cleaned in the laboratory prior to use in the field to confirm no contamination from them.

5.3.3 SPME Fiber and Rod Field Sampler

The fiber-retracted field water sampler device in Figure 5-2 was constructed with copper tube and caps and a commercial SPME 100 μm PDMS fiber assembly. [22] A Silco steel-treated tube with an inner diameter (0.76 mm) was used as the diffusion path. In this trial, the length of the diffusion path was adjusted to 4 mm for all of the samplers. The opening of the device was covered with a copper mesh to avoid biofouling from the sampling environment and PDMS/ Teflon septa were used for sealing the device.

When preparing for sampling, the fiber was conditioned at 250 °C for 1 h. The copper tube, the Silcosteel tube, and sampler caps were cleaned and baked at 250 °C for 1 h. After the copper tube and caps were cooled, the SPME fiber was placed into the diffusion tube and the cap (used to fix the fiber assembly) was tightly screwed in place. A copper mesh was placed in the sampling opening, the cap was tightly screwed, and the sampler was then ready for sampling. All of the samplers were constructed in water to eliminate any air

in the systems. Prior to deployment, the cap was removed from the sampler opening and the samplers were then deployed at the sampling sites for a set period of time.
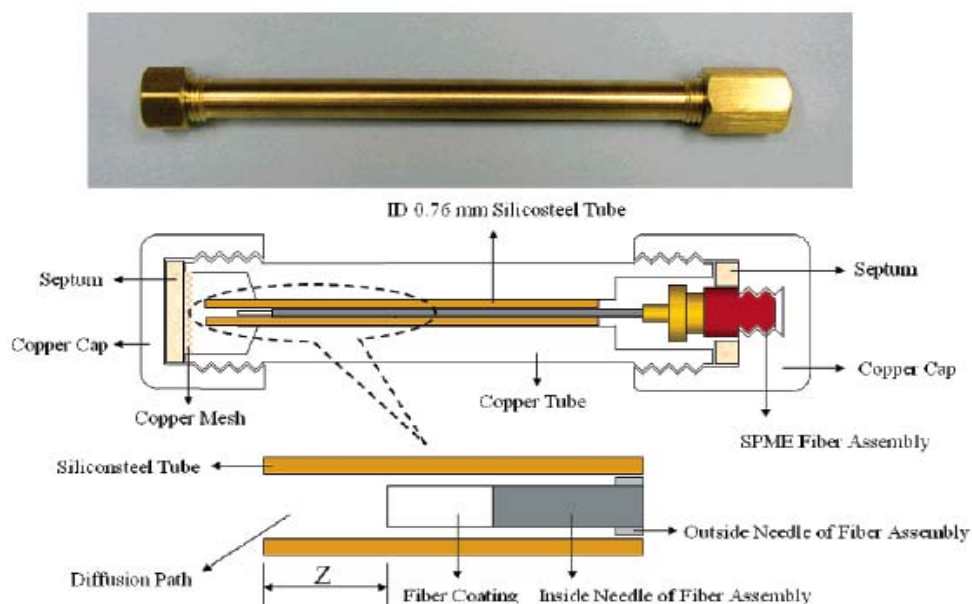
Figure 5-2 SPME fiber-retracted field water sampler

The SPME PDMS-rod samplers were 1 cm long with a diameter of 1mm and a volume of about 7.85 μL. They were conditioned at 250 °C for 1 h prior to use.

5.3.4 Initial Loading of the Standard onto the Thin Film and Rod Samplers

There were two internal standards chosen for these experiments: deuterated fluoranthene and deuterated pyrene. The initial loading of the standards onto the thin-film or rod was optimized and subsequently used for field sampling. The loading was conducted by placing the rod or thin film directly into the standard aqueous solution with agitation. A standard solution (25 ng/mL) was prepared by spiking 2.5 μL of 100 μg/mL deuterated standard solution into a 10 mL (for rod) or 20 mL (for thin film) vial containing 10 mL of nanopure water. After mixing, either the PDMS rod or the PDMS thin film was

added into the vial, and the vials were then placed in the agitator of the autosampler at 35 °C and 500 rpm. It was determined that the standards had reached equilibrium with the thin film after 45 min or rod after 2 hours so these were the extraction time used for the standards. The amount of initial standard loaded onto the samplers was calculated by analyzing these samplers and quantified with the external calibration method. The loaded samplers were maintained at low temperature (0 °C) during storage and transportation.

5.3.5 Field Trial

5.3.5.1 Field Sampling Techniques

Before trip to the sampling sites, when three replicates of each thin film, SPME fiber and rod sampler were ready for on site deployment, they were placed into sealed copper cages and, for transportation, were placed in sealed glass jars at low temperature. At the sampling sites, all of the samplers were removed from the glass jars but still kept in copper cages. The cages can secure the devices and protect them from the sampling environment. But the cages did not restrict the flow of analytes from the bulk water sample to the samplers. All the cages with the samplers were then placed into plastic baskets.

At the sampling locations, the samplers were placed at three different depths at the sample location. At each depth, plastic baskets containing the samplers were deployed onto stationed moors that were positioned and maintained by the Technical Operations Services group at Environment Canada. Three replicates of each sampler were deployed at each depth to study the reproducibility of the sampling device. The samplers were then deployed at the sampling sites for a set period of time (approximately one month).

After the sampling period was completed, the samplers were removed from the sampling site. The thin film and rod samplers were placed in silane-treated glass vials, sealed, and kept cool until analysis. The fiber-retracted devices were sealed with the caps. During storage and transportation, the samplers were kept at low temperatures to minimize the amount of analyte or standard lost.

Once transported to the laboratory (at the University of Waterloo), the thin films and rods were removed from the copper cages and rinsed with nano-pure water to remove the very thin layer of excess silt, which was attached to the samplers. The thin films or rods were then placed into the GC liners and analyzed to determine the amount of PAHs in the samples. The SPME fibers were gently dried with a lint-free tissue and then the SPME fiber holder was used to introduce the fibers into the GC injector port for desorption, separation and quantification.

The thin films were analyzed a second time to determine the residual PAH remaining on the thin film after analysis. Blank analyses were also conducted between each sample. Both the carryover analysis and the blanks illustrated much smaller (< 5%) levels of PAHs than the thin film samples.

5.3.5.2 TWA Water Sampling Using Thin Film Sampler in September, October and November, 2005

The Meuse River was heavily polluted with various inorganic and organic substances in the 1960s and 1970s.[29] The major contamination sources are agricultural activities and urban pollution.[30] Heavy metals and organic pollutants such as PAHs, polychlorinated

biphenyls, and chlorinated pesticides have accumulated in high concentrations in the water. Many countries are working together to cleanup this drinking water source. [31-32] The thin-film samplers were first used in the Meuse River in Eijsden, the Netherlands, where the river first enters the country. Samplers were deployed from the side deck of a barge for a time period of 28 days.

Sampling in Hamilton Harbour in Lake Ontario, located on the western tip of Lake Ontario, ON, Canada occurred in one month intervals over a period of three months. Two sampling sites were chosen in the harbour. Site 1 was in Windermere Arm in the south eastern corner of the harbour. Site 2 was located in the middle of the harbour in a location known as the Deep Hole. There are several steel factories along Hamilton Harbour, which contribute to the high levels of pollutants in the harbour (PAHs, in particular).

At each site, plastic baskets containing the samplers were placed at three different depths: surface water, middle-depth water, and deep water. At site 1, the depths were 1, 11.5, and 21 m (which is approximately 1 m above the bottom of the lake). At site 2, the depths were 2.5 (because of convenience of placing the samplers on existing lines), 11.5 m, and 22.5 m (approximately 1 m above the bottom of the lake). Three samplers were placed at each depth in both sites.

5.3.5.3 TWA Water Sampling Using Thin Film, SPME Fiber and Rod Field Samplers in July and August, 2006

Three types of SPME TWA field water samplers, thin film, fiber and rod, were tested in Hamilton Harbour. The sampling site was located in the middle of the harbour, which

has been identified as one of the most polluted spots in the harbour, based on data from Environment Canada. The samplers were deployed 1m below the surface, considered surface water, 11 m below the surface, considered middle water, and 21 m below the surface, considered bottom water.

Six PAH compounds were selected as the target analytes, including acenaphthene, fluorene, phenanthrene, anthracene, fluoranthene, and pyrene. The fiber-retracted SPME devices were deployed in June and retrieved in August (2 month sampling period). The minimum sampling time was estimated with equation 5.6, where n was 1 pg, the detection limit of the instrument, and $\overline{C}$ was the approximate concentration of the target analyte in the sample, which is based on the reference data. The SPME PDMS rod and PDMS thin film samplers were also deployed in June, but retrieved after 1 month and replaced with new samplers (too long sampling time will cause all of the preloaded standards to be lost). The new samplers were retrieved in August.

5.3.6 Instrument

5.3.6.1 Thin Film and Rod Analysis

For the analysis of the PDMS thin films, the thin films were coiled and rotated for insertion into the gas chromatography (GC) liners (Figure 5-3). These liners were purchased specifically from ATAS for this purpose. The top was sealed using a crimped cap, and the bottom was open to the GC column. The liners were held on a cooled DTD tray until analysis. During analysis, the thin films or rods remained in the GC inlet at 280°C for the entire GC runtime.

The thin films or rods were analyzed using an Agilent 6890 GC and 5973 Mass spectrum detector (MSD) equipped with a total analytical system (ATAS) Optic 3 direct thermal desorption (DTD) large volume injector (LVI) system (Veldhoven, the Netherlands). The ATAS system, in combination with the CombiPAL autosampler (Leap Technologies, Carrboro, NC), was used for the pneumatic exchange of liners between the cooled autosampler tray to the GC injector. A Varian (Chrompack) CP Sil 8 CB column (5% diphenyl–95% PDMS, 30 m, 0.25 mm i.d., 0.25 μm film thickness) was used with a splitless helium flow as the carrier gas at a flow rate of 1 mL/min.
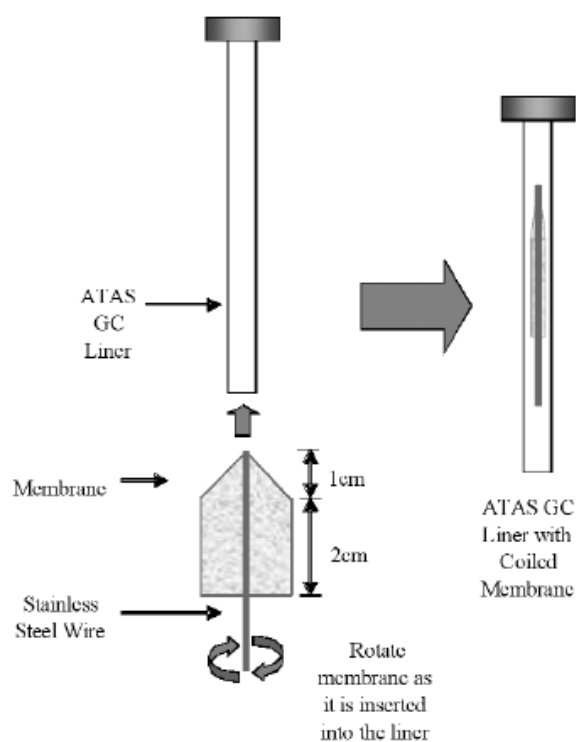
Figure 5-3 Thin film design and insertion into liner for analysis

Because the ATAS system was equipped with a cryotrap to focus the analytes, the temperature of the cryotrap was 0 °C for the first 10 min and then increased to 280 °C for the duration of the run. The GC oven temperature started at 40°C, where it was held

constant for 13 min, and then increased at a rate of 15°C/min to 250°C and held constant for 3 min. The total GC run time was 30 min. The MS system was operated in the electron ionization mode and tuned with perfluorotributylamine. A mass scan from 40 to 300 was obtained, and the base peak of each compound was selected and integrated.

The instruments were calibrated with six-point calibration curves, which were plotted with six methanolic standard solutions. The concentrations of the solutions ranged from 1 ng/mL to 100 μg/ mL. Peak shape quality, resolution, and retention times were also carefully monitored to ensure that the chromatography was within the required specifications.

5.3.6.2 SPME Fiber Analysis

A Varian 4000 ion trap GC/MS system fit with a SPB-5 column (30 m, 0.25 mm i.d., 0.25 μm film thickness) (Supelco, Mississauga, ON, Canada) was used for the analyses of the SPME fibers. Helium as the carrier gas was set to 1 mL/min. For SPME injection, the 1079 injector was set to 270 °C, and the desorption time was set at 10 min. For liquid injection, the injector was set at 40 °C and then increased to 250 °C at a rate of 100 °C/min. A 1093 SPI liner was used for the 1079 injector to ensure the sample transfer efficiency was the same for both the SPME injection and the liquid injection. The column temperature was maintained at 40 °C for 2 min and then programmed at 30 °C/ min to 250 °C, held for 5 min, then programmed at 30 °C/min to 280 °C, and held for 15 min. The total run time was 30 min. The MS system was operated in the electron ionization mode and tuned with perfluorotributylamine. A mass scan from 40 to 300 was obtained, and the

base peak of each compound was selected and integrated. The instruments were calibrated with the same method as described in thin film analysis.

5.4 Results and Discussion

5.4.1 Validation of Kinetic Calibration Method in the Thin Film Extraction in Flow through System

A standard flow-through system has been developed by Ouyang *et al.* that employs the use of DispoDialyzers (Spectrum Laboratories, Rancho Dominguez, CA) for the permeation of PAHs into a flowing water system. The concentration of PAHs in the system is known to remain constant throughout the sampling period. [33] This same system was used with the PDMS thin films. Pyrene was used as the target analyte and deuterated pyrene as the standard. Three thin films were first loaded with the standard using an aqueous solution with a concentration of 10 ng/ mL and 45 min exposure time of the thin film to the standard solution. They were then exposed in the flow through system for periods of 2, 4, 6, and 14 h. After removal and analysis, the amounts of pyrene extracted by thin film and deuterated pyrene remained on the thin films were determined. Equation 5.5 was used to calculate the pyrene concentrations in the flow through system. The results were then compared with the concentrations determined by SPME spot sampling, and the results by two methods were similar, as shown in Table 5-1. This demonstrated experimentally the feasibility of kinetic calibration method in thin film extraction.

The SPME method consisted of direct extraction of analytes from a 10 mL vial containing a 10 mL sample of water withdrawn from the flow-though system. It was

completed with three replicates using a 100 μm PDMS fiber. Equilibrium was reached for these PAHs with SPME within 30 min.

Table 5-1 Concentration of pyrene determined using thin film extraction with kinetic calibration as compared to the results obtained by SPME fiber spot sampling.

	Concentration				
Analyte	2 h	4 h	6 h	14 h	SPME
Pyrene	10.2	11.1	11.1	16.3	15.8

5.4.2 Sampling by Thin Film Sampler in September, October and November in 2005

5.4.2.1 Meuse River Results

The samplers that were placed in the Meuse River were part of a study by the Screening Method for Water Data Information in support of the implementation of the Water Framework Directive (SWIFT-WFD). The SWIFT-WFD objectives include improving, protecting, and preventing further deterioration of water quality across Europe. SWIFT-WFD is a multi-disciplinary project with many different types of spot, continuous, and passive samplers. The results of the larger study illustrated that PAH concentrations are typically within the low to sub ng/L range in the Meuse River, which inhibits detection by most conventional passive samplers. [34] The three samplers from the Netherlands had slightly different concentrations of target analytes on the thin films. In the river water samples, the amount of the PAHs was found to be in the sub ng/ L range. For fluoranthene,

the concentration range was from 0.154–0.346 ng/L, and for pyrene, the concentration range was between 0.165–0.482 ng/L. These results were within the expected concentration range of the study.

5.4.2.2 Hamilton Harbour Results

The concentrations of contaminants in Hamilton Harbour were determined over one-month intervals throughout a three-month period at two sampling sites and at three different depths at each site. The results in Table 5-2 illustrate that the concentrations of fluoranthene and pyrene were in the low ng/ L levels at all of the sampling locations. Generally, the PAH concentrations were higher in the surface water compared with the deeper water depths. This may be because of constant sources of pollution that are fed into the lake water. Also, the thin film extraction in the surface water were found close to equilibrium after the one month sampling period, but the extraction at the other two depths were far away to reach equilibrium. This may be because of the higher turbulence in the surface water compared with the deeper water, which improves the sampler kinetics.

The PAH concentrations at the second sampling site were found to be slightly lower than those at the first site at the lower sampling depths, likely because the second sampling site was in the middle of the lake, farther from the steel factory effluents. However, higher concentrations of PAH were detected in the shallow sampling depths at both sampling sites.

The data from both sample sites in the Hamilton Harbour were comparable to the results obtained by traditional liquid–liquid extractions completed by C. Marvin of the

Water Science and Technology Directorate at Environment Canada. [35] The PAHs were measured in the water from the harbour and the total concentration of fluoranthene is in the range of 2–152 ng/ L and between 1–141 ng/ L for pyrene. [35] The data in Table 5-2 are based on the average of three samplers at each sampling site and depth. The RSD values for the samplers were generally less than 20%. For the samplers at the 2.5 m depth for September site 2, there was only 1 sampler analyzed for that point because the other two had been lost from the sampling basket during sampling because of broken wire in the sampling basket.

Table 5-2 Concentrations of fluoranthene and pyrene during three months in Year 2005 in Hamilton Harbour.

Analyte	Date	Concentration (ng/L)					
		Site 1			Site 2		
		1 m	11.5 m	21m	2.5m	11.5m	22.5m
Fluoranthene	Sept	7.2±1.4	8.5±0.4	2.4±1.0	2.5±0.4	2.7±1.3	2.4±2.0
	Oct	15.0±2.4	8.7±2.6	2.3±0.4	20.5±3.9	3.2±0.9	2.6±0.2
	Nov	9.6±2.3	2.1±0.2	2.1±0.2	8.4±0.7	7.9±0.1	6.5±0.6
Pyrene	Sept	11.9±8	10.8±1.4	4.9±1.5	1.8	4.4±2.1	6.2±1.9
	Oct	16.6±2.4	10.3±3.1	3.8±0.2	38.4±4.5	3.7±0.3	3.7±1.1
	Nov	10.4±1.5	2.9±0.3	2.6±0.5	22.0±1.4	19.4±0.1	12.7±0.2

5.4.3 Sampling by Three Types of SPME Samplers in July, August, 2006

5.4.3.1 Hamilton Harbour Results

For the fiber-retracted devices, the TWA concentrations of the target analytes in the sampling environment were calculated with equation 5.6. The average temperatures at the three different depths were used as the approximate temperature for sampling. Figure 5-4 illustrates the temperature profile of different depths in Hamilton Harbour on June 19. For the PDMS rod and PDMS thin film samplers, the TWA concentrations of the target analytes in the sampling environment were calculated with equation 5.5.
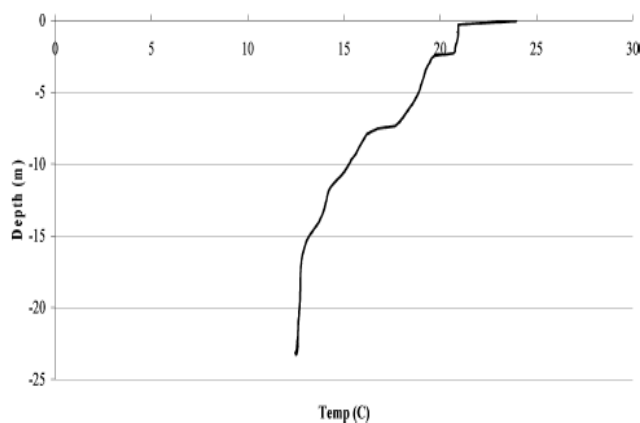
Figure 5-4 Temperature profile of different depths in Hamilton Harbour

Table 5-3 presents the TWA concentrations of target analytes at the sampling sites, as determined by the three types of SPME passive samplers. The results illustrate that the concentrations of PAHs were in the low ng/L levels and were a little higher in the surface water compared with the other sampling depths. This may be due to the source of the pollution typically discharged at surface depths. The data in Table 5-3 are the average values of PAHs as detected by the three samplers. For the PDMS rod and PDMS thin film samplers, only fluoranthene and pyrene were quantified since only deuterated fluoranthene

and deuterated pyrene were loaded as the internal standards. The results in Table 5-3 illustrate that the concentrations of fluoranthene and pyrene at different depths obtained by three types SPME passive samplers were quite close. The results obtained by the SPME fiber retracted devices and the PDMS rod and PDMS membrane samplers are in the range of the data obtained by spot sampling with traditional liquid-liquid extractions, as reported by C. Marvin. [35]

Table 5-3 PAH Concentrations in Hamilton Harbour obtained by three types of SPME samplers in Year 2006.

		Concentration (ng/ L)					
Depth	Sampler	Acenaphthen	Fluorene	Phenanthene	Anthrancene	Fluoranthene	Pyrene
1 m	Fiber	17.6±2.3	21.7±3.7	28.3±4.0	3.7±0.8	18.9±0.4	22.9±3.4
	Rod	NQ	NQ	NQ	NQ	17.7±1.7	26.5±3.8
	Thin film	NQ	NQ	NQ	NQ	14.4±1.6	28.6±2.6
11 m	Fiber	15.2±0.7	ND	ND	ND	7.8±0.8	10.1±0.5
	Rod	NQ	NQ	NQ	NQ	8.7±2.5	8.4±0.9
	Thin film	NQ	NQ	NQ	NQ	8.3±1.4	10.1±2.5
21 m	Fiber	15.5±2.9	19.2±2.3	ND	ND	8.6±0.8	9.9±1.2
	Rod	NQ	NQ	NQ	NQ	6.8±1.4	7.3±1.4
	Thin film	NQ	NQ	NQ	NQ	5.4±0.5	8.3±1.8

ND, not detected; NQ, not quantitated.

5.4.3.2 Effect of Turbulence

One problem that is commonly encountered during field sampling is the effect of turbulence on the sampling environment.

Table 5-4 Levels of the extracted analytes and the remaining standards on the rod and thin film samplers at three different depths.

Sampler	Depth (m)	Mass (ng)			
		Fluoranthene	d10-fluoranthene	Pyrene	d10-pyrene
Rod	1	3.8±0.2	3.1±0.3	4.8±0.3	2.4±0.2
	11	0.6±0.2	37.6±9.6	1.1±0.2	45.5±7.7
	21	0.5±0.1	85.7±3.2	0.6±0.1	77.1±4.3
Thin Film	1	36.7±7.1	3.3±0.3	68.8±8.2	2.9±0.2
	11	5.0±1.5	90.4±12	8.8±0.7	32.9±2.1
	21	3.2±0.2	110.6±1.5	7.3±0.3	52.8±1.6

The amount of preloaded standards were about 168 ng for d10-fluoranthene and 176 ng For d10-pyrene.

For field water sampling, the flow rate of surface water sites should be higher than the deeper water sites, since the surface can be easily affected by the wind and moving boat traffic. Table 5-4 presents the amounts of the extracted analytes and the remaining standards on the PDMS rod and PDMS thin film samplers at different depths in Hamilton Harbour after a 1 month sampling period. The results indicate that the higher flow rate of the surface water contributed to the higher rate of loss of the preloaded standard.

Conversely, the amounts of the target analytes extracted on the PDMS rod and PDMS thin film samplers at the surface water were greater than the amounts extracted at other depths. These observations confirm that the kinetic calibration method can effectively compensate for the turbulence factor that can be encountered in field sampling.

For the fiber-retracted SPME device, it has been proven that the mass uptake is independent of the face velocity, due to the extremely small inner diameter of the fiber needle. [22] In this field trial, the concentrations of fluoranthene and pyrene at different depths were quite close to the results obtained by the rod and thin film samplers, which demonstrated that the flow rate of the sampling environment did not affect the mass uptake of the fiber retracted SPME field water sampler.

For all three types of SPME passive samplers, the effect of the turbulence was avoided or effectively compensated for with a preloaded standard. This feature is desirable for long-term field water sampling, especially where the convection conditions of the sample environment are difficult to measure and calibrate.

5.4.3.3 Comparison of three types of SPME samplers

The three types of SPME passive samplers that were used in this field trial possess all of the advantages of SPME: they are solvent-free, combine sampling isolation and enrichment into one step, and can be directly injected into a GC for analysis without further treatment. The three types of SPME passive samplers were easy to deploy and retrieve.

The cost of the field sampler is a very important factor for application. A sampler that

is manufactured of PDMS thin film or PDMS rod is inexpensive. Conversely, the cost of the fiber-retracted device is higher. The data in Table 5-3 illustrate the difference in quantification for the three types of SPME passive samplers. For the fiber-retracted SPME device, all of the analytes were quantified and no internal standard was required. Conversely, the rod and thin film samplers can only quantify analytes with a corresponding internal standard. This is due to the fact that the kinetic calibration method can only calibrate analytes with similar physicochemical properties to the preloaded standard.

With different sampling approaches and different surface to volume ratio, the sampling rate of three SPME passive samplers were different. Figure 5-5 illustrates the sampling rates of three types of SPME passive samplers at different sampling depths.

$$R_s = n / \overline{C}t \qquad\qquad \text{Equation 5.8}$$

where R_s is the sampling rate, n is the extracted amount of analyte, $\overline{C}$ is the TWA concentration of analyte in the sample, and t is the sampling time.
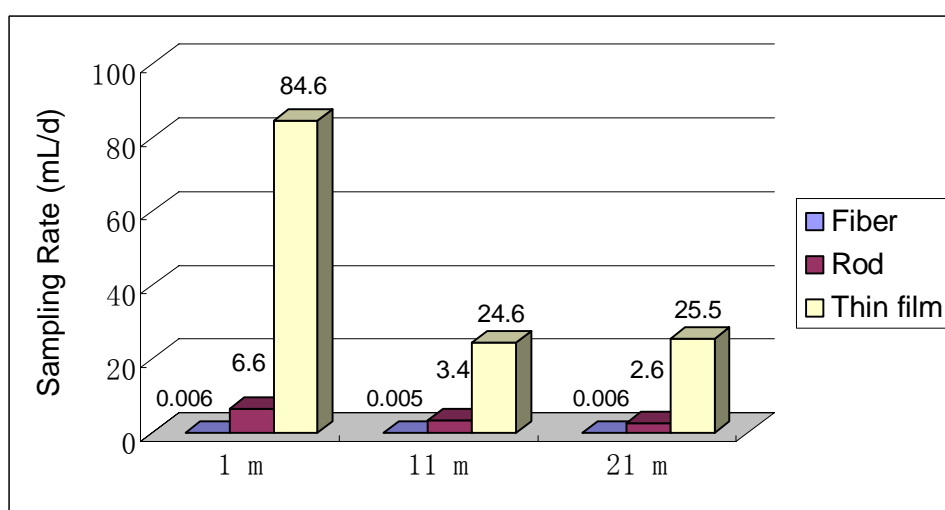
Figure 5-5 Sampling rates of three types of SPME samplers at different sampling depths

The thin film sampler exhibited the highest sampling rate, due to the large surface-to-volume ratio. The sampling rate of the fiber-retracted SPME device was much lower than the rod and thin film samplers, because the extraction phase did not contact the sample matrix directly and the diffusion of the analyte molecules was very slowly in water. This illustrates that the sensitivity of this type sampler is lower than that of the rod and thin film samplers. The sampling rates of the rod and thin film samplers at the surface sampling depth were obviously higher than other depths because the flow rate of the surface water was higher than the deeper waters.

5.5 Conclusion

The feasibility of kinetic calibration method in poly (dimethylsiloxane) (PDMS) thin film extraction was experimentally proven for the analysis of polycyclic aromatic hydrocarbons (PAHs) in the flow through system. On site sampling in Hamilton Harbour in 2005 and determination of TWA concentrations of PAHs based on kinetic calibration were successfully completed using thin film extraction. In addition, the thin film sampler, a modified fiber-retracted SPME field water sampler, and a SPME PDMS rod, were used simultaneously to determine the TWA concentrations of PAHs in Hamilton Harbour in 2006. The thin film sampler exhibited the highest sampling rate compared to the other water samplers, due to its large surface-to-volume ratio.

Chapter 6

Passive Water Sampling Using Thin Film and Worms

6.1 Introduction

Monitoring persistent organic pollutants such as PAHs represents an ongoing challenge to the environmental chemist because of their extremely low solubility in water. Biomonitoring as an integrative technique can effectively be used to continuously sample an aquatic environment. In aquatic organisms, the bioconcentration of lipophilic compounds from water results in increased tissue concentrations, which greatly exceed those in the external water environment. [1] Due to their low solubility in water it is much easier to determine the concentrations of these compounds in the organisms than it is in water.

Many organisms fulfill the criteria for passive sampling. Living organisms commonly used as biomonitors include: fish, blue mussels, freshwater mussels, yellow eels, bivalves (including modern clams, scallops and oysters) and benthic invertebrates. [1, 2] Optimal biomonitors are usually resident species, since migratory species do not reflect the pollutant levels at any particular location. In addition, the organism selected for use as a biomonitor should be widely distributed over the examined area and be easy to collect. They should come from a stable population to ensure long-term monitoring. Tissue concentrations of pollutants in free-living organisms integrate both uptake from water (which is largely passive), and uptake from diet (which is largely active). This can be either an advantage or a disadvantage depending on whether one is looking for an estimate

of uptake solely from water (bioconcentration) or from the entire environment including diet (biomagnification).

Comparatively, passive sampling devices will not die from diseases, get eaten by predators or die from suboptimal environmental conditions. Several passive sampling devices have been developed for the determination of PAHs in water, such as ceramic dosimeter and Semipermeable membrane devices (SPMDs). [3] SPMDs can be deployed for long periods of time (days to months). PAHs have been shown to accumulate in SPMDs in rivers following a flood and in ocean water. [4, 5] However, the main disadvantage of the SPMD technique is the time-consuming sample treatment procedure. Polyethylene membrane without lipid was reported to be more convenient for assessing hydrophobic organic compounds in aquatic environments. [6, 7] Nevertheless, most permeation and diffusion devices still utilize solvent as a collecting medium or for analyte desorption.

The passive extraction approach with solid phase microextraction (SPME) is widely accepted for monitoring organic compounds in environmental samples. SPME is a solventless sample preparation and extraction technique deployed as a fiber coated with a liquid polymeric sorbent coating in a sample matrix. [8-11] For passive sampling the fiber coating is withdrawn a known distance into its needle during the sampling period. [12-15] The well-defined geometry of the diffusion zone allows for diffusion-based calibration of the mass uptake. SPME technique has been used to evaluate liposome-water partitioning coefficients for assessing bioaccumulation potential of hydrophobic organic chemicals (HOCs). [16] Matrix SPME was compared to Tenax extraction to evaluate the bioavailability of hydrophobic contaminants from sediment. [17]

Recently, another two techniques of SPME, including a PDMS rod and a PDMS thin-film have been developed. [18, 19] PDMS thin-film possessed the highest surface to volume ratio, which resulted in the highest sensitivity and mass uptake. Unlike the thick coatings of SPME rods, the high extraction rate of the thin-film SPME technique with very thin extraction phase allows for the extraction of larger amounts of analyte within a shorter period. Therefore, a higher extraction efficiency and sensitivity can be achieved without sacrificing analysis time. [19]

Van der Heijden *et al*. compared SPME fibers to aquatic worms (Lumbriculus variegatus), polyoxymethylene solid-phase extraction (POM-SPE), and hydroxypropyl-beta-cyclodextrin-(HPCD) for predicting PAH bioavailability in sediment.[20] In our study, we aim to investigate the feasibility of the thin-film sampler for measuring the bioavailability of PAHs in aquatic environment. Considering the higher extraction efficiency by thin film technique compared to common fiber SPME, the performance of two passive sampling techniques: thin-film extraction and bioconcentration by black worms (*Lumbriculus variegatus*) were compared in a flow-through system. The black worm was chosen as biomonitor because it has low demand and it is easy to handle and to culture. This study also investigated the relationships among three relevant PAH coefficients: partition coefficient between octanol and water (K_{ow}), partition coefficient between thin film and water (K_{tfw}), and bioconcentration factor (BCF) of worms in water.

6.2 Experimental Section

6.2.1 Chemicals and Supplies

Methanol (HPLC grade) was obtained from BDH (Toronto, ON, Canada). Stock solutions of PAHs in methanol (100 mg/L) were prepared from pure solid standards of acenaphthene, fluorene, anthracene, fluoranthene, pyrene, purchased from Supelco (Oakville, ON, Canada). Deionized water was obtained using a Barnstead/Thermodyne NANO-pure ultrapure water system (Dubuque, IA, USA). The polydimethylsiloxane (PDMS) thin film (SSPM 100, 127 μm thick), was purchased from Specialty Silicone Products Inc (Ballston Spa, NY). Helium (ultrahigh-purity grade) was purchased from Praxair (Kitchener, ON, Canada). Black worms were obtained from Ward's Natural Science Company, (St. Catharines, ON, Canada).

6.2.2 Thin Film Sampler and Worm Sampler

The PDMS thin-film was cut into a 1 mm × 1 cm rectangle. The surface area of one side was 10 mm^2 and the weight of each thin-film was about 0.0025 g. The thin film was conditioned for 1 hour at 250 ºC in a GC injection port before being used. Between consecutive extractions a blank run of the same PDMS thin film was analyzed, confirming that there was no carryover of the target analytes on the thin film from the previous desorption.

Lumbriculus variegates is a freshwater Oligochaete. They live throughout North America and Europe in shallow water marshes, ponds, and swamps, feeding on microorganisms and organic material. On average, an adult black worm can have 150 to

250 segments. In this study, the average weight of the worms was approximately 0.02 g. The black worms were cultured with small pieces of paper towel in deionized water. Throughout the whole experiment, all the worms remained healthy and alive.

6.2.3 PAH Concentrations in Flow through System

The flow-through system for the generation of a standard PAHs aqueous solution has been previously described. [21] Unlike the commonly used spiking approach, this system utilized a DispoDialyzer to generate constant PAHs aqueous solution, which avoided the effect of solvent on the experiments. The PAH concentrations in the flow-through system were determined by SPME direct extraction. Ten milliliters of the effluent was collected and agitated at 500 rpm (Gerstel Agitator). The SPME procedures were performed automatically with a Gerstel MPS2 autosampler. A 30 min extraction was followed by fiber desorption in the GC injector. External calibration was used for the quantification.

6.2.4 Uptake by Passive Samplers in Flow through System

A 1 L sampling chamber with an inlet close to its bottom and an outlet near its top was used to collect the effluent after passing through the sampling cylinder. The extractions by thin-films and black worms were performed in this chamber at the room temperature $(25^{o}C)$ up to 11 days. The upper outlet of the chamber was high enough so that the worms could not climb up and escape from it.

Approximately 20 pieces of PDMS thin-films and 50 black worms were placed in the

sampling chamber. They were exposed to the same contaminated solution at the same time. Each time, one thin-film and three or four black worms were collected from the system at the same time to evaluate and compare the concentration of target organic contaminants. After the uptake of PAHs, each group of worms was weighed and sealed in a small vial and frozen at -20 °C prior to subsequent chemical analyses.

6.2.5 Sample Treatment of Worm Samples

After thawing, the worms were placed in a specially made test tube. Five milliliters of acetone and 0.1 g of anhydrous Na_2SO_4 solid were added. The mixture was homogenized by 10 passes with a Polytron at 900 rpm. When the solution thickened and the tissue was crushed completely, 5 mL of hexane was added to the mixture. The residue on the Polytron and the tube was then rinsed with a mixed solvent of 1:1 acetone and hexane. The homogenate was filtered in a funnel with the aid of suction with the mixed solvent. The filtrate was collected in a glass Erlenmeyer flask and transferred to a 25×150 mm test tube. The filtrate was vigorously shaken for 1 minute to mix the two phases thoroughly, and centrifuged at 3000 rpm for 5 minutes to separate the lower acetone layer and the upper hexane layer containing the extracted PAHs. One milliliter of deionized water was carefully added along the side of the tube to form a division between the two layers. The tube was placed in dry ice until the intermediate aqueous phase was frozen. The top layer (hexane with PAHs) was decanted into a second test tube and was evaporated to near dryness using nitrogen. 1.5 mL of hexane was then added to the test tube to reconstitute the worm extract. Finally, 1 μL of reconstituted solution was injected

into GC for analysis.

6.2.6 Instrument

Gas chromatography was performed on an Agilent 6890 GC and 5973 MSD equipped with a Multipurpose Sampler (MPS 2) system (Gerstel GmbH, Mulheim, Germany). The Thermal Desorption System (TDS-2) unit was mounted on the GC via the Cooled Injection System (CIS-4) inlet for the thermal desorption of the analytes. The thin-film was placed in a glass tube of (187 mm length, 6 mm o.d., and 4 mm i.d.) for desorption.

CIS-4 has a Septum-Less Head (SLH), which eliminates contamination from septum bleed or particles and prevents loss of analytes. A Thermal Desorption Unit (TDU) was used for large volume injection (LVI). The tube with the sampler was heated in order to transfer the compounds into the CIS-4. The CIS-4 acts as cryogenic trap by focusing and concentrating the components to be determined; it is then heated, transferring the components to the capillary column. The temperature of the CIS-4 was 0 ºC for the first 5 minutes, during which time the temperature of TDU was increased to 280 ºC for analyte desorption. After desorption, the cooled liner with the thin film was removed from the TDU, followed by a temperature increase of the CIS-4 to transfer the analytes to the GC column. The transfer line situated between the thermodesorption device and the CIS-4 was set at 300 ºC.

An HR-1 capillary column (30 m, 0.25 mm i.d., 0.25 μm film thickness) (Shinwa, Kyoto, Japan) was used with helium as the carrier gas, at a flow rate of 1 mL/min. For the analysis of the PDMS thin film, column temperature was maintained at 40 ºC for 2

minutes, then programmed to increase at a rate of 15 ºC /min to 280 ºC, and then held constant for 2 minutes. The total run time was 20 min. The MS system was operated in the electron ionization (EI) mode and tuned to perfluorotributylamine (PFTBA). A mass scan from 50 to 300 m/z was acquired and the base peak of each compound was selected and integrated.

Absolute amounts of the target analytes were calibrated by the injection of liquid standards. Peak area, shape quality, resolution, and retention times were carefully monitored to ensure all chromatography was within required specifications.

6.3 Results and Discussion

6.3.1 Extraction of PAHs by Thin Film

The average concentrations of acenaphthene, fluorene, anthracene, fluoranthene and pyrene in the flow through system (n = 3) were 3.51, 1.03, 0.62, 0.13 and 0.14 μg/L, respectively, determined by SPME direct extraction. PDMS thin-film was used to investigate the uptake of the analytes, both prior to equilibrium and at equilibrium. Figure6-1 (A) shows the PAHs concentrations in the thin film samplers after 4, 6, 7, 10, and 11 days of exposure. These concentrations were calculated by dividing the extracted amount in a thin film by its accurate weight ($ng·g^{-1}$). The extraction of all the analytes by the thin film reached equilibrium after 10 days.

(A)
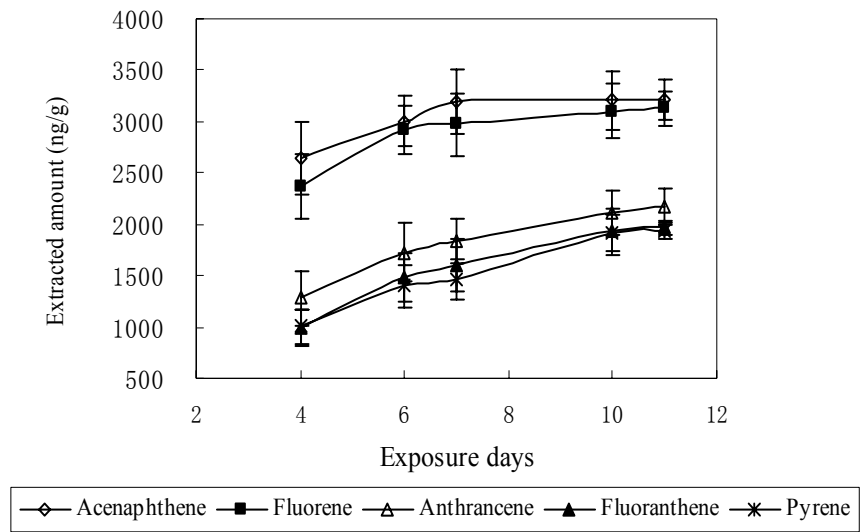
(B)
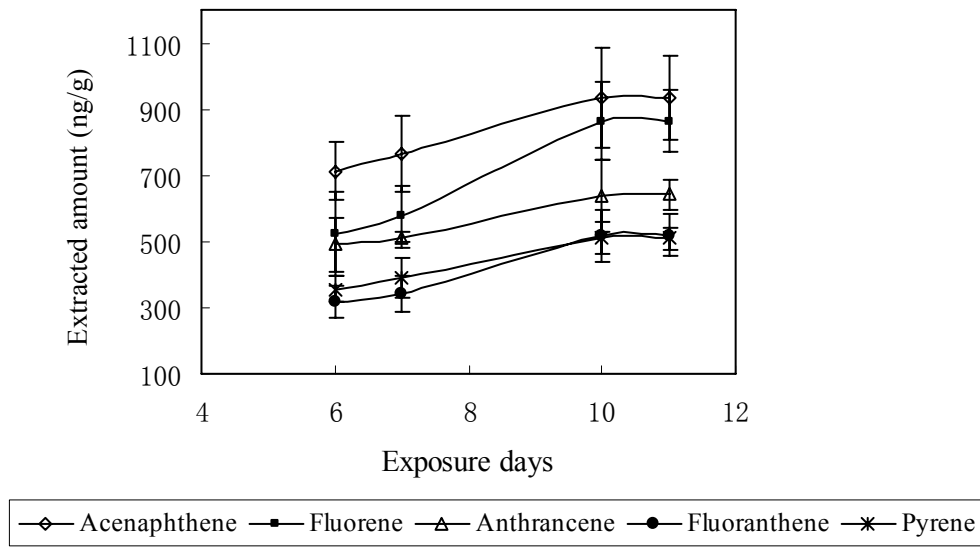
Figure 6-1 Extraction time profiles of five PAHs by thin films (A) and worms (B) in the

flow-through system.

Table 6-1 lists the partition coefficients (K_{tfw}) determined by using equilibrium concentrations in the thin film and aqueous concentrations in the flow-through system. K_{ow} is the compound's partition coefficient between water and octanol, and is the most accepted indicator of a compound's hydrophobicity. The PAH log K_{ow} values are from Huckins *et al.* [22]

Table 6-1 Partition coefficients and bioconcentration factors of five PAHs.

Analytes	Partition coefficient (K_{tfw})	Bioconcentration factor (experimental)	Bioconcentration factor (literature) (ref. 29)	Log K_{ow}
Acenaphthene	913	266	387	4.22
Fluorene	3010	838	506, 315	4.38
Anthrancene	3422	1032	NA	4.54
Fluoranthene	14851	3992	14836, 2705	5.20
Pyrene	13629	3635	4810, 1400	5.30

In Figure 6-2 (A), the K_{tfw} are plotted against log K_{ow}. The partitioning of PAHs in the thin film increased with increasing hydrophobicity. The K_{tfw} was reasonably well correlated with K_{ow} values ($R^2 = 0.92$), as shown in the following equation:

$$LogK_{tfw} = 0.98LogK_{ow} - 1.0 \qquad \text{Equation 6.1}$$

It should be remembered that the trends are only valid for compounds within the same group with similar structures, such as aromatic hydrocarbons. They cannot be used to

make comparisons between different groups of compounds, due to different analyte activities in the polymers.

(A)

Log K_{tfw} = 0.98Log Kow - 1.0
R^2 = 0.92

(B)

Log Ktfw = 0.0018(RI) + 0.4541
R^2 = 0.94
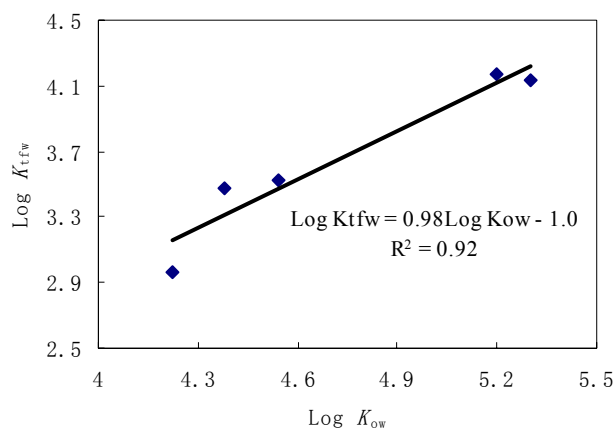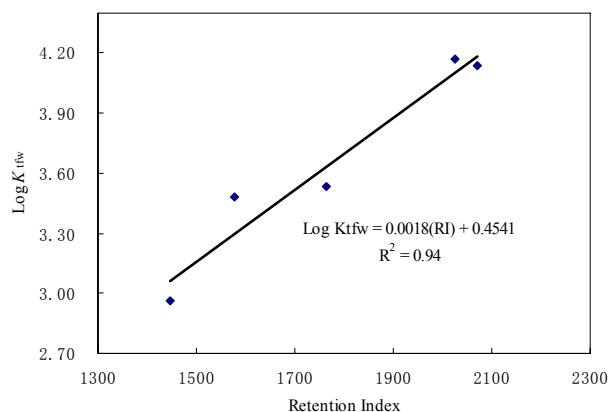
Figure 6-2 Relationship between log K_{tfw} and log K_{ow} (A); relationship between log K_{tfw} and retention index (B).

The equation for the relationship between log K_{tfw} and retention index (RI) for five PAHs is presented in Figure 6-2 (B). The RI values used were from literature. [23-27] The r-squared correlation coefficient for Log K_{tfw} as a function of RI was 0.94 and indicated

that Log K_{tfw} is linearly related to RI, as demonstrated by Saraullo *et al.* [28]

Compared to the PDMS thin film investigated previously with a surface area of 10 cm^2, the thin films used in this study had a surface area of only 0.2 cm^2 (0.1cm^2/side × 2). They extracted an insignificant portion of the target analytes; therefore, they did not affect the partition in the system and avoided the depletion of the analytes during extraction.

6.3.2 Bioconcentration in Black Worms

A blank analysis of worm was conducted and PAH compounds were not detected. The complicated process of sample treatment of the worm samplers after uptake of PAHs led to the inevitable loss of a portion of the analytes. Recovery of the analytes during the sample treatment was evaluated using blank worms and a recovery yield was applied to the concentrations. The blank worms were mixed with 500 ng of acenaphthene, fluorene, anthracene, fluoranthene and pyrene, followed by the sample treatment. The amounts of each compound remaining in the worms after sample treatment were determined. This remaining amount was divided by 500 ng to obtain the recovery for each individual compound. The recovery of standards averaged 55.8 % for acenaphthene, 65.4 % for fluorene, 72.6 % for anthracene, 82.4 % for fluoranthene and 83.7 % for pyrene. The recoveries increased with increasing molecular weight (M_w). Clearly, the lower volatilities of the high M_w compounds reduced the degree of loss during the sample treatment.

The bioconcentration factor (BCF) is the ratio of the concentrations of a chemical in the biotic and water phases at equilibrium. The bioconcentration factors of five PAHs in the worms were calculated and listed in Table 6-1. This was achieved by using the

concentrations of PAHs in the worms and the dissolved phase concentrations of the compounds in the flow-through system. This data analysis was performed based on the results obtained on the 10th day, since the steady-state levels in Oligochaetes were reached after 10 days as indicated in Figure 6-1 (B). The U.S. EPA's ECOTOX database (U.S. EPA 2006a) is the largest compilation of ecotoxicity data, providing information on the effects of single chemical to aquatic and terrestrial species. [29] The reported BCF values are comparable to the values in this study.

(A)

Log BCF = 0.95log Kow - 1.4
$R^2 = 0.92$

(B)

Log BCF = 0.0017(RI) - 7E-05
$R^2 = 0.95$
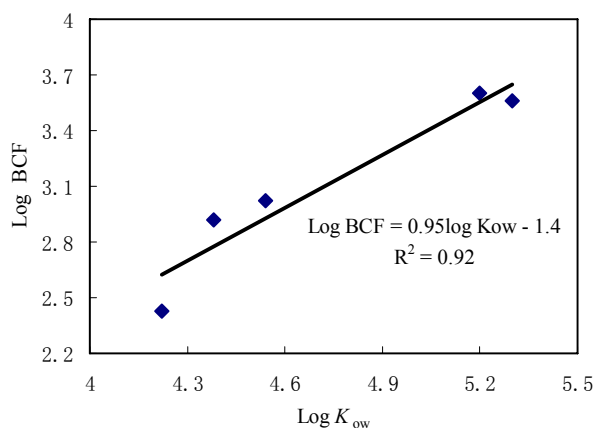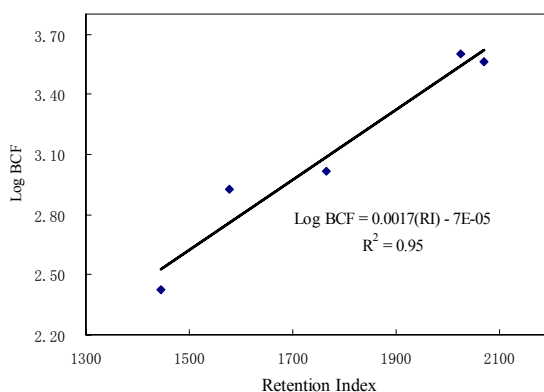
Figure 6-3 Relationship between log BCF and log K_{ow} (A); relationship between log BCF and retention index (B).

The logs of the BCFs listed in Table 6-1 were plotted against the log K_{ow} in Figure6-3(A). The log BCFs of five PAHs were linear to their log K_{ow}s ($R^2 = 0.92$). The following relation was obtained:

$$LogBCF = 0.95LogK_{ow} - 1.4 \qquad \qquad \text{Equation 6.2}$$

The log BCF increased from 2.43 to 3.56 for PAHs with log K_{ow}s, which ranged between 4.22 and 5.30. This trend was similar to the logs of the thin-film partition coefficients. Figure 6-3 (B) also presents the linear relationship between Log BCF and retention index.
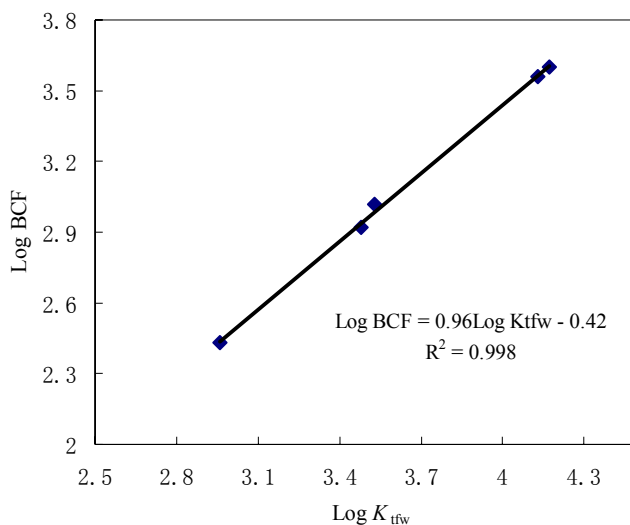
Figure 6-4 Relationship between log BCF and log K_{tfw}.

Figure 6-4 shows a good linear relationship between log BCF and log K_{tfw}, with R^2 values as high as 0.998, which exhibits much better linearity than Log BCF/ Log K_{ow} and Log K_{tfw}/ Log K_{ow}

$$LogBCF = 0.96LogK_{tfw} - 0.42 \qquad \qquad \text{Equation 6.3}$$

Equation 6.3 can be used to predict the bioconcentration factors of PAHs with different K_{tfw}s, which provides a means to measure the bioavailability of environmental contaminants.

6.3.3 Comparison of Thin Film Sampler and Worm Sampler

The cost of the sampler is always an important consideration in an environmental analysis. The black worm has a high cost and requires lethal sampling. On the contrary, the cost of thin-film is very low and it can be reused. The precision of the two sampling methods was indicated by the standard deviations for the triplicate analysis. The relative standard deviations (%RSDs) of three replicates by thin-film uptake ranged from 5 % to 15 %. In the case of the worms, %RSDs were about 20 %. The reason could be the variability of locations occupied by the worms while in the solution. Support for this reasoning came from the observation that most of the worms huddled in the centre of the solution, which resulted in a decreased access to the solution for the worms in the middle of the huddle. These conditions may have reduced their uptake of target analytes.

We also compared the PAHs uptake ability of worms and thin-films in the flow-through system. In Figure 6-1 (A), the uptake of PAHs by thin-film was rapid. By day 7, thin-film had extracted significant amounts of acenaphthene and fluorene, and the concentrations appeared to reach steady-state values. These concentrations were around 3,000 ng·g^{-1} and 3,200 ng·g^{-1} on the thin-film weight basis. Extraction of anthracene, fluoranthene, pyrene reached equilibrium after 10 days. Likely a faster equilibrium was reached by the thin-film than by the worms because the thin film had a thinner extraction

phase than the worm body.

When we investigated the concentrations in the two samplers after the same time period (Figure 6-1 (A) and (B)), it was found that thin films could uptake much more analytes than the worms. Saint-Denis and Styrishave *et al*. observed the metabolism of PAHs in the tissues of earthworms, either by cytochrome P450 pathways or via free radical oxidation. [30, 31] Metabolism of PAHs involves the conversion of these hydrophobic xenobiotics into more polar compounds. [30] That is, the metabolism of PAHs associated with an increased duration, may have accounted for a lower net uptake by the worms. Furthermore, compared to the pure liquid PDMS extraction phase of the thin-film, the worm body contained high water content. This hypothesis might also explain the larger slope of Figure 6-2 (A), than that of Figure 6-3 (A). The integration of biochemical techniques with an enhanced knowledge of worm metabolism will facilitate an understanding of the mechanisms by which worms are able to uptake pollutants.

In the initial extraction stage, the rate of SPME extraction is proportional to the surface area of the extraction phase: [19]

$$\mathrm{d}n / \mathrm{d}t = (DA / \delta) C \qquad\qquad \text{Equation 6.4}$$

where D is the analyte's diffusion coefficient in the sample fluid, A is the surface area, δ is the boundary layer thickness and C is the concentration of analyte in the sample.

Equation 6.4 can be transformed to equation 6.5:

$$\mathrm{d}n / A\mathrm{d}t = (D / \delta) C \qquad\qquad \text{Equation 6.5}$$

The sampling environment and the characteristic of a sampler determine the boundary layer thickness. The thin-films and worms were exposed in the same sampling system; the

only difference between the two samplers was their behaviors during the uptake. The worms were alive and swam slowly. On the other hand, the thin-films didn't move by themselves but just floated in the flowing environment. Thus, the difference in their relative motions to sample fluid might cause a slight decrease in boundary layer thickness of the worm extraction than of the thin film extraction. As a result, there is a slight increase in extracted amounts of certain PAHs per unit surface area by the worms than by the thin-films after the same extraction time (Figure 6-5). Day 6 was chosen because it was in the initial extraction region.
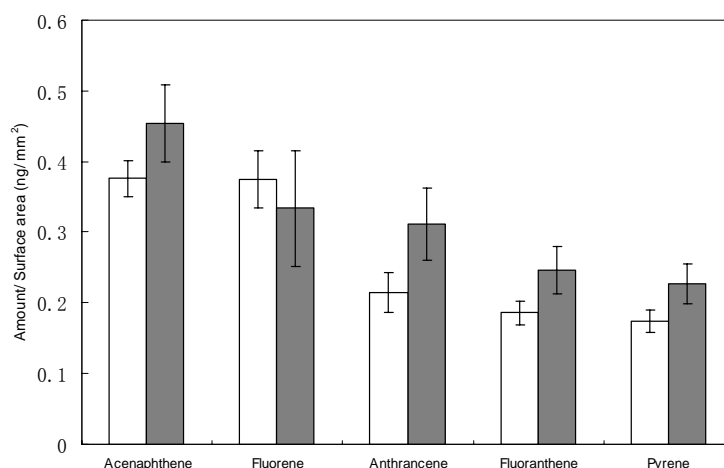
Figure 6-5 Extracted amount of PAHs by thin film of unit surface area (white) and by worms of unit surface area (grey) after 6 days.

6.4 Conclusion

As a solventless and integrative sampling technique, thin film extraction was used to investigate the partition of PAHs in the flow through system and compared to biomonitoring by black worms. Initial extraction rate per surface area by thin film and

black worms were similar indicating that thin film samplers could mimic the behavior of black worms for passive monitoring. In the 11 day sampling period, equilibrium was reached faster by the thin film than by the black worms.

The film-water partition coefficients and worm bioconcentration factors of PAHs were linearly correlated to their retention indexes and octanol-water partition coefficients. An even better linear relationship ($R^2=0.998$) between the bioconcentration factors and the film-water partition coefficients of PAHs was achieved. Compared to the lengthy and inconvenient process in sample preparation for worms and other passive sampling devices, the thin film sampler is a promising approach for future determination of TWA concentrations and bioavailability of hydrophobic organic compounds in aquatic environments.

Chapter 7

Skin and Breath Analysis Using Thin Film

7.1 Introduction

There is currently a great deal of emphasis on monitoring the chemical composition of fractions sampled from solid living organisms, such as vegetables, animals and humans, as well as those of the volatile fractions released from them. These chemical compositions can be regarded as important biosensors – which are diagnostic of changes taking place in the metabolism of living organisms.[1] Human odor results from the action of both skin glands and bacterial populations localized at skin surfaces, which survive by metabolizing and transforming organic compounds that they absorb from the external environment. Any alteration of this equilibrium induces changes to both the nature and the amount of volatile compounds contributing to the smell of skin. Practitioners of ancient medicine understood the significance of odors in relation to human health, and commonly diagnosed human diseases by analyzing body odor. Conventional western medicine recognizes that certain pathologies produce unpleasant characteristic odors (e.g. diabetes and some hepatic diseases).[2]

Researchers have performed substantial tasks of prospecting for disease markers using various techniques.[3] Some methods are based on adsorption of sebum on an opalescent material or on a glass surface, followed by photometric analysis.[4-5] These techniques have some merits but suffer from poor reproducible sampling. Another method utilized direct collection of the sebum at the skin surface by solvent rinsing; which was harmful due to

138

the introduction of a solvent directly to the skin.[6] An alternative to this was the extraction

of the sebum sampled on an adsorbing material (such as Sebutape) followed by thin layer

chromatography analysis.[7] However, this approach required a time-consuming sample

preparation step. Sweat is sampled as it drips from the skin surface (usually the elbow) or

by enclosing a limb (normally an arm) in a plastic bag (polythene) or by enclosing the

whole body in a much larger bag, which is then rinsed with water to wash off sweat. The

limb has often been cleaned with surfactant and distilled water and air-dried prior to

sampling.[8-11] Uncontrolled losses of volatiles, bacterial contamination of the collected

sweat accompanied by hydrolysis, and oxidative transformations of the compounds

involved, confound any attempts at accurate characterization of profiles of volatile organic

compounds. The conditions to which the participants have been subjected to often induce

sweating, involve thermal stress or intense exercise, and as such the samples are not

representative of the range of sweating mechanisms.[12]

In recent years, solid phase microextraction (SPME) as a solventless extraction

technique has been successfully applied to pharmaceutical and clinical samples.[13-15]

Bruheim *et al*. compared a thin sheet of a polydimethylsilicone (PDMS) thin film to

SPME fiber for the extraction of semivolatile analytes through both direct and headspace

modes.[16] Higher extraction efficiency and sensitivity were achieved with the thin film than

with the fiber because of the larger surface area/extraction phase volume ratio. For planar

sampling on the skin surface, a tape composed of flexible PDMS sheet was developed to

provide good contact with the skin. The tape was 15 mm × 4 mm for thermo desorption

and 15 mm × 12 mm for liquid desorption, with a film thickness of 0.5 mm. The sorptive

tape extraction (STE) technique studied the effects on sebum composition, both before and after cosmetic treatment through in vivo sampling at the human skin surface. The tapes were non-occlusive and sampling was ambulatory, easy and fast, which meant that large panels of volunteers could be studied. Moreover, this method is highly reproducible and predictable.[17] PDMS membrane sampling-patches that conform to the anatomical contours of the human body were investigated to assess the analytical functionality of adsorptive approaches, with an emphasis on the reproducibility, selectivity and sample stability.[12]

Human breath analysis can be used as a diagnostic tool. The organic compounds that are produced by metabolic processes, partition from the blood stream via the alveolar pulmonary membrane into the alveolar air. Therefore, the concentration measured in the breath is related to the concentration in the blood. Increased or decreased concentrations of certain compounds in human breath have been associated with a variety of diseases or altered metabolism.[18] The major advantage of breath analysis is that it is a noninvasive procedure, and is more convenient to collect compared to blood or urine samples.

Human breath contains many volatile substances derived from both internal metabolism and external exposure to vapors and gases. Normal humans differ from one another in the composition of their breath, both qualitatively and quantitatively. Breath analysis has been used for lung cancer, liver disease, and exposure to environmental pollutants.[19-20] Acetone was detected in the breath of patients suffering from diabetes; a chronic disorder in which either the pancreas is unable to produce insulin or the body is unable to effectively use insulin.[21-22] Almost all conventional breath sampling devices capable of collecting alveolar air have a common disadvantage: adsorptive losses on the

surface of the material may be significant, particularly when trace levels of analyte are being measured.

Some researchers have explored the application of SPME in breath analysis. The breath samples can be easily obtained in the patient's room without having to carry any large equipment. The SPME fiber device, as shown in Figure 7-1, can either be exposed directly to the air or to a sample collected in a gas-sampling bulb. [23] The validation of the method was based on ethanol, acetone, and the non-polar compound isoprene, which was found to be the main endogenous hydrocarbon in human breath.
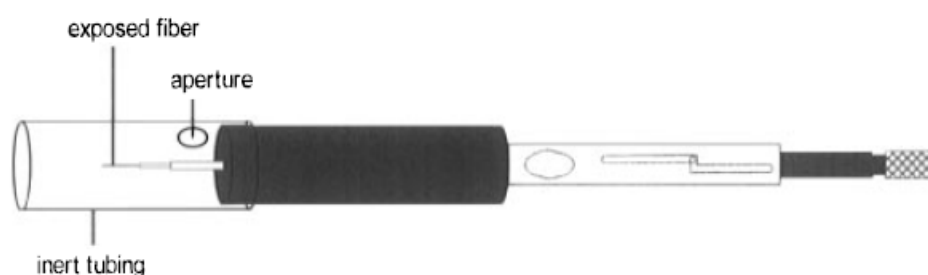
Figure 7-1 SPME device for breath analysis

Membrane extraction with a sorbent interface (MESI), another SPME technique, has been developed to allow rapid routine analysis and long-term continuous monitoring of volatile organic compounds in various environmental matrixes.[24] It minimizes the loss of analytes by interfacing the membrane extraction module directly to a capillary gas chromatograph. The sample is exposed to one side of the membrane, and a gas flows along the other side, transporting the extracted analyte molecules into a cooled sorbent trap. The analytes are desorbed from the sorbent trap by heating and are then transferred to the GC for analysis.[25]

In this study, thin film SPME as an effective sampling and sample preparation method

was investigated for in-vivo analysis of human skin and breath. The sampling times in all experiments were no more than 5 minutes, and the shortest sampling time could be 15-20 seconds. Calculation of retention index combined with mass spectrum comparison as a fast qualitative method was used to identify the compounds. For risk assessment purposes, factors that would affect the extraction of analytes were studied. These included sampling time, sampling area, and static sampler or rotated sampler.

7.2 Theory

The most popular way to measure retention was proposed by Kovats.[26] He proposed that Retention Indexes (RIs) were calculated under isothermal conditions, and reference substances (usually a homologous series of hydrocarbons), were used by performing a logarithmic interpolation. Van den Dool and Kratz further developed this approach, in the case of temperature-programmed GC analyses, following an approximately linear scale.[27]

Linear Temperature Programmed Retention Indices (LTPRI) were calculated using n-alkanes as reference compounds using the following expression:[27]

$$LTPRI(x) = 100 \times z + \frac{RT(x) - RT(z)}{RT(z+1) - RT(z)}$$

Equation 7.1

where RI (x) is the retention index of the unknown compound x; z is the number of carbon atoms of the n-alkane eluted before the unknown compound x; z + 1 is the number of carbon atoms of the n-alkane eluted after the unknown compound x; RT (x) is the retention time of the unknown compound x; RT (z) is the retention time of the n-alkane eluted before the unknown compound x; and RT (z + 1) is n-alkane eluted after the unknown compound x. All the indices were calculated by performing three replicated

measurements.

7.3 Experimental Section

7.3.1 Chemicals and Supplies

HPLC grade methanol was purchased from BDH (Toronto, ON, Canada). Retention index probes – an alkane mixture consisting of C8–C20 and C21–C40 straight-chain alkanes, with a concentration of 40 mg/L in hexane and toluene, respectively – were purchased from Fluka (Buchs, Switzerland). Compressed air that was used for the analytical instruments was obtained from Praxair (Kitchener, ON, Canada). The water used in these experiments was Nano-pure water from a Barnstead water system (Dubuque, IA). Ultrahigh-purity helium was purchased from Praxair (Kitchener, ON, Canada). The PDMS thin film, with a thickness of 127 μm, was purchased from Specialty Silicone Products Inc. (Ballston Spa, NY). A portable 7.2 V Makita drill with a constant agitation speed of 600 rpm was used.

7.3.2 Thin Film Sampler and Thin Film Extraction

For skin analysis, the dimension of the thin film was 1 × 1 cm. The surface area for one side was 1 cm^2, and the total volume of each thin-film was 0.0127 cm^3. For breath analysis, the thin film was 2 × 2 cm with a 1 cm high triangle on the top of the square. The surface area for one side was 5 cm^2, and the total volume of each thin-film was 0.0635 cm^3. These dimensions were optimized for ease of analysis so that the device could be coiled and fit inside a gas chromatography (GC) liner for injection. The thin films were

conditioned before use with a 2 hour bake out period in the GC injector port at 250°C, with a helium flow rate of 1 mL/min. Between consecutive extractions, a blank run of the same PDMS thin film was analyzed, proving that there was no carryover of the target analyte on the thin film from the previous desorption.

For the skin analysis, the thin film was placed in direct contact with human skin, and then covered with aluminum foil to prevent environmental contamination and analyte loss by evaporation. In order to ensure no contamination from aluminum foil, a conditioned blank thin film was wrapped with the foil for 5 minutes and then analyzed. No skin-related compound was detected. For the breath analysis, the thin film was placed in front of a human mouth while the person was exhaling (Figure 7-2). After extraction, the thin film was carefully removed from the skin or breath and inserted into the liner. The liner containing the thin film was inserted into the thermal desorption unit for automated analysis by thermo-desorption GC-MS. The thin film was analyzed immediately to minimize analyte loss.

Figure 7-2 Thin film extraction for breath analysis

7.3.3 Instrument

Gas chromatography was performed on an Agilent 6890 GC and 5973 MSD equipped with a Multipurpose Sampler (MPS 2) (Gerstel GmbH, Mullheim, Germany) system. The

Thermal Desorption System (TDS-2) unit was mounted on the GC via the Cooled Injection System (CIS-4) inlet for the thermal desorption of analytes. The thin film was placed in a liner of 187 mm length, 6 mm O.D. and 4 mm I.D. The liner with the sampler was heated so that the compounds to be determined were transferred into the CIS-4. The CIS acts similarly to cryogenic trapping; focusing and concentrating the components to be determined. The temperature of the CIS was 0°C for the first 5 minutes, during which time the temperature of TDU was increased to 250°C and the analyte was desorbed. After desorption, the cooled liner with the thin film was removed from the TDU, followed by a temperature increase of the CIS to transfer the analyte to the GC column. The transfer line situated between the thermo desorption device and the CIS, was set at 270°C.

An HR-1 capillary column (30 m, 0.25 mm i.d., 0.25 μm film thickness) (Shinwa, Kyoto, Japan) was used, with helium as the carrier gas at a flow rate of 1 mL/min. Column temperature was maintained at 40°C for 1 minute, then programmed to increase at a rate of 10°C/min to 280°C (for skin analysis) or at a rate of 5°C/min to 200°C (for breath analysis). The MS system was operating in the electron ionization (EI) mode, and tuned to perfluorotributylamine (PFTBA). A mass scan from 40 to 300 was acquired, and the base peak of each compound was selected and integrated.

7.4 Results and Discussion

7.4.1 Loading of Retention Index Probes onto the Thin Film

After a blank experiment of thin film, it was spiked with the retention index probes of 1μL followed by GC-MS analysis. This retention index loading experiment was repeated

every 10 injections during the sample analysis sequence, to confirm the exact retention times of the probes. Repeatability of the retention times of the retention index probes was in the range from 1 to 5%.

Table 7-1 Retention times of retention index probes

	Compound	Molecular weight	Retention time (min)
C9	nonane	128	5.06
C10	decane	142	6.68
C11	undecane	156	8.28
C12	dodecane	170	9.87
C13	tridecane	184	11.33
C14	tetradecane	198	12.69
C15	pentadecane	212	13.97
C16	hexadecane	226	15.17
C17	heptadecane	240	16.31
C18	octadecane	254	17.39
C19	nonadecane	268	18.43
C20	eicosane	282	19.42
C21	heneicosane	296	20.36

As seen in Table 7-1, when the temperature-programmed rate of GC was linear, the correlation between the retention times of members of a homologous series, and the

number of carbon atoms, was also linear.

7.4.2 Skin Analysis by Thin Film Extraction

7.4.2.1 Identification of Compounds

The identification of compounds was achieved by a combination of two paths. The first was a library search based on the comparison of the experimental mass spectra with those stored in the National Institute of Standards and Technologies (NIST) library. Ambiguous identifications often happened, especially in the case of structurally related compounds that give similar spectra, thus reducing the possibility of obtaining a complete characterization of the compounds under investigation. Therefore, the second useful path in identification was GC retention indices (RI), which are independent from the operating conditions – except for the polarity of the utilized stationary phase. This approach avoided the use of time-consuming procedures in which identification would have been based on the injection of pure compounds. Furthermore, when complex matrices containing hundreds of compounds have to be analyzed, the injection of pure standards could be a limiting factor; because such compounds may not be commercially available or they may be very expensive.

No degreasing was done before sampling; only the tap water was applied to clean the skin. The sampling area was on the skin surface close to the pulse of right wrist, because the surface temperature close to the pulse is a little higher than at other reachable surfaces of the human body. Analyses, including the analysis of skin samples, conducted in triplicate, and the blank experiments were performed using one thin film without any

significant change in sensitivity. The second thin film was not required. Skin-related compounds across the entire chromatogram were evaluated (integrated). These compounds were not necessarily the most intensive peaks in the chromatogram. In the rare cases of overlapped peaks, the peak quality for the evaluated compounds was considered satisfactory when the valley between two consecutive peaks was less than 10% of the peak height. Automatic integration was inspected and manually re-integrated if necessary. In Table 7-2, retention indices are indicated as integers, because RI values with a decimal digit are meaningless, taking into account that a difference of 0.1 in the RI should correspond to a difference of about 0.5 second in the retention time of the analyte. [29]

Table 7-2 Compounds identified in the skin samples

Compounds	Retention Time (min)	Retention Index (experimental)	Retention Index [28] (literature)
decanoic acid	12.27	1369	1372
dodecanoic acid	14.88	1575	1570
tetradecanoic acid	17.14	1777	1769
pentadecanoic acid	18.14	1872	1869
hexadecanol	18.38	1895	1875
ethyl hexadecanoate	19.25	1983	1978
propan-2-yl hexadecanoate	19.64	2024	2013
docosane	21.27	2202	2200

Sebum is produced by the sebaceous glands, which are epidermal appendixes located in the dermis. In the glands, the sebum is mainly composed of squalene, wax esters and triglycerides (ca. 60%) with some traces of cholesterol and its derivatives. During the move from the glands to the skin surface, some of the triglycerides are converted into free fatty acids by the resident microflora.[17] The skin surface composition is very complex; only some of the peaks in the chromatogram were selected at random from across the range of retention times and elucidated. The LTPRI values in Table 7-2 calculated from the retention times obtained in this study mostly exhibited good agreement with the literature values. The most common substances present in human skin odor were found, such as: esters, alcohols, and fatty acids in the C10 to C15 range originating from the bacterial decomposition of the triglycerides.

7.4.2.2 Reproducibility and Carryover Study

A necessary prerequisite for a suitable sampling procedure for skin analysis is its reproducibility. Retention indices (RI) precision was assessed by performing replicated injections under the same experimental conditions: differences less than 1U were observed for all the compounds. The repeatability experiment was carried out when sampling time was 5 minutes. Skin samples were continuously collected one at a time for each subject. Table 7-3 shows RSDs ($n = 3$) of all the compound peak areas within the range of 1.1–7.1 %. This RSD is small considering the fact that the sample was collected on a living human being. Carryover ratio of the sample, calculated through carryover absolute peak area *versus* average uptake peak area, was in the 0.9-6.7 % range. This proves that the residues

on the thin film after thermal desorption were low and negligible compared to the amount absorbed onto the sampler.

Table 7-3 RSD and carryover in skin analysis by thin film extraction

Compounds	Average	RSD (%)	Carryover	Carryover Ratio (%)
decanoic acid	2096818	5.7	108437	5.2
dodecanoic acid	88428503	2.6	4309939	4.7
tetradecanoic acid	170556281	2.7	10898877	6.4
pentadecanoic acid	72038805	7.1	4637972	6.7
hexadecanol	127009529	6.9	1089205	0.9
ethyl hexadecanoate	242633168	2.0	6064930	2.5
propan-2-yl hexadecanoate	27607488	1.7	1077469	3.9
docosane	28451656	1.1	1424182	4.9

7.4.2.3 Effect of Sampling Areas

An important feature of thin film extraction used in skin analysis is its simplicity and convenience, because no sample preparation step is required and the sample is collected on a very small skin surface (10 mm x 10 mm). These features show that thin film extraction may be extremely useful to simultaneously study several skin areas of one person and compare their compositions. On the right arm of a subject, three conditioned

thin films of the same size were placed on three sites: wrist, forearm and back of the arm. Three samples were collected after 5 minutes.
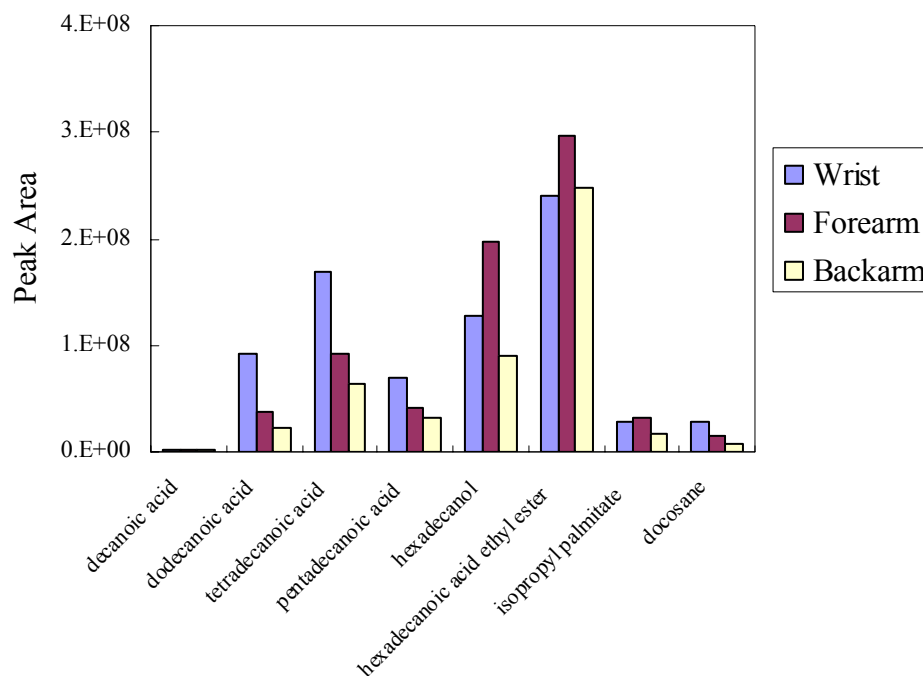
Figure 7-3 Effect of sampling areas in skin analysis by thin film extraction

The GC-MS profiles of the skin surfaces at the three sites are qualitatively similar, but quantitatively different. Figure 7-3 reports the mean absolute peak areas from three experiments at three sites. For most compounds, the uptake amounts at the wrist were more than those at the forearm and back arm. One of the possible explanations is that this increase might be related to the higher temperature at the wrist than at other areas on the arm, which contributes to the emission of human skin odor. Although the peak areas obtained at the three sites look very different, it is difficult to hypothesize a more thorough explanation of the biological phenomena involved.

7.4.2.4 Effect of Sampling Times

The amount of an analyte extracted by thin film was controlled by the partition between the skin and the extraction material.
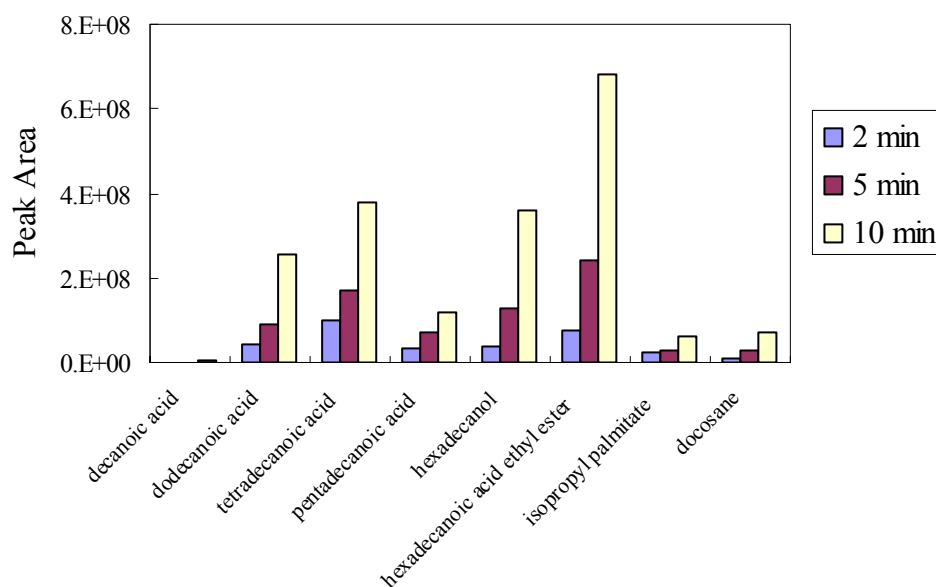
Figure 7-4 Effect of sampling time in skin analysis by thin film extraction

Figure 7-4 shows the peak areas versus time plot for skin surface components. The skin surface close to the pulse of right wrist was sampled in triplicate for three different lengths of time: 2 minutes, 5 minutes and 10 minutes. These results clearly show that analyte uptake was strongly influenced by the sampling time, even under very short sampling time conditions. The uptake amount of all the analytes increased with the increasing sampling time. The extracted amounts after a sampling time of 10 minutes were approximately 3-5 times and 2 times higher, than the amounts after 2 minutes and 5 minutes, respectively. This illustrates that the entire sampling procedure over the course of 10 minutes, was still within the region of linear uptake, and a sampling time of 10 minutes

is far from the equilibrium for the analytes between the two media.

7.4.2.5 Effect of Sampling Subject

In the sampling of live solid matrices, the only parameters that can be varied are the sampling area and sampling time; since the sampling rate cannot be increased by modifying the temperature, the stirring of sample, or matrix volume as in the liquid solutions. However, an advantage of sampling on a biological matrix is that it can monitor a variety of different living individuals. For example, in the human skin analysis, there is a high variability in the skin composition among humans of different nationalities, or between male and female individual persons. The goal of this experiment was to demonstrate the effectiveness of thin film extraction in the characterization of the skin of different persons, and to investigate the volatile fractions of cosmetic products that were released from the skin.

Table 7-4 reports the compounds identified on the skin of a second person, who applied a hand cream several hours prior to being sampled. The following compounds were different from those found on the first person: methyl-4-hydroxybenzoate (methylparaben), estra-1, 3, 5 (10)-trien-17b-ol, (9Z)-octadec-9-enoic acid and octadecanol. Methylparaben is known to be one of the main chemicals responsible for the fragrance in hand cream products. Its presence in the extracted compounds by thin film, shows that there is significant potential for the use of thin film extraction in the cosmetic industry.

Table 7-4 Compounds identified in skin samples of person Ⅱ

Name	Retention time (min)	Retention index (literature)	Retention index (experimental)
decanoic acid	12.28	1372	1370
methyl-4-hydroxybenzoate	13.58	1459	1470
dodecanoic acid	14.87	1570	1575
tetradecanoic acid	17.22	1769	1785
pentadecanoic acid	18.20	1869	1878
hexadecanol	18.40	1875	1898
estra-1,3,5 (10)-trien-17b-ol	19.38	1949	1996
(9Z)-octadec-9-enoic acid	19.99	2097	2061
octadecanol	20.39	2086	2104

Neither of the participants reported any problems with wearing the PDMS skin sampler. No skin irritation or skin damage was observed to be associated with the application of thin film. Both persons appeared to be comfortable throughout the sampling procedure and were not restricted from undertaking normal office-based or laboratory-based activities.

7.4.3 Breath Analysis by Thin Film Extraction

7.4.3.1 Effect of Garlic Diet

7.4.3.1.1 Headspace of Ground Garlic

Garlic is a perennial plant that is mainly used as a food flavoring agent and condiment in various foods and spices. Characteristic flavors of fresh garlic are associated with thiosulfinates and related compounds formed enzymatically by odorless precursors when the plants are cut or crushed.[30] The most important precursor of garlic flavor is allicin (2-propene-1-sulfinothioic acid *S*-2-propenyl ester). Allicin is not a stable compound and it readily degrades to form secondary products, a variety of sulfides, which contribute to the characteristic flavor and taste of garlic.[31]

Approximately 3 g of commercially available fresh garlic samples were ground and placed in a 20 mL vial. A thin film was hung in the headspace above the sample and the vial was capped with an aluminum cap for 10 minutes at room temperature. After extraction, the thin film was removed from the sampling vial and immediately inserted into the desorption liner for instrumental analysis.

Table 7-5 presents the compounds identified from the ground garlic flavors. Similar to the skin analysis, the identification was based on the mass spectral and GC retention indices of chromatogram peaks. Using thin film extraction, a variety of sulfides were found to be the predominant flavor components in the garlic samples, such as diallyl disulfide and 2-vinyl-1, 3-dithiane. The unstable compound allicin was not observed with this technique. The peak area of each characteristic compound was large enough to ensure sufficient sensitivity.

Table 7- 5 Compounds identified in the headspace of ground garlic

Compounds	Retention Time (min)	RI (experimental)	RI (literature)
2-ethyl-2-pentenal	6.962	917	891
2,4-dimethyl thiophene	8.37	950	898
methyl 2-propenyl disulfide	8.761	959	924
diallyl disulfide	13.646	1082	1079
2-vinyl-1,3-dithiane	14.35	1101	1152
3-vinyl-1,2-dithiocyclohex-5-ene	17.322	1192	1134
diallyl tetrasulfide	26.943	1550	1540

7.4.3.1.2 Breath Analysis by Static Thin Film Extraction

A healthy person exhales 500 mL of air or more with each breath. The PDMS thin film is similar to the non-polar lipid bilayer cell membrane of the alveoli, across which many compounds must travel to be expired into air. The cell membrane is relatively non-polar and preferentially transports non-polar compounds. As a result, the compounds present in the breath are relatively non-polar; these are the compounds that are best extracted by PDMS thin film.

For the detection of heptanol, diallyl disulfide and 2-vinyl-1,3-dithiane in the breath, the sample was collected from a person after eating two cloves of raw fresh garlic. Samples were collected over a 100-minute period, and the abundance of compounds in the

breath was related to the length of time after the diet of garlic. The three sampling times were just after the ingestion of garlic, 40 minutes after ingestion and 100 minutes after ingestion. Each measurement used an extraction time of 5 minutes with breath being exhaled onto the thin film sampler every half minute.
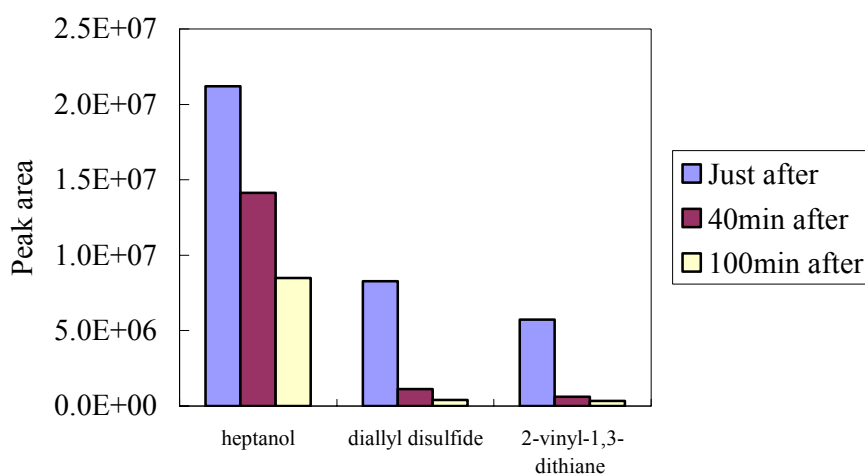
Figure 7-5 Effect of time intervals in breath analysis by static thin film extraction

Figure 7-5 presents the results obtained for the extraction of the three compounds from the human breath under varying time intervals after consuming the garlic. The compounds related to garlic were initially present at high levels shortly after the subject ate the garlic. After a longer time period, the amount of compounds extracted started to drop off to very low levels. Diallyl disulfide and 2-vinyl-1,3-dithiane dropped rapidly to nearly non-detectable levels after 100 minutes. The sampling method was simple with low requirements from the subject. It provided a convenient means to monitor the breath of individuals.

7.4.3.1.3 Breath Analysis by Rotated Thin Film Extraction

Rapid sampling is beneficial for breath analysis and optimization of the analytical method. In order to provide the most comfortable sampling environment for the subject, a sampling time that is as short as possible is important; a high sampling rate is required to achieve this goal. It is known that the diffusion of the analyte in the boundary layer between the sample and the extraction phase controls the extraction rate. Decreasing the boundary layer thickness through stirring the sample can increase the extraction rate. This experiment used a portable electric drill attached to the thin film to constantly rotate the film, which sped up the flow-rate of the sample and thus allowed high extraction efficiency. Only one deep breath from the subject was sampled instead of having the breath be exhaled for 5 minutes. This showed that the sampling time could be shortened to only 15-20 seconds.
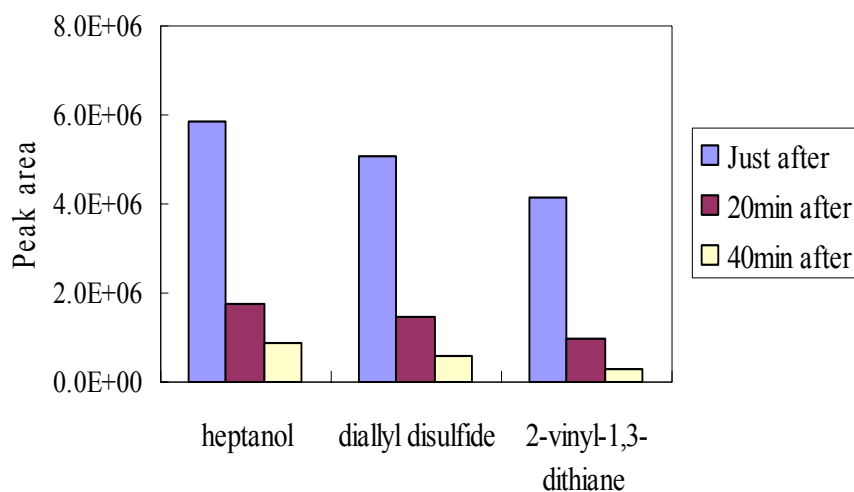
Figure 7-6 Effect of time intervals in breath analysis by rotated thin film extraction

Figure 7-6 illustrates that the sampling time interval had a significant effect on the

amount of the three analytes in the breath sample. Although the abundance of compounds extracted by dynamic thin film was lower than those extracted by static thin film, this difference is insignificant considering the notable reduction in sampling time (i.e. from 5 minutes to 20 seconds).

7.4.3.2 Effect of Smoking

To evaluate the usefulness of thin film in pre-concentrating analytes present at low concentration in human breath, breath samples were also analyzed for the volatile compounds arising from cigarette smoking. To identify which components originated from smoking, this study compared volatile profiles among breath samples acquired before smoking, during smoking and after smoking. Extraction time in this case was 5 minutes.
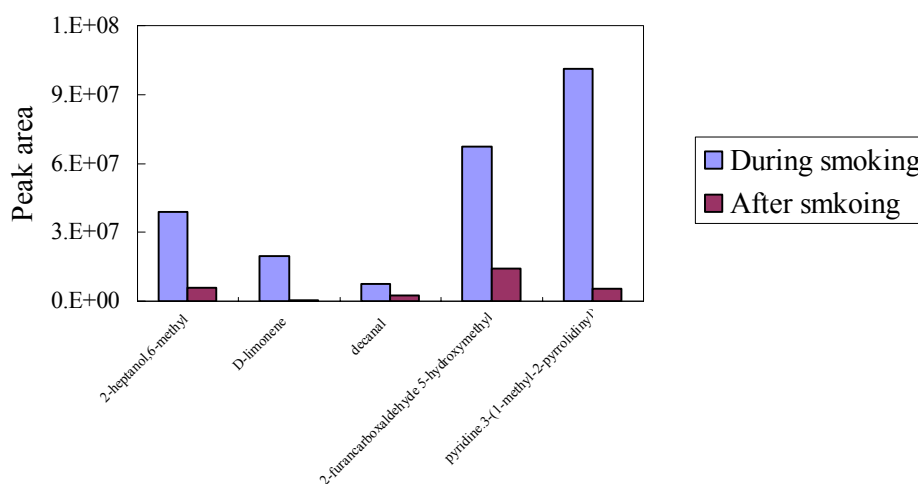
Figure 7-7 Analysis of the breath of a smoke during smoking and after smoking

By comparing the results obtained before smoking and during smoking – although some peaks were common to both profiles – several more peaks responsible for cigarette smoking appeared in the profile during smoking, such as limonene. However, the amount

of the compounds extracted decreased rapidly when the breath sample was collected after the subject stopped smoking, as shown in Figure 7-7.

7.5 Conclusion

The work described has shown that thin film extraction is applicable for the collection of samples from both human skin and breath. Compared to the sampling techniques currently used (which are usually cumbersome and expensive), thin film extraction is a rapid and convenient method – because the sampling process takes only 5 minutes and has a high sample sensitivity. Providing a skin or breath sample does not require very much effort from the test subject.

Thin film extraction is also useful to simultaneously study several skin areas of one person, and to characterize the skin of several different persons. Based on the investigation of the volatile fractions of cosmetic products that were released from the skin, this technique shows significant potential for the cosmetic industry. It is noted that the sampling time in the breath analysis can be further reduced to 20 seconds when the thin film is rotated with a portable drill.

Further research into accurate quantification of skin and breath concentrations will improve the thin film extraction technique, and may be beneficial in the study of skin and breath physiology.

Chapter 8

Summary

8.1 Thin Film Extraction

SPME technique is a solvent-free, fast and simple technique, which combines extraction, concentration and sample introduction into one step. PDMS thin film possesses large surface area-to-volume ratio, which enhances its sensitivity without sacrificing analysis time. It is demonstrated in the previous chapters that thin film extraction technique is feasible for both spot sampling and time weighted average (TWA) sampling in laboratory and on site.

A rotated thin PDMS film or PDMS fiber was used for rapid analysis of PAHs in water samples. A mass transfer model was proposed to quantitatively describe direct extraction of PAHs with rotated thin film extraction. Compared to the fiber, the rotated thin film coupled with an electric drill achieved high extraction sensitivity without sacrificing equilibrium time. The amount of the analytes extracted by the thin film was around 100 times higher than those obtained by the fiber, for both 5 minute rapid sampling as well as equilibrium extraction. A new thin film active sampler included a portable electric drill, a copper mesh pocket, a piece of thin film and a liner. It facilitated on-site sampling, sample preparation, storage and transport. Laboratory experiments indicated that sampling remained in the linear uptake region with this sampler up to 8 minutes for the PAHs. Field tests illustrated that this novel sampler was excellent for rapid on-site water sampling.

161

The comparison between a PDMS thin film and a PDMS-coated stir bar at a constant stirring speed, showed that the extraction rate was roughly proportional to the surface area of the extraction phase during the initial stage of the extraction process; the amount of analyte extracted at equilibrium was proportional to the extraction phase volume. Different agitation and stirring rates of the thin-film and stir bar were applied for extraction, revealing that extraction efficiency can be improved by increasing rotation rate.

The mass transport process of pyrene into a SPME PDMS fiber or PDMS thin film from a static aqueous solution and the simultaneous desorption process of calibrant into the solution from the extraction phase were simulated by COMSOL Multiphysics. Modeling gave the concentration distribution of PAH in the extraction phase and demonstrated the symmetry of absorption and desorption for both fiber extraction and thin film extraction. Moreover, modeling illustrated the feasibility of the kinetic calibration method for fiber SPME in a flow through system and aqueous sample with the presence of binding matrix. The concentration of total analyte rather than free dissolved analyte was determined in the complex sample matrix.

Thin film extraction was successfully used for on-site sampling in Hamilton Harbour in 2005 and the determination of TWA concentrations of PAHs based on the kinetic calibration method. In 2006, a thin film sampler, a modified fiber-retracted SPME field water sampler and a SPME PDMS rod were used simultaneously to determine the TWA concentrations of PAHs in Hamilton Harbour. For the fiber-retracted device, all of the analytes were quantified and no internal standard was required. Conversely, the rod and thin film samplers can only quantify the analytes with a corresponding internal standard.

However, the kinetic calibration method can effectively compensate for the turbulence factor that can be encountered in field sampling.

PDMS thin films were simultaneously exposed to the contaminated water stream, along with black worms used as biomonitors. After equal extraction times in the initial extraction stage, the extracted amount per surface area by the two samplers were similar. Equilibrium was reached faster by the thin-film samplers than by the black worms. Film-water partition coefficients of PAHs could be used to calculate the BCFs and therefore eliminate the need of worms for this purpose. Compared to the lengthy and inconvenient process of liquid-liquid extraction in the worm treatment, thin-film is a solventless sampling technique, which simplifies the sample pretreatment procedure by integrating sampling and sample preparation. The whole analysis procedure, including sample transfer, thermal desorption, and instrumental analysis, can be automated. Thin film samplers provide an alternative technology for measuring the bioavailability of hydrophobic organic compounds in aquatic environments.

Thin film extraction was experimentally proven to be applicable for the analysis of human skin and breath samples under normal conditions or when the subjects performed different activities, such as eating, applying cosmetics or smoking. Factors affecting the extraction of analytes were studied, including: sampling time, sampling area, sampling subject and static sampler or rotated sampler. The sampling times were no more than 5 minutes, and the shortest sampling time could be only 15-20 seconds. Providing a skin or breath sample did not require much effort from the subject.

8.2 Perspective

Thin film extraction technique has achieved breakthroughs for both spot and TWA sampling. Future research in this area could consist of a number of applications.

Firstly, future applications of thin film extraction in the area of skin and breath can include the recording of VOC profiles present in skin cancer or other skin diseases, and buccal disorders. The research on metabolomics of skin and breath using this approach will lead to the discovery of clinical and therapeutic markers, and be beneficial to the study of skin and breath physiology. In addition, based on the investigation of the volatile fractions of cosmetic products that were released from the skin, this technique shows significant potential for the cosmetic industry.

Secondly, commercially available thin films are made of different materials (with the exception of PDMS), and they possess varying thicknesses. These coatings satisfy the needs for analysis of various organic compounds, in many applications. The extension of thin film extraction technique for different coatings and thicknesses is needed.

Glossary

a	Time constant
A	Surface area of extraction phase
b	Radius of a SPME fiber
B	Geometric factor
$\overline{C}$	TWA concentration
C_c	Concentration of calibrant in extraction phase
C_f	Concentration of analyte in extraction phase
C_s	Concentration of analyte in sample
D_a	Diffusion coefficient in air
D_f	Diffusion coefficient in extraction phase
D_s	Diffusion coefficient in sample
E	Constant depends on Reynolds number
$\mathbf{F}$	Body force
$\overline{h}$	Average mass transfer coefficient
K	Partition coefficient
K_{es}	Extraction phase/ sample partition coefficient
K_{ow}	Octanol/ water partition coefficient
K_{tfw}	Thin film/ water partition coefficient
L	Length of fiber coating
M	Stiff-spring velocity
n	Amount of analyte absorbed onto extraction phase

n_e	Amount of analyte absorbed onto extraction phase at equilibrium
p	Pressure
Q	Amount of calibrant remaining on extraction phase after time t
q_0	Initial amount of calibrant loaded onto extraction phase
R_s	Sampling rate
R_e	Reynolds number
S_c	Schmidt number
t	Sampling time
t_e	Equilibrium time
u	Linear speed of fluid
$\mathbf{u}$	Velocity vector
v	Kinematic viscosity
V_e	Volume of extraction phase
V_s	Volume of sample matrix
Z	Diffusion path length
δ	Thickness of boundary layer
ρ	Density of fluid

References

Chapter 1

(1) Pawliszyn, J., Ed. *Sampling and Sample Preparation for Field and Laboratory*. Elsevier, Amsterdam. 2002.

(2) Pawliszyn, J. *Anal. Chem.* **2003**, *75*, 2543.

(3) Thurman, E.; Mills, M. *Solid-Phase Extraction*; John Wiley: New York, 1998.

(4) Liska, I. *J. Chromatogr. A* **2000**, *885*, 3.

(5) Handley, A., Ed.; *Extraction Methods in Organic Analysis;* Sheffield Academic Press: Sheffield, U K., 1999.

(6) Bao, L.; Dasgupta, P. *Anal. Chem.* **1992**, *64*, 991.

(7) Gorecki, T.; Namiesnik, J. *Trends Anal. Chem.* **2002**, *21*, 276.

(8) Murray, D. A. J. *J. Chromatogr*. **1979**, *177*, 135.

(9) Thielen, D. R.; Olsen, G.; Davis, A.; Bajor, E.; Stefanovski, J.; Chodkowski, J. *J. Chromatogr. Sci*. **1987**, *25*, 12.

(10) Arthur, C. L.; Pawliszyn, J. *Anal. Chem*. **1990**, *62*, 2145.

(11) Pawliszyn, J. *Solid Phase Microextraction – Theory and Practice*; Wiley – VCH; New York, 1997.

(12) Grote, C.; Pawliszyn, J. *Anal. Chem.* **1997**, *69*, 587.

(13) Ouyang, G.; Pawliszyn, J. *Anal. Bioanal. Chem*. **2006**, *386*, 1059.

(14) Lambropoulou, D.; Albanis, T. A. *J. Chromatogr. A* **2001**, *922*, 243.

(15) Zeng, Z.; Qui, W.; Huang, Z. *Anal. Chem.* **2001**, *73*, 2429.

(16) Alpendurada, M. *J. Chromatogr. A* **2000**, *889*, 3.

(17) Felix, T.; Hall, B. J.; Brodbelt, J. S. *Anal. Chim. Acta* **1998**, *371*, 195.

(18) Pawliszyn, J.; Pedersen-Bjergaard, S. *J. Chromatogr. Sci.* **2006**, *44*, 291.

(19) Baltussen, E.; Sandra, P.; David, F.; Cramers, C. *J. Microcolumn Separations*, **1999**, *11*, 737.

(20) McComb, M.; Giller, E.; Gesser, H. D. *Talanta* **1997**, *44***, 2137.

(21) Zhao, W.; Ouyang, G.; Alaee, M.; Pawliszyn, J. *J. Chromatogr. A* **2006**, *1124*, 112.

(22) Koziel, J.; Jia, M.; Pawliszyn, J. *Anal. Chem*. **2000**, *72*, 5178.

(23) Bruheim, I.; Liu, X.; Pawliszyn, J. *Anal. Chem*. **2003**, *75*, 1002.

(24) Ramsey, S. A.; Mustacich, R. V.; Smith, P. A.; Hook, G. L.; Eckenrode, B. A. *Anal. Chem*. in press.

(25) Isetun, S.; Nilsson, U.; Colmsjo, A. *Anal. Bioanal. Chem*. **2004**, *380*, 319.

(26) Mayer, P.; Vaes, W.; Wijnker, F.; Legierse, K.; Kraaij, R.; Tolls, J.; Hermens, J. *Environ. Sci. Technol*. **2000**, *34*, 5177.

(27) Zeng, E. Y.; Tsukada, D.; Diehl, D. W. *Environ. Sci. Technol*. **2004**, *38*, 5737.

(28) Pawliszyn, J. (Ed.), Applications of Solid Phase Microextraction, RSC, Cornwall, UK, 1999.

(29) Doong, R. A.; Chang, S. M. *Anal. Chem*. **2000**, *72*, 3647.

(30) Shurmer, B.; Pawliszyn, J. *Anal. Chem*. **2000**, *72*, 3660.

(31) Chen, Y.; Pawliszyn, J. *Anal. Chem*. **2006**, *78*, 5222.

(32) Carasek, E.; Pawliszyn, J. *J. Agric. Food Chem*. **2006**, *54*, 8688.

(33) Ouyang, G.; Zhao, W.; Alaee, M.; Pawliszyn, J. *J. Chromatogr. A* **2007**, *1138*, 42.

(34) Martos, P. A.; Pawliszyn, J. *Anal. Chem*. **1999**, *71*, 1513.

(35) Lee, I. S.; Tsai, S. W. *Anal. Chim. Acta* **2008**, *610*, 149.

(36) Chen, C. Y.; Hsiech, C.; Lin, J. M. *J. Chromatogr. A* **2006**, *1137*, 138.

(37) Chen, Y.; Pawliszyn, J. *Anal. Chem.* **2003**, *75*, 2004.

(38) Ouyang, G.; Chen, Y.; Pawliszyn, J. *Anal. Chem.* **2005**, *77*, 7319.

(39) Koziel, J.; Jia, M.; Pawliszyn, J. *Anal. Chem.* **2000**, *72*, 5178.

(40) Tuduri, L.; Desauziers, V.; Fanlo, J. L. *Analyst* **2003**, *128*, 1028.

(41) Paschke, A.; Popp, P. *J. Chromatogr. A* **2004**, *1025*, 11.

(42) Chen, Y.; Koziel, J. A.; Pawliszyn, J. *Anal. Chem.* **2003**, *75*, 6485.

(43) Ai, J. *Anal. Chem.* **1997**, *69*, 1230.

(44) Ai, J. *Anal. Chem.* **1997**, *69*, 3260.

(45) Chen, Y.; O'Reilly, J.; Wang, Y.; Pawliszyn, J. *Analyst* **2004**, *129*, 702.

(46) Chen, Y.; Pawliszyn, J. *Anal. Chem.* **2004**, *76*, 5807.

(47) Ouyang, G.; Cai, J.; Zhang, X.; Li, H.; Pawliszyn, J. *J. Sep. Sci*. **2008**, *31*, 1167.

Chapter 2

(1) Pawliszyn, J. *Solid Phase Microextraction – Theory and Practice*; Wiley – VCH; New York, 1997.

(2) Pawliszyn, J. Applications of solid phase microextraction. RSC, Cornwall, UK, 1999.

(3) Ai, J. *Anal. Chem*. **1997**, *69*, 1230.

(4) Ai, J. *Anal. Chem*. **1997**, *69*, 3260.

(5) Chen, Y.; Pawliszyn, J. *Anal. Chem*. **2004**, *76*, 5807.

(6) Chen, Y.; O'Reilly, J.; Wang Y.; Pawliszyn, J. *Analyst* **2004**, *129*, 702.

(7) Wang, Y.; O'Reilly, J.; Chen, Y.; Pawliszyn, J. *J. Chromatogr. A* **2005**, *1072*, 13.

(8) Ouyang, G.; Zhao, W.; Pawliszyn, J. *Anal. Chem*. **2005**, *77*, 8122.

(9) Bragg, L.; Qin, Z.; Alaee, M.; Pawliszyn, J. *J. Chromatogr. Sci*. **2006**, *44*, 317.

(10) Zhao, W.; Ouyang, G.; Alaee, M.; Pawliszyn, J. *J. Chromatogr. A* **2006**, *1124*, 112.

(11) Musteata, F. M.; Musteata, M. L.; Pawliszyn, J. *Clin. Chem*. **2006**, *52*, 708.

(12) Zhou, S. N.; Zhang, X.; Ouyang, G.; Es-haghi, A.; Pawliszyn, J. *Anal. Chem*. **2007**, *79*, 1221.

(13) Li, Q.; Ito, K.; Wu, Z.; Lowry, C.; Loheide II, S. *Groud Water* **2009**, *47*, 480.

(14) Wang, J.; Dual, J. *J. Phys. A: Math. Theor*. **2009**, *42*, 285502.

(15) Lawrence, B.; Devarapalli, M.; Madihally, S. *Biotechnol. & Bioeng*. **2009**, *102*, 935.

(16) Koyamaa, T.; Neretnieksb, I.; Jing, L. *Int. J. Rock Mech. & Min*. **2008**, *45*, 1082.

(17) Artug, G.; Roosmasari, I. *Sep. Sci. & Technol*. **2007**, *42*, 2947.

(18) Comini, G.; Savino, S. *Appl. Therm. Eng*. **2009**, *29*, 2863.

(19) Breure, B.; Peters, E.; Kerkhof, P. *Chem. Eng. Sci* **2009**, *64*, 2256.

(20) Joly, A.; Perrard, A. *Math. & Comput. Simulat* **2009**, *79*, 3492.

Chapter 3

(1) Pawliszyn, J. *Solid Phase Microextraction - Theory and Practice*; Wiley-VCH: New York, 1997.

(2) Chen, Y.; Pawliszyn, J. *Anal. Chem*. **2004**, *76*, 6823.

(3) King, A.; Readman, J.; Zhou, J. *Anal. Chim. Acta* **2004**, *523*, 259.

(4) Ouyang, G.; Pawliszyn, J. *J. Chromatogr. A* **2007**, *1168*, 226.

(5) Zhou, S.; Zhang, X.; Ouyang, G.; Pawliszyn, J. *Anal. Chem*. **2007**, *78*, 1221.

(6) Pawliszyn, J., Ed. *Sampling and Sample Preparation for Field and Laboratory*; Elsevier: Amsterdam, 2002.

(7) Bruheim, I.; Liu, X.; Pawliszyn, J. *Anal. Chem*. **2003**, *75*, 1002.

(8) Ouyang, G.; Pawliszyn, J. *Trends Anal. Chem*. **2006**, *25*, 692.

(9) Ouyang, G.; Pawliszyn, J. *Anal. Bioanal. Chem*. **2006**, *386*, 1059.

(10) Pawliszyn, J. *Trends Anal. Chem*. **2006**, *25*, 633.

(11) Gorecki, T.; Namiesnik, J. *Trends Anal. Chem*. **2002**, *21*, 276.

(12) Digiano, F.; Elliot, D.; Leith, D. *Environ. Sci. Technol*. **1988**, *22*, 1365.

(13) Vrana, B.; Popp, P.; Paschke, A.; Schuurmann, G. *Anal. Chem*. **2001**, *73*, 5191.

(14) Kot-Wasik, A. *Anal. Chem*. **2004**, *49*, 691.

(15) Ouyang, G.; Chen, Y.; Pawliszyn, J. *Anal. Chem*. **2005**, *77*, 7319.

(16) Ouyang, G.; Zhao, W.; Alaee, M. *J. Chromatogr. A* **2007**, *1138*, 42.

(17) Vrana, B.; Mills, G.; Allan, I.; Dominiak, E.; Svensson, K.; Knutsson, J.; Morrison, G.; Greenwood, R. *Trends Anal. Chem*. **2005**, *24*, 845.

(18) Ouyang, G.; Pawliszyn, J. *Anal. Chim. Acta* **2008**, *627*, 184.

(19) Huckins, J.; Petty, J.; Orazio, C.; Lebo, J.; Clark, R.; Gibson, V.; Gala, W.; Echols, K. *Environ. Sci. Technol*. **1999**, *33*, 3918.

(20) Murdock, C.; Kelly, M.; Chang, L.; Davison, W.; Zhang, H. *Environ. Sci. Technol*. **2001**, *35*, 4530.

(21) Chen, Y.; Koziel, J.; Pawliszyn, J. *Anal. Chem*. **2003**, *75*, 6485.

(22) Koziel, J.; Jia, M.; Pawliszyn, J. *Anal. Chem*. **2000**, *72*, 5178.

(23) Hilpert, R.; *Forsch. Geb. Ingenieurwes*. **1933**, *4*, 215.

(24) Knudsen, J.; Katz, D. *Fluid Dynamics and Heat Transfer*, McGraw-Hill: New York, 1958.

(25) Carslaw, H.; Jaeger, J. *Conduction of Heat in Solids*, 2nd Edition, Clarendon Press, Oxford, 1986.

Chapter 4

(1) Lioy, P.; Greenberg, A. *Toxicol. Ind. Health* **1990**, *6*, 209.

(2) Dennis, M.; Massey, R.; Cripps, G.; Venn, I.; Howarth, N.; Lee, G. *Food Addit. Contam.* **1991**, *8*, 517.

(3) Wong, K.; Wang, J. *Environ. Pollut.* **2001**, *112*, 407.

(4) Biziuk, M.; Pryjazny, A.; Czerwinski, J.; Wiergowski, M. *J. Chromatogr. A* **1996**, *754*, 103.

(5) Vreuls, J.; Brinkman, U.; de Jong, G.; Grob, K.; Artho, A. *J. High Resol. Chromatogr.* **1991**, *14*, 45.

(6) Brouwer, E.; Hermans, A.; Hingeman, H.; Brinkman, U. *J. Chromatogr. A* **1994,** *45*, 669.

(7) Louter, A.; Vreuls, J.; Brinkman, U. *J. Chromatogr. A* **1999**, *842*, 391.

(8) Sabaliu-nas, D.; Lazutka, J.; Sabaliu-niene, I. *Environ. Pollut.* **2000**, *109*, 251.

(9) Petty, J.; Orazio, C.; Cranor, W. *J. Chromatogr. A* **2000**, *879*, 83.

(10) Arthur, C.; Pawliszyn, J. *Anal. Chem.* **1990**, *62*, 2145.

(11) Baltussen, E.; Sandra, P.; David, F.; Cramers, C. *J. Microcolumn Separations* **1999**, *11*, 737.

(12) Pawliszyn, J. Ed. *Application of Solid-Phase Microextraction*; Royal Society of Chemistry: Cornwell, UK, 1999.

(13) Ouyang, G.; Pawliszyn, J. *Anal. Bioanal. Chem.* **2006**, *386*, 1059.

(14) Ouyang, G.; Pawliszyn, J. *Trends Anal. Chem.* **2006**, *25*, 692.

(15) Chen, Y.; Begnaud, F.; Chaintreau, A.; Pawliszyn, J. *Flavour Fragr. J.* **2006**, *21*, 822.

(16) Zhao, W.; Ouyang, G.; Alaee, M.; Pawliszyn, J. *J. Chromatogr. A* **2006**, *1124*, 112.

(17) Zhao, W.; Ouyang, G.; Pawliszyn, J. *Analyst* **2007**, *132*, 256.

(18) Montero, L.; Popp, P.; Paschke, A.; Pawiliszyn, J. *J. Chromatogr. A* **2004**, *1025*, 17.

(19) Bruheim, I.; Liu, X.; Pawliszyn, J. *Anal. Chem.* **2003**, *75*, 1002.

(20) Grob, K.; Habich, A. *J. Chromatogr. A* **1985**, *321*, 45.

(21) Burger, B.; Munro, Z. *J. Chromatogr. A* **1986**, *370*, 449.

(22) Bicchi, C.; Amato, A.; David, F.; Sandra, P. *Flavor Flagr. J.* **1988**, *3*, 143.

(23) Baltussen, E.; David, F.; Sandra, P.; Janssen, H.; Cramers, C. *J. Chromatogr. A* **1998**, *805*, 237.

(24) www. Gerstel. com

(25) Popp, P.; Bauer, C.; Weinrich, L. *Anal. Chim. Acta* **2001**, *436*, 1.

(26) Popp, P.; Bauer, C.; Hauser, B.; Keil, P.; Wennrich, L. *J. Sep. Sci.* **2003**, *26*, 961.

(27) Kreck, M.; Scharrer, A.; Bilke, S.; Mosandl, A. *Eur. Food Res. Technol.* **2001**, *213*, 389.

(28) Luan, F.; Mosandl, A.; Gubesch, M.; Wust, M. *J. Chromatogr. A* **2006**, *1112*, 369.

(29) Soini, H.; Wiesler, D.; Apfelbach, R.; Konig, P.; Vasilieva, N.; Novotny, M. *J. Chem. Ecol.* **2005**, *31*, 1125.

(30) Zhang, J.; Soini, H.; Bruce, K.; Wiesler, D.; Woodley, S.; Baum, M.; Novotny, M. *Chem. Senses* **2005**, *30*, 727.

(31) Pawliszyn, J. *Solid Phase Microextraction – Theory and Practice*, Wiley – VCH, New York, 1997.

(32) Motlagh, S.; Pawliszyn, J. *Anal. Chim. Acta* **1993**, *284*, 265.

(33) Gorecki, T.; Pawliszyn, J. *Anal. Chem.* **1996**, *68*, 3008.

(34) Carasek, E.; Pawliszyn, J. *J. Agric. Food Chem.* **2006**, *54*, 8688.

(35) Ouyang, G.; Chen, Y.; Pawliszyn, J. *J. Chromatogr. A* **2006**, *1105*, 176.

Chapter 5

(1) Kot, A.; Zabiegala, B.; Namiesnik, J. *Trends Anal. Chem.* **2000**, *19*, 446.

(2) Namiesnik, J.; Zabiegala, B.; Kot-Wasik, A.; Partyka, M.; Wasik, A. *Anal. Bioanal. Chem.* **2005**, *381*, 279.

(3) Vrana, B.; Mills, G. A.; Allan, I. J.; Dominiak, E.; Svensson, K.; Knutsson, J.; Morrison, G.; Greenwood, R. *Trends Anal. Chem.* **2005**, *24*, 845.

(4) Gorecki, T.; Namiesnik, J. *Trends Anal. Chem.* **2002**, *21*, 276.

(5) Prest, H. F.; Jacobson, L. A.; Wilson, M. *Chemosphere* **1997**, *35*, 3047.

(6). Luellen, D. R.; Shea, D. *Environ. Sci. Technol.* **2002**, *36*, 1791.

(7). Huckins, J. N.; Petty, J. D.; Orazio, C. E.; Lebo, J. A.; Clark, R. C.; Gibson, V. L.; Gala, W. R.; Echols. K. R. *Environ. Sci. Technol.* **1999**, *33*, 3918.

(8) Prest, H. F.; Jacobson, L. A.; Huckins. J. N. *Chemosphere* **1995**, *30*, 1351.

(9) Litten, S.; Mead, B.; Hassett, J. *Environ. Toxicol. Chem.* **1993**, *12*, 639.

(10) Audunsson, G. *Anal. Chem.* **1986**, *58*, 2714.

(11) DiGiano, F. A.; Elliot, D.; Leith, D. *Environ. Sci. Technol.* **1988**, *22*, 1365.

(12) Huckins, J. N.; Tubergen, M. W.; Lebo, J. A.; Gale, W.; Schwartz, T. R. *J. Assoc. Off. Anal. Chem.* **1990**, *73*, 290.

(13) Pawliszyn, J. *Solid Phase Microextraction*s*Theory and Practice*, Wiley-VCH: New York, 1997.

(14) Arthur, C. L.; Pawliszyn, J. *Anal. Chem.* **1990**, *62*, 2145.

(15) Pawliszyn, J. *Applications of Solid Phase Microextraction*, RSC: Cornwall, UK, 1999.

(16) Ouyang, G.; Pawliszyn, J. *Anal. Bioanal. Chem.* **2006**, *386*, 1059.

(17) Ouyang, G.; Pawliszyn, J. *Trends Anal. Chem.* **2006**, *25*, 692.

(18) Martos, P. A.; Pawliszyn, J. *Anal. Chem.* **1999**, *71*, 1513.

(19) Khaled, A.; Pawliszyn, J. *J. Chromatogr. A* **2000**, *892*, 455.

(20) Chen, Y.; Pawliszyn, J. *Anal. Chem.* **2003**, *75*, 2004.

(21) Chen, Y.; Pawliszyn, J. *Anal. Chem.* **2004**, *76*, 6823.

(22) Ouyang, G.; Chen, Y.; Pawliszyn, J. *Anal. Chem.* **2005**, *77*, 7319.

(23) Ai, J. *Anal. Chem.* **1997**, *69*, 1230.

(24) Ai, J. *Anal. Chem.* **1997**, *69*, 3260.

(25) Chen, Y.; O'Reilly, J.; Wang, Y.; Pawliszyn, J. *Analyst* **2004**, *129*, 702.

(26) Chen, Y.; Pawliszyn, J. *Anal. Chem.* **2004**, *76*, 5807.

(27) Wang, Y.; O'Reilly, J.; Chen, Y.; Pawliszyn, J. *J. Chromatogr. A* **2005**, *1072*, 13.

(28) Hayduk, W.; Laudie, H. *AlCheE J.* **1974**, *20*, 611.

(29) Lahr, J.; Maas-Diepeveen, J. L.; Stuijfzand, S. C.; Leonards, P. E.G.; Druke, J. M.;
Lucker, S.; Espeldoorn, A.; Lerkum, L.C. M.; Stee, L. L. P. V.; Hendriks, A. J. *Water Res.*
2003, *37*, 1691.

(30) Schildermand, P. A. E. L.; Moonen, E. J. C.; Maas, L. M.; Welle, I.; Kleinjans, J. C.S.
Ecotoxicol. Environ. Saf. **1999**, *44*, 241.

(31) Miermans, C. J. H.; Van der Velde, L. E.; Frintrop. P. C. M. Chemosphere **2000**, *40*,
39.

(32) Vanderpoorten, A. *Environ. Pollut.* **1999**, *104*, 401.

(33) Ouyang, G.; Chen, Y.; Pawliszyn, J. *J. Chromatogr. A* **2006**, *1105*, 176.

(34) G. Mills. Personal communication. SWIFT-WFD. Portsmouth, U.K., 2005.

(35) C. Marvin. Personal communication. Water Science and Technology Directorate, Environment Canada, Burlington, Ontario, Canada, 2006.

Chapter 6

(1) Kot, A.; Zabiegata, B.; Namiesnik, J. *Trends Anal. Chem.* **2000**, *19*, 446.

(2) Leppanen, M.; Kukkonen, J. *Environ. Toxicol. Chem.* **1998**, *17*, 2196.

(3) Bopp, S.; McLachlan, M.; Schirmer, K. *Environ. Sci. Technol.* **2007**, *41*, 6868.

(4) Petty, J.; Poulton, B.; Charbonneau, C.; Huckins, J.; Jones, S.; Caneron, J.; Prest, H. *Environ. Sci. Technol.* **1998**, *32*, 837.

(5) Komarova, T.; Bartkow, M.; Rutishauser, S. *Environ. Pollut.* **2009**, *157*, 731.

(6) Anderson, K.; Sethajintanin, D.; Sower, G.; Quarles, L. *Environ. Sci. Technol.* **2008**, *42*, 4486.

(7) Adams, R.; Lohmann, R.; Fernandez, L.; Macfarlane, J.; Gschwend, P. *Environ. Sci. Technol.* **2007**, *41*, 1317.

(8) Pawliszyn, J. *Solid Phase Microextraction – Theory and Practice*, Wiley – VCH, New York, 1997.

(9) Ouyang, G.; Pawliszyn, J. *Anal. Bioanal. Chem.* **2006**, *386*, 1059.

(10) Chen, Y.; Begnaud, F.; Chaintreau, A.; Pawliszyn, J. *Flavour Fragr. J.* **2006**, *21*, 822.

(11) Zhou, S.; Zhang, X.; Ouyang, G.; Pawliszyn, J. *Anal. Chem.* **2007**, *78*, 1221.

(12) Gong, Y.; Eom, I.; Lou, D.; Hein, D.; Pawliszyn, J. *Anal. Chem.* **2008**, *80*, 7275.

(13) Chen, Y.; Pawliszyn, J. *Anal. Chem.* **2003**, *75*, 2004.

(14) Chen, Y.; Pawliszyn, J. *Anal. Chem.* **2004**, *76*, 6823.

(15) Ouyang, G.; Chen, Y.; Pawliszyn, J. *Anal. Chem.* **2005**, *77*, 7319.

(16) Van der Heijden, S.; Jonker, M. *Environ. Sci. Technol.* **2009**, *43*, 8854.

(17) You, J.; Landrum, P.; Lydy, M. *Environ. Sci. Technol*. **2006**, *40*, 6348.

(18) Zhao, W.; Ouyang, G.; Alaee, M.; Pawliszyn, J. *J. Chromatogr. A* **2006**, *1124*, 112.

(19) Bruheim, I.; Liu, X.; Pawliszyn, J. Anal. Chem. **2003**, *75*, 1002.

(20) Van der Heijden, S.; Jonker, M. *Environ. Sci. Technol*. **2009**, *43*, 3757.

(21) Ouyang, G.; Chen, Y.; Pawliszyn, J. *J. Chromatogr. A* **2006**, *1105*, 176.

(22) Huckins, J.; Petty, J.; Orazio, C.; Lebo, J.; Clark, R.; Gibson, V.; Gala, W.; Echols, K. *Environ. Sci. Technol*. **1999**, *33*, 3918.

(23) Ansorena, D.; Astiasarán, I.; Bello, J. *J. Agri. Food Chem.* **2000**, *48*, 2395.

(24) Wang, Z.; Fingas, M.; Li, K. *J. Chromatogr. Sci*. **1994**, *32*, 367.

(25) Naikwadi, K.; Charbonneau, G.; Karasek, F.; Clement, R. *J. Chromatogr.* **1987**, *398*, 227.

(26) Lundstedt, S.; Haglund, P.; Öberg, L. *Environ. Toxicol. Chem*. **2003**, *22*, 1413.

(27) Piao, M.; Chu, S.; Zheng, M.; Xu, X. *Chemosphere* **1999**, *39*, 1497.

(28) Saraullo, A.; Martos, P. ; Pawliszyn, J. *Anal. Chem*. **1997**, *69*, 1992.

(29) http://cfpub.epa.gov/ecotox/quick_query.htm.

(30) Saint-Denisa, M.; Narbonneb, J.; Arnaudb, C.; Thybaudc, E.; Ribera, D. *Soil Biol. Biochem*. **1999**, *31*, 1837.

(31) Rewitz, K.; Styrishave, B.; Løbner-Olesen, A.; Andersen, O. *Comp. Biochem. Phys. C* **2006**, *143*, 363.

Chapter 7

(1) Bicchi, C.; Cordero, C.; Liberto, E.; Rubiolo, P.; Sgorbini, B.; Sandra, P. *J. Chromatogr. A* **2007**, *1148*, 137.

(2) Di Natale, C.; Macagnano, A.; Paolesse, R.; Tarizzo, E.; Mantini, A.; D'Amico, A. *Sens. Actuators B* **2000**, *65*, 216.

(3) Deng, C.; Zhang, X.; Li, N. J. Chromatogr. B **2004**, *808*, 269.

(4) Pierard, G. E. *Appl. Skin Physiol.* **2000**, *13*, 372.

(5) St Leger, D. *Arch. Dermatol. Res*. **1979**, *265*, 79.

(6) Ruggieri, M. R. *Advances in Thin Layer Chromatography, Clinical and Environmental Applications*, Ed. J. C. Touchstone, Publ. John Wiley & Sons, New York, USA, 1982.

(7) Nordstrom, K. M. *J. Invest. Dermatol*. **1986**, *87*, 260.

(8) Yokoyama, Y.; Aragaki, M.; Sato, H.; Tsushiya, M. *Anal. Chim. Acta* **1991**, *246*, 405.

(9) Shirreffs, S. M.; Maughan, R. J. *J. Appl. Physiol.* **1997**, *82*, 336.

(10) Patterson, M. J.; Galloway, S. D.; Nimmo, M. A. *Exp. Physiol.* **2000**, *85*, 869.

(11) Patterson, M. J.; Galloway, S. D.; Nimmo, M. A. *Acta Physiol. Scand.* **2002**, *174*, 41.

(12) Riazanskaia, S.; Blackburn, G.; Harker, M.; Taylor, D.; Thomas, C. L. P. *Analyst* **2008**, *133*, 1020.

(13) Liu, Z.; Pawliszyn, J. *J. Chromatogr. Sci.* **2006**, *44*, 366.

(14) Stashenko, E. E.; Martinez, J. R. *Trends Anal. Chem*. **2004**, *23*, 553.

(15) Zhou, S. N.; Zhang, X.; Ouyang, G.; Eshaghi, A.; Pawliszyn, J. *Anal. Chem*. **2007**, *79*, 1221.

(16) Bruheim, I.; Liu, X.; Pawliszyn, J. *Anal. Chem*. **2003**, *75*, 1002.

(17) Sisalli, S.; Adao, A.; Lebel, M.; Le Fur, I.; Sandra, P. *LC–GC Europe*, **2006**, *19*, 33.

(18) Manolis, A. *Clin Chem*. **1983**, *29*, 5.

(19) Gordon, S. M.; Szidon, J. P.; Krotoszynski, B. K.; Gibbons, R. D.; O'Neill, H. J. *Clin. Chem*. **1985**, *31*, 1278.

(20) Kaji, H.; Hisamura, M.; Saito, N.; Murao, M. *Clin. Chim. Acta* **1978**, *85*, 279.

(21) Rooth, G.; Ostenson, S. *The Lancet* **1966**, *ii*, 1102.

(22) Crofford, O. B.; Mallard, R. E.; Winton, R. E. *Trans. Am. Clin. Climatol. Assoc*. **1977**, *88*, 128.

(23) Grote, C.; Pawliszyn, J. *Anal. Chem*. **1997**, *69*, 587.

(24) Yang, M. J.; Pawliszyn, J. *Anal. Chem*. **1993**, *65*, 2538.

(25) Lord, H; Yu, Y.; Segal, A.; Pawliszyn, J. *Anal. Chem*. **2002**, *74*, 5650.

(26) Kovats, E. *Adv. Chromatogr*. **1965**, *1*, 229.

(27) Van den Dool, H.; Kratz, P. D. *J. Chromatogr*. **1963**, *11*, 463.

(28) NIST 2.0 Mass spectral data base.

(29) Ettre, L. S. *Chromatographia* **2003**, *58*, 491.

(30) Han, J.; Lawson, L.; Han, G.; Han, P. *Anal. Biochem*. **1995**, *225*, 157.

(31) Lee, S.; Kim, N.; Lee, D. *Anal. Bioanal. Chem*. **2003**, *377*, 749.